Deciphering the impact of lipopolysaccharide and high-fat diet on disease pathogenesis in Parkinson's and Huntington's disease rat models

Dissertation

zur Erlangung des Grades eines Doktors der Naturwissenschaften

der Mathematisch-Naturwissenschaftlichen Fakultät
und
der Medizinischen Fakultät
der Eberhard-Karls-Universität Tübingen

vorgelegt

von

Reema Chowdhury
aus Serampore, Indien

2025

Tag der mündlich Prüfung: 20.10.2025

Dekan der Math.-Nat. Fakultät: Prof. Dr. Thilo Stehle

Dekan der Medizinischen Fakultät: Prof. Dr. Bernd Pichler

1. Berichterstatter: Prof. Dr. med. Olaf Rieß

2. Berichterstatter: Prof. Dr. Julia Schulze-Hentrich

Prüfungskommission: Prof. Dr. med. Olaf Rieß
Prof. Dr. Julia Schulze-Hentrich
Prof. Dr. Vanessa Nieratschker
Dr. rer. nat. Thorsten Schmidt

Erklärung/Declaration

Ich erkläre hiermit, dass ich die zur Promotion eingereichte Arbeit mit dem Titel ”Deciphering the role of environmental factors on disease pathogenesis in Parkinson’s and Huntington’s disease rat models” selbständig (ohne fremde Hilfe) angefertigt, nur die angegebenen Quellen und Hilfsmittel benutzt und aus anderen Arbeiten wörtlich oder inhaltlich übernommene Stellen als solche kenntlich gemacht habe. Ich versichere an Eides statt, dass diese Angaben der Wahrheit entsprechen und ich nichts verschwiegen habe. Mir ist bekannt, dass die Abgabe einer falschen eidesstattlichen Erklärung mit Freiheitsstrafe bis zu drei Jahren oder mit Geldstrafe bestraft werden kann.

I hereby declare that I have produced the work entitled “Deciphering the role of environmental factors on disease pathogenesis in Parkinson’s and Huntington’s disease rat models”, submitted for the award of a doctorate, on my own (without external help), have used only the sources and aids indicated and have marked passages included from other works, whether verbatim or in content, as such. I swear upon oath that these statements are true and I have not concealed anything. I am aware that making a false declaration under oath is punishable by a term of imprisonment of up to three years or by a fine.

Tübingen,

Datum/Date: 13.11.2025 Unterschrift/Signature

Acknowledgements

This thesis is the outcome of my research work at the Institute of Medical Genetics and Applied Genomics in Tübingen. During this period, I had the privilege of working and engaging with many remarkable individuals. I take this opportunity to thank all of them for their continuous support and help.

First, I would like to express my sincere gratitude to my supervisors Prof. Dr. Julia Schulze-Hentrich and Prof. Dr. med. Olaf Rieß for their constant and invaluable academic and personal support throughout my research period. I am especially grateful to Prof. Dr. Julia Schulze-Hentrich, my internal supervisor, for her continuous mentorship and support during my Ph.D. journey. Without her guidance, this would not have been possible. I would like to thank my advisory board members, Prof. Dr. Julia Schulze-Hentrich, Prof. Dr. med. Olaf Rieß, Prof. Dr. Vanessa Nieratschker, and Dr. rer. nat. Thorsten Schmidt for their suggestions and for reviewing my Ph.D. project.

Thanks to all my collaborators in the EPIROM project, Dr. Jonas Neher, Dr. Ping Liu, Dr. Kathrin Kattler-Lackes, Dr. Thomas Hentrich, Dr. M. Sadman Sakib, Dr. Jonasz Jeremiasz Weber, Priscila Pereira Sena, Xidi Yuan, Dr. rer. nat. Nicolas Casadei and Dr. Yogesh Singh.

On the lab front, I was very happy to be a part of the Institute of Genetics, where I got the opportunity to grow and learn as a scientist. I am immensely thankful to Dr. Jonasz Jeremiasz Weber and Priscila Pereira Sena for their constant support during the last days of my Ph.D. Dr. Jonasz Jeremiasz Weber truly guided me through the wet-lab experiments, and I really appreciated how he patiently listened to my complaints and offered support throughout. I would like to thank our technical assistant Celina Tomczak for her support in the animal work. I would also like to thank my lab members Linda Sofan, Anna Hendlinger, Jacqueline Jung, Mahkameh Abeditashi, Rana Dilara Incebacak Eltemur, Dr. rer. nat. Libo Yu-Taeger and Dr. Elisabeth Singer for the constant support during my Ph.D.

I would like to thank my best friends, Sudeshna Karmakar and Aishwarya Murali, for standing by my side through all the high and low moments during my time in Germany. I would also like to thank my friends Sromona Chatterjee, Diksha Gadhoke, Nikita Srivastava, Puja Mishra, Aarya Lakshmireddy, Johanna Rodriquez, Shrunal Mane, Patricia Buzzatto, Pallabi Paul, Marta Ibanez, and my newfound friends-turned-family in Darmstadt – Omveer Singh, Shaifali Mehta, and Anurag Tiwari – for their unwavering support and warmth throughout this journey. Most importantly, I am truly grateful to my parents and extended family members for their support, which has been my greatest strength throughout every step of this journey. Their trust and sacrifices made this possible.

Abstract

Neurodegenerative diseases such as Alzheimer's, Parkinson's, and Huntington's disease affect millions of people worldwide, with no effective treatments currently. They are often characterised by the accumulation of misfolded proteins, such as tau, amyloid beta, alpha-synuclein, and huntingtin (Sweeney et al. 2017). Aging, genetic, and environmental factors play a significant role in the progression of these diseases. Thus, a detailed understanding of these diseases would shed light on the development of therapeutic targets.

Parkinson's and Huntington's diseases are associated with neuronal loss in the motor and sensory systems (Troncoso-Escudero et al. 2020). A combination of genetic and environmental factors contributes to Parkinson's disease, with only 10-15% of cases resulting from genetic mutations, while the rest are sporadic. (Ball et al. 2019). Many environmental factors, including pesticides and heavy metals, have been linked to the onset of Parkinson's disease. Neuropathologically, Parkinson's disease is characterized by the presence of Lewy bodies, which are composed of aggregates of alpha-synuclein (Wakabayashi et al. 2007). In comparison to Parkinson's, Huntington's disease is an autosomal dominantly inherited disorder caused by a trinucleotide repeat expansion (CAG) within the gene Huntingtin HTT (Nopoulos 2016). CAG codes for the amino acid glutamine, and the expansion of polyglutamine tracts results in the formation of neuronal aggregates containing the mutant HTT (Kshirsagar et al. 2021).

For the pathophysiology of neurodegenerative diseases, the role of misfolded proteins leading to neurodegeneration has been discussed earlier. Recently, substantial evidence suggests that neuroinflammation plays a role in the pathogenesis of these diseases (Kwon and Koh 2020). Neuroinflammation can be triggered by environmental pollutants, including metals, diet, pollution and exposure to pesticides (Langley et al. 2022). It is crucial to understand how neuroinflammatory factors can trigger neurodegeneration and whether environmental factors play a role as risk factors in these diseases. Previous studies have demonstrated that inflammatory stimuli can induce long-term epigenetic memory in microglia, thereby significantly influencing the deposition of amyloid beta plaques in the brain of an Alzheimer's mouse model (Wendeln et al. 2018). Studies have also shown that neuroinflammation plays a significant role in the pathogenesis of Parkinson's and Huntington's diseases (W. Zhang et al. 2023). However, the role of microglial immune memory in influencing pathogenesis in Parkinson's and Huntington's disease remains unknown.

This thesis aims to investigate how immune memory is triggered with bacterial lipopolysaccharide, LPS, and high-fat diet, HFD, and whether this immune memory shapes neuropathology in Parkinson's and Huntington's disease. Here, we use the BAC SNCA and BAC HD rat models, which were generated using a bacterial artificial chromosome (BAC) containing the entire human SNCA or HTT genomic sequence with 97 polyQ repeats and all regulatory elements (Nuber et al. 2013; Yu-Taeger et al. 2012).

In summary, we report on changes in body weight of the BAC SNCA and BAC HD rats when exposed to bacterial lipopolysaccharides and a high-fat diet. LPS-induced sickness

behavior in the rats led to temporary weight loss after the injections. In contrast, HFD rats gained weight within four weeks compared to the control group. The changes in body weight were compared with different cytokine responses and indicated that after the first LPS injection (1xLPS), an increase in the pro-inflammatory cytokines (IFN-ɣ, IL-1β, TNF-α) was observed, but repeated injections of LPS (2xLPS and 4xLPS) resulted in a suppression of the cytokine levels (P. Liu 2022). Several post-translational modifications are associated with alpha-synuclein, and patients with Parkinson's disease have alpha-synuclein phosphorylated at Serine 129 (Kawahata, Finkelstein and Fukunaga 2022). This is typically found in the neuronal cells of patients and is more pronounced in the late stages of the disease. Additionally, alpha-synuclein phosphorylation is widespread in Lewy body pathology (Takahashi et al. 2002). At the histological level, we observed the presence of phosphorylated alpha-synuclein in the forebrain of the BAC SNCA rat model at the age of 9 months. Upon quantification of the signal, an increase in the area of phosphorylated serine 129 deposits could be observed with HFD and LPS treatments. In the BAC HD rat model, histological nuclear localization of the mutant huntingtin could be observed following LPS treatment.

Accordingly, we emphasized that HFD showed opposite effects at the level of insoluble protein detection in BAC SNCA and BAC HD rat models. On one hand, HFD leads to an increase in insoluble alpha-synuclein protein aggregates. On the other hand, it reduces the accumulation of insoluble huntingtin in the forebrain at the age of 9 months. Moreover, we also detected soluble-level alpha-synuclein and huntingtin in both models, and an expression pattern of full-length and fragmented alpha-synuclein could be observed. Different forms of alpha-synuclein, including monomeric, dimeric, trimeric, tetrameric, and oligomeric forms, could be detected. HFD led to an increase in the oligomeric forms of alpha-synuclein. Although the detection of huntingtin soluble protein revealed the presence of the full-length huntingtin protein along with the fragmented portion, no treatment-based effects of LPS and HFD could be observed in our BAC HD rat model. Furthermore, bulk RNA sequencing of the 9-month-old BAC SNCA model revealed oxidative phosphorylation as one of the altered pathways, thereby verifying mitochondrial dysfunction at the OXPHOS protein level in the BAC SNCA rat model. HFD and LPS treatment showed a reduction in the complex V of the mitochondrial complex. Even when there are alterations in the accumulation of alpha-synuclein and huntingtin protein levels, no autophagy response could be observed in the BAC SNCA and BAC HD disease models. Inflammatory markers were used to check the role of HFD and LPS in inducing inflammation in the BAC SNCA model. A reduction in LPS groups with β-arrestin 1 confirms the stimulation of microglial immune responses.

Overall, the data in this thesis demonstrate the role of LPS and HFD in triggering immune responses in the brain in BAC SNCA and BAC HD rat models. It also provides the first evidence that LPS and HFD modulate brain pathology responses in these disease models.

Contents

List of Figures

List of Tables

Acronyms

a-syn	alpha-synuclein.
AD	Alzheimer' disease.
BAC	Bacterial artificial chromosome.
CNS	Central nervous system.
ELISA	Enzyme-linked immunosorbent assay.
FACS	Fluorescence-activated cell sorting.
HD	Huntington's disease.
HFD	High fat-diet.
htt	huntingtin.
IF	Immunofluorescence.
IHC	Immunohistochemistry.
LPS	Lipopolysaccharide.
mhtt	mutant huntingtin.
ND	Neurodegenerative diseases.
PCR	Polymerase chain reaction.
PD	Parkinson's disease.
qPCR	Quantitative polymerase chain reaction.
TG	Transgenic animals.
WB	Western blotting.
WT	Wildtype animals.

Chapter 1

Introduction

1.1 Motivation

Neurodegenerative diseases are characterized by the degeneration of neurons in the central nervous system (CNS), such as Parkinson's (PD), Huntington's (HD), and Alzheimer's disease (AD). Immune responses play a critical role in neurodegeneration, and the interplay between immune responses and neuroinflammation has been recently studied (Doty, Guillot-Sestier and Town 2015). Two kinds of memory exist in mammals: Innate and Adaptive. Innate immunity is the first response to a pathogen, whereas adaptive immunity forms an immunological memory to a previously encountered pathogen (Netea, Joosten et al. 2016). Contrary to the adaptive response, innate immune memory responses are rapid, but have much less specificity than adaptive responses (Netea, Joosten et al. 2016). Innate immune memory is a crucial phenomenon that occurs in response to environmental stimuli, altering the immune responses (Sherwood et al. 2022). It is a change in the reactivity of the innate immune cells, leading to either a stronger (immune training) or weaker (immune tolerance) response to a previous stimulus. Both immune training and immune tolerance are associated with epigenetic alterations (Neher and Cunningham 2019). Varied environmental and lifestyle factors like Western diet, surgery and systemic infections can trigger inflammation and contribute in shaping the immune responses, and thus it is essential to know how these environmental factors are contributing to the pathology of neurodegenerative diseases.

Microglia are the brain-resident macrophages that are responsible for mediating the immune responses in the CNS and it has been established that peripheral stimulation triggers microglia and could lead to epigenetic reprogramming of microglia (Neher and Cunningham 2019). Neuroinflammation leads to the presence of disease-associated microglial subtypes during the disease (Tay et al. 2018). Microglia exist in a ramified morphological state under normal physiological conditions, and transform themselves into an amoeboid morphology under pathological conditions (Stratoulias et al. 2019). This change of microglial phenotype from a neuroprotective state to a neurotoxic state suggests that microglia have a disease-associated signature in neurodegenerative diseases (Joers et al. 2017). The role of innate immune memory was studied in Alzheimer's mouse models, and some genes related to disease-associated microglia were also found in this study (Wendeln et al. 2018). It was concluded that the innate immune cells develop a memory of a previously encountered pathogen. Upon administering a single dose of

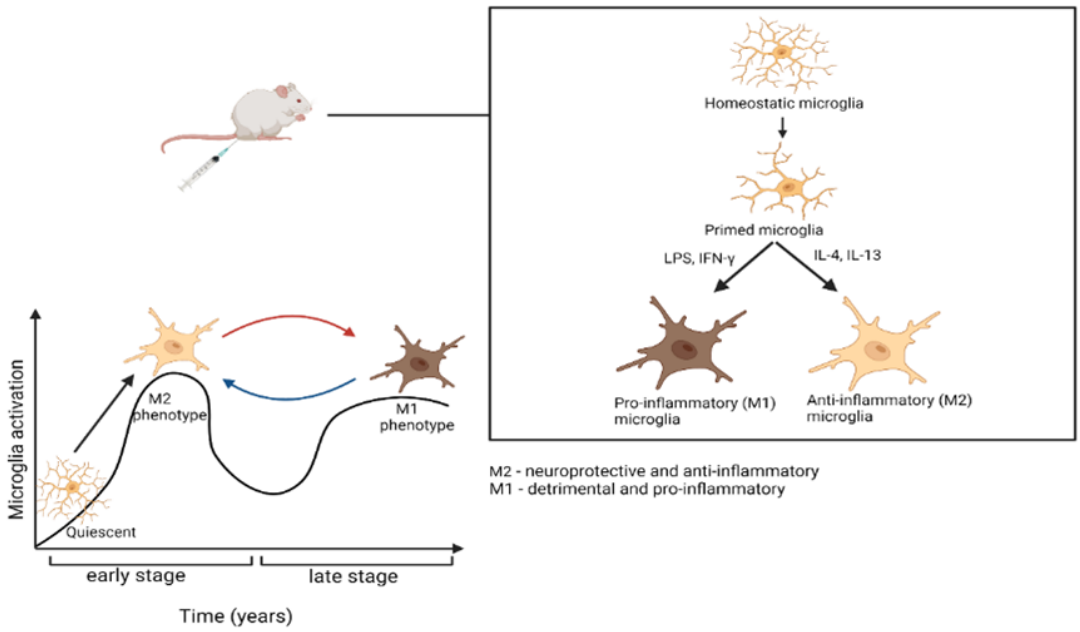

Figure 1.1: Microglial polarization in neurodegeneration.
The enhancement and reduction of microglial immune responses occurring upon integration of multiple stimuli as described by Wendeln et al. shows the different roles of microglia in diseases (Wendeln et al. 2018). The modulation of microglia polarization from M1 to M2 plays an important role in NDs (adapted from (Shen, Bao and R. Wang 2018; Neher and Cunningham 2019). This figure has been generated with BioRender.com.

Lipopolysaccharide (LPS), microglia developed a form of immune memory, known as training, which increased the production of inflammatory responses and led to a higher deposition of amyloid beta in the brain, ultimately causing the death of neurons after 6 months. On the other hand, upon injecting four doses of LPS, microglia developed immune tolerance, which ultimately leads to neuronal survival (Wendeln et al. 2018).

1.2 Interlinking immune responses and neuroinflammation

1.2.1 Introduction to innate immune memory and microglia acting as a key mediator in innate immune responses

Innate immune memory is a mechanism where the reactivity of the innate immune cells are altered while encountering a previous stimulus (Boraschi and Italiani 2018). It differs from adaptive immunity in a way that it is usually short-lived and involves epigenetic reprogramming of the innate immune cells (Boraschi and Italiani 2018). Innate immune responses can exist in two forms: 'training' or 'tolerance'. Training could be a heightened response to the primary response and tolerance could be the lack of responsiveness to

the primary response (Boraschi and Italiani 2018). Thus, innate immune memory in the brain could be used as a risk factor for ND, and targeting innate immune memory could be a powerful therapeutic paradigm for treating NDs.

Studies have shown that peripheral inflammation can lead to the epigenetic reprogramming of microglia (Wendeln et al. 2018). When no stimulus is present, microglia are in a homeostatic state. Usually, immune training induced by the microglia could be referred to as a 'priming stimulus' and immune tolerance as the 'desensitising stimulus' (Neher and Cunningham 2019). Depending upon the intensity of the infection or injury, microglia get activated and adopt either an M1 or an M2 polarization state. M1 state is the neurotoxic state of microglia that produces pro-inflammatory cytokines like IL-1β and TNF-α, causing neuroinflammation. Alternatively, M2 is the neuroprotective state of microglia producing anti-inflammatory cytokines and suppressing neuroinflammation (Zhou et al. 2017). Immune memory in microglia has been associated with varied epigenetic modifications like DNA methylation, histone modifications and chromatin remodelling (Yeh and Ikezu 2019). Histone and DNA modifications are considered to play an important role in regulating macrophage phenotypes (Cheray and Joseph 2018). A long-term regulation of microglia by epigenetic modifications has happened and this has been passed onto generations, strengthening the bond between the switch of microglial phenotypes and epigenetic mechanisms (Cheray and Joseph 2018). The involvement of microglia in innate immune responses has opened new doors in the approach to the treatment of neurological disorders.

1.2.2 Inflammation in neurodegenerative disease and its potential as a therapeutic agent

In ND, neuroinflammation is a process following microglial activation and injury, occurring in the CNS. It can be triggered by signals coming from damaged neurons and an imbalance between pro-inflammatory and anti-inflammatory responses (Wyss-Coray and Mucke 2002). Other triggers could be aggregated proteins, accumulation of abnormal cellular constituents, neuronal triggers, and imbalance in the regulation of inflammatory mechanisms (Wyss-Coray and Mucke 2002).

Microglia account for 5-20% of the total glial cells in the CNS and switch between neuroprotective and neurotoxic states upon being triggered by various stimuli. The polarization of microglia mediates the immune responses in the CNS (Jha, W. H. Lee and Suk 2016). Understanding neuroinflammation has been crucial in treating NDs, as anti-inflammatory drugs are being developed to target peripheral inflammation to treat ND. Drugs developed to target inflammation and pro-inflammatory cytokines, and transcriptional modifiers could restore the immune system to a balanced level (Elodie Kip and Louise C. Parr-Brownlie 2022).

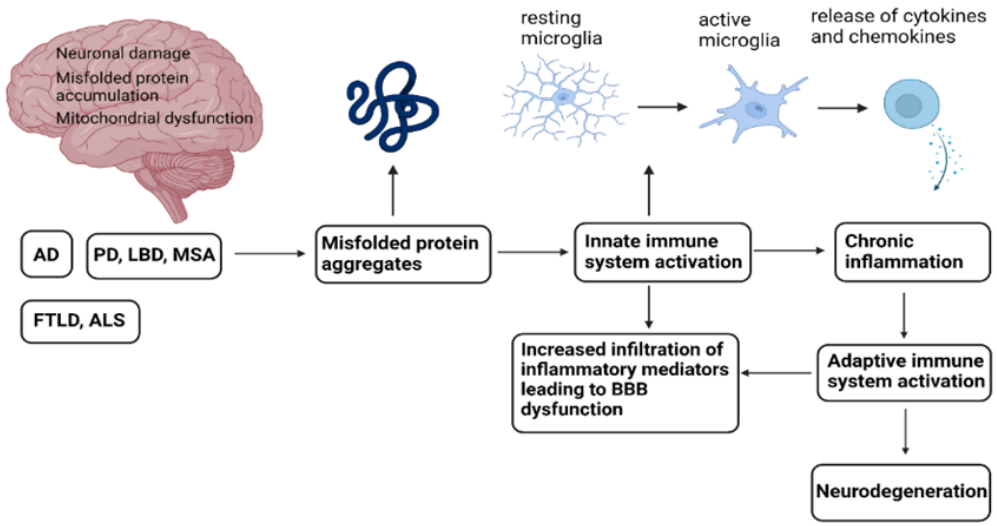

Figure 1.2: Central and peripheral immune response in neurodegeneration.
Misfolded protein aggregates lead to the activation of the innate immune system, which activates microglia, subsequently leading to the release of cytokines and chemokines in the brain. This increased infiltration of the inflammatory mediators leads to the dysfunction of the BBB. Therefore, a relationship between protein deposition in the brain, activation of the innate immune system, and neurodegeneration has been established (Ciccocioppo 2020). This figure has been generated with BioRender.com (adapted from (Ciccocioppo 2020)).

1.3 Background of disease models

1.3.1 Parkinson's disease (PD)

Neurodegeneration refers to the loss of function of neurons, ultimately leading to cell death. Examples include Alzheimer's, Parkinson's, Huntington's, Amyotrophic lateral sclerosis, multiple system atrophy and prion diseases. Neurodegeneration affects most of the body's activities like movement, speech, breathing, heart and lung functionality, etc., and most of these diseases are incurable to date (Serge Przedborski and Vernice Jackson-Lewis 2003). These diseases pose a great health risk in today's world. A lot of factors like activated immune responses, bioenergetics, metabolism, genetic and environmental interactions are contributors to neurodegeneration (Wareham et al. 2022). Thus, an in-depth study of these multifactorial events would provide a link towards the therapeutic strategies of these diseases.

PD is a common neurodegenerative disorder of the CNS, affecting the motor system. It affects 2-3% of the population over 65 years of age and worsens with advancing age (Poewe et al. 2017). The dopaminergic neuron degeneration in the substantia nigra pars compacta is the hallmark of PD which causes the symptoms of tremor, rigidity, slowness and difficulty in walking, followed by decline in cognition at a later stage (Beitz 2014). PD is also characterized by the intracellular depositions of alpha-synuclein in the brain, in the form of Lewy bodies (Kouli, Torsney and Kuan 2018). Diagnosis is mainly based on the development of motor symptoms. Apart from the motor symptoms, it also causes

neuropsychiatric disturbances in an individual's mood and behaviour. Approximately 78% of the people with Parkinson's develop severe dementia (Gomperts 2016). PD could be either familial or sporadic (Carr et al. 2003). Familial PD is usually caused by a mutation in a single gene, and sporadic PD is generally caused by a combination of genetic and environmental factors. Both familial and sporadic PD are known to cause cognitive impairment (Carr et al. 2003).

1.3.1.1 Neuropathology of PD

As stated earlier, PD prevalence increases with age and affects the population over 65 years of age (Storstein 2017). The most common cause of PD is the loss of dopaminergic neurons in the substantia nigra and the loss of dopamine neurons contributes towards cognitive decline in the CNS (Beitz 2014). The substantia nigra is a part of midbrain that plays a critical role in the motor system control of the basal ganglia and loss of pigmented neurons in this region is a hallmark of PD (Goetz 2011). According to a study, genetic variation accounts for approximately 25% of the PD cases (Day and Mullin 2021). Mutations in SNCA, LRRK2, PARK2, PARK7, PINK1 and VPS35 are involved with the pathogenesis of PD (Houlden and Singleton 2012). The association of environmental toxins and PD has been well debated. Some studies have drawn a strong association of pesticide exposure with PD (De Miranda et al. 2022).

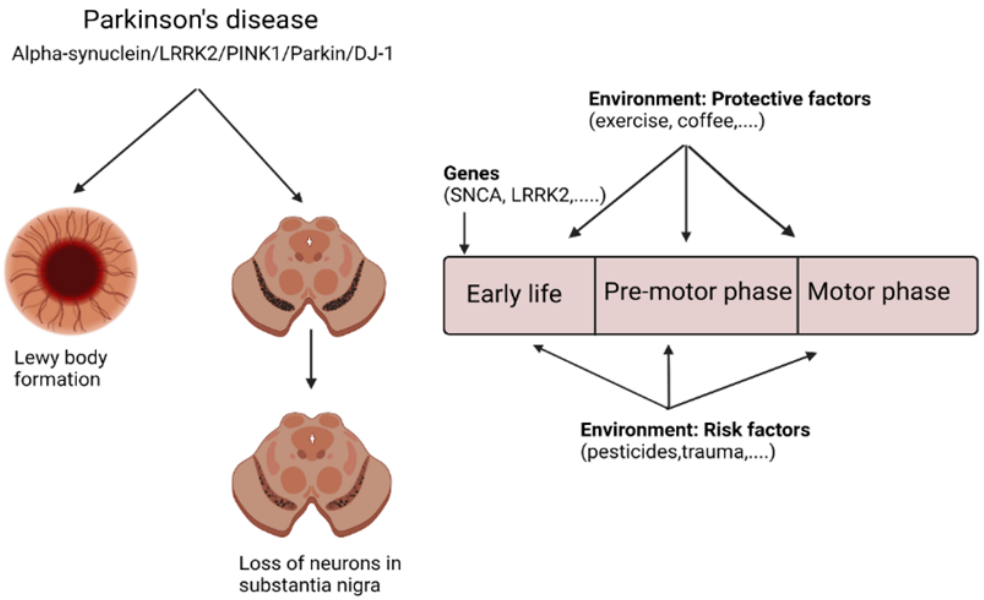

Figure 1.3: The interplay of genes, Lewy body formation and cell death in inherited PD. The recessive genes Parkin, PINK1 and DJ-1 contribute towards neuronal loss, whereas on the other hand, the dominant genes alpha-synuclein and LRRK2 play a role in both neuronal loss and Lewy body formation (Vlag, Havekes and Heckman 2020). This figure has been generated with BioRender.com.

PD pathology has been best described by Braak staging, which supports the Lewy body formation (Braak et al. 2003). It is divided into 6 stages, starting from the onset of non-motor symptoms to the development of motor symptoms. According to Braak staging, Lewy bodies are first visible in the olfactory bulb and medulla oblongata, with patients

displaying few non-motor symptoms. As the disease progresses, Lewy body formation occurs in the substantia nigra, leading to dopaminergic neuronal loss further (Braak et al. 2003). Apart from the alpha-synuclein misfolding, mitochondrial dysfunction, abnormalities in proteasomal pathways, and neuroinflammation also contribute to the pathology of PD (D. W. Dickson 2018).

The misfolding and aggregation of alpha-synuclein is also considered one of the key factors responsible for PD (Beitz 2014). The cause of cell death involves the presence of Lewy bodies, which are abnormal aggregates of various proteins like alpha-synuclein (Beitz 2014). Lewy bodies are intracytoplasmic inclusions that consist of a granular protein core and a halo consisting of fibrillar elements (Kouli, Torsney and Kuan 2018). Lewy bodies ubiquitously express a variety of proteins, including alpha-synuclein (Spillantini et al. 1997). Lewy bodies have also been found in patients displaying clinical PD (Hughes et al. 1992; Dhavale et al. 2024). Altogether, different formations of Lewy bodies provide different aspects towards disease progression, either acting as a toxic or a protective mechanism in PD (McNaught et al. 2002; Olanow et al. 2004). Thus, studying the interplay of aging, genetic, and environmental factors in PD would provide insight into the impairment of the biogenesis of different cellular processes that drives the progression of PD pathogenesis (Pang et al. 2019).

1.3.1.2 Parkinson's disease animal models

PD is a complex disorder in which the link between causes and disease progression is still unclear. Patient-derived data provide limitations for usage, and that is why animal models are used to study the pathogenesis of PD. PD disease models are divided into: neurotoxin models and genetic models (Blesa and Przedborski 2014). Neurotoxin models are models where chemicals are used to induce toxicity in the brain and for genetic models, mutated genes are used to induce PD phenotypes. The selection of the right animal model is very important, as the animal model should reproduce all the disease features of clinically diagnosed PD.

Some common examples of neurotoxin models would be 6-OHDA, MPTP, rotenone, and paraquat (Blesa and Przedborski 2014). 6-Hydroxydopamine, known as 6-OHDA, has a similar structure to dopamine, with the presence of an additional hydroxyl bond. This chemical compound could not cross the blood-brain barrier junction (Tieu 2011). Thus, 6-OHDA is stereo-tactically injected in a unilateral position to the substantia nigra (Blandini, Armentero and Martignoni 2008; Tieu 2011), medial forebrain bundle or striatum, leading to the degeneration of neurons within 12 hours to a maximum of 3 days (Faull and Laverty 1969; Jeon, V. Jackson-Lewis and Burke 1995). However, in this neurotoxic model, no production of clinical Lewy-body inclusion happens and thus replication of the PD model does not happen (Blesa and Przedborski 2014). 1-Methyl-4-phenyl-1,2,3,6-tetraydropyridine (MPTP) is another widely used neurotoxin in PD and the association of MPTP with PD as an environmental contaminant has already been established earlier (B L Goodwin 1998). In contrast to 6-OHDA, MPTP crosses the blood-brain barrier, making it more selective for dopaminergic neurons (Snow et al. 2000). The drawback of this model is the absence of Lewy body inclusion (Shimoji et al. 2005). Exposure to herbicides and pesticides, for example, paraquat and rotenone, respectively, also drives some features of PD (Blesa and Przedborski 2014). Rotenone, administered intraperitoneally, intravenously, or subcutaneously, reproduces all features

of PD, including pathologically visible alpha-synuclein deposition (T. B. Sherer et al. 2003). Like rotenone, paraquat also reproduces pathological features of PD (Manning-Bog et al. 2002). However, both these compounds offer high mortality rates in animal models and a slower loss of dopaminergic neurons (Manning-Bog et al. 2002; Alam, Mayerhofer and Schmidt 2004; Xiong et al. 2009).

Genetic models, on the other hand, provide better insight into the pathogenesis of the disease and could suggest the potential of understanding monogenic forms of PD in a better way (Bezard and Przedborski 2011). Alpha-synuclein (a-syn) was linked to dominant, familial PD and is the main component of Lewy body pathology, as described earlier. Transgenic mice expressing either mutated or wild-type human a-syn were generated using different promoters (Bezard and Przedborski 2011). A30P, A53T, and E46K have been commonly used to study the pathogenesis of PD, containing missense mutations (Zarranz et al. 2004; T. M. Dawson, H. S. Ko and V. L. Dawson 2010; Vekrellis et al. 2011). They also showed altered neuronal function with a-syn aggregation. Thus, these models are useful to study the relation between a-syn and the onset of PD. In addition to these models, a transgenic rat with a bacterial artificial chromosome (BAC) model carrying the full-length human SNCA gene was also identified, which reproduced the neuropathology of PD and the progressive loss of dopaminergic neurons (Nuber et al. 2013). Although mutations in the SNCA gene have been widely studied, other mutations in LRRK2, PINK-1, Parkin, DJ-1, and ATP13A2 have also been in focus (Bezard and Przedborski 2011). Thus, while choosing an animal model, the genetics of the species and the background of the reproducibility of the neuropathology should be taken into account.

1.3.1.3 Etiology: Understanding the gene-environment axis of PD

PD is caused by a combination of genetic and environmental factors and aging is considered as one of the important factors for PD (Storstein 2017). Epidemiological evidence has shown that aging is the primary cause of PD, with a higher incidence rate of 70 years for both men and women (Pang et al. 2019). Although there are theories to support aging with dopaminergic loss in PD, there is a lack of evidence for this, and additional genetic and environmental factors contribute towards the loss of dopaminergic neurons. Alpha-synuclein is considered to be playing a central role in Lewy body pathology, and thus is important for sporadic and genetic PD (Spillantini et al. 1997). Alpha-synuclein, encoded by the SNCA gene, aggregates into oligomers and fibrils, and adopts a cytotoxic state while accumulating in Lewy bodies. As described earlier, the post-translational modifications like phosphorylation, ubiquitination, truncation and nitration plays a crucial factor in a-syn aggregation process (Stefanis 2012), especially phosphorylation at serine 129 (Oueslati 2016; Ghanem et al. 2022). Other gene mutations with PD involves Parkin gene, which is responsible for causing early onset PD (Kitada et al. 1998). Mutations in PINK1/PARK7 are involved with autosomal recessive form of PD (Day and Mullin 2021). Mutations in Protein deglycase DJ-1 (PD protein 7) is thought to cause autosomal recessive, early onset PD (Bonifati et al. 2003). Altogether, Parkin, DJ-1 and PINK1 regulates the ubiquitin-proteasome system and plays an important role in maintaining the mitochondrial structure (Xiong et al. 2009). For sporadic PD, point mutations in leucine-rich repeat kinase 2 (LRRK2) is the common cause for autosomal dominant PD (J.-Q. Li, Tan and Yu 2014). The presence of LRRK2 leads to an increased kinase activity which interferes with the normal physiological functions (Day and Mullin 2021), and

LRRK2 kinase activity is increased in the brains of idiopathic PD patients who lack LRRK2 variants, thus providing a link between genetic and idiopathic forms of PD (Di Maio et al. 2018).

The discovery of 1-Methyl-4-phenyl-1,2,3,6-tetrahydropyridine (MPTP) shifted the focus of the causes of PD towards environmental toxins. The dopaminergic neurotoxicant MPTP converts to N-methyl-4-phenylpyridine (MPP+), crosses the blood-brain barrier and gains access to the dopaminergic neurons. Since its discovery, MPTP is known to mimic the toxic herbicides paraquat and rotenone (Meredith and Rademacher 2011) MPTP is known to induce neurotoxicity by increasing oxidative stress. Thus, environmental toxins similar to MPTP cause idiopathic PD (Javitch et al. 1985). In addition to genetic factors, exposure to pesticides and heavy metals, head trauma, and high dairy intake have been associated with an increasing risk of PD (Jason R. Cannon and Greenamyre 2013). There is a direct link between alpha synuclein and the deposition of pesticides. It has been concluded that exposure to pesticides accelerates the rate of alpha synuclein formation (Manning-Bog et al. 2002). Mitochondrial complex I inhibition has been associated with rotenone, causing degeneration of the dopamine region in the brain, thus leading to PD (Todd B. Sherer et al. 2003).

1.3.1.4 Alpha-synuclein in PD

A-syn is a protein encoded by the SNCA gene and is associated with the neuropathology of PD (Stefanis 2012). Its importance was described when it was found to be a component of Lewy body pathology (Spillantini et al. 1997). A-syn (14 kDa) is a small protein that is present in the central and peripheral nervous system (Burre, Sharma and Sudhof 2018). It regulates synaptic vesicle trafficking and is also known to promote SNARE (Soluble NSF Attachment Protein Receptor) complex assembly (Yoo, Shin and N. K. Lee 2023). A-syn could either exist in a monomer form or a tetramer form, and an imbalance between these forms could potentially give rise to aggregated forms of a-syn (Bartels and Leenders 2010; Calabresi et al. 2023). A-syn is usually characterized by three modules, the N-terminal region, the hydrophobic NAC region which is prone to aggregation and the C-terminal region (Burre, Sharma and Sudhof 2018). Being an intrinsically disorder protein, it can undergo oligomerization processes under pathological conditions, leading to the formation of beta-sheet structured aggregates (Villar-Pique, Lopes da Fonseca and Outeiro 2016). A-syn oligomers are neurotoxic in nature. They could produce a higher ER stress, resulting in mitochondrial dysfunction (Du, Xie and R. T. Liu 2020).

The abnormal accumulation of a-syn aggregates in neurons is a hallmark of alpha-synucleinopathies, which might be indicative of dopaminergic neuronal loss (Kshirsagar et al. 2021). Also, the ability of a-syn to form β-sheet structure under pathological conditions is important for understanding the pathogenesis of PD (Stefanis 2012). Apart from in-vivo experimental studies, in-vitro studies shows that a-syn oligomers form aggregates inside the cell body, leading to secondary processes called neurodegeneration (Rosencrans et al. 2021). A-syn under certain conditions may undergo modifications like phosphorylation, oxidation, nitrosylation, glycation, or glycosylation, and amongst all modifications, the frequently studied one is phosphorylation, which has clinical relevance and has been found in Lewy body pathology (Stefanis 2012). Serine 87 and Serine 129 are the major phosphorylated sites of a-syn (Okochi et al. 2000; Fujiwara et al. 2002). High degree of

phosphorylated and aggregated a-syn is visible in post-mortem brains of PD patients, and is also present in Lewy body dementia (Anderson et al. 2006; Y. Wang et al. 2012). 90% of PD patients have a-syn phosphorylated in serine 129, and it is one of the dominant pathological conditions visible in Lewy body disease (Anderson et al. 2006; Arawaka et al. 2017). This post-translational modification is initiated on a-syn aggregation and has a negative impact on neuronal function (Ghanem et al. 2022). Phosphorylation at serine 129 is indeed interesting to study, as it plays a lot of physiological roles including regulation of a-syn turnover, inhibiting a-syn membrane binding, stress-induced synaptic plasticity, enhancement of dopamine uptake, modulating a-syn protein-protein interaction, and regulating a-syn nuclear localization (Burre, Sharma, Tsetsenis et al. 2010; Machiya et al. 2010; Pfefferkorn, Jiang and J. C. Lee 2012; Goncalves and Outeiro 2013; Snead and Eliezer 2014; Oueslati 2016). Antibodies specific to phosphorylated a-syn have been widely used as a marker to evaluate the relationship between pathology, disease severity and subsequently cell loss (Ghanem et al. 2022).

1.3.1.5 Elucidating the role of neuroinflammation in PD

Neuroinflammation is a term coined for the inflammation happening in the CNS. Although the etiology of the disease is unknown, neuroinflammation is one of the major factors that lead to the progression of the disease, leading to dopaminergic neuronal loss (Kaur et al. 2017). Parkinson's disease, a disease of the motoric system, usually starts with the dysfunction in the non-motor system in the prodromal phase and an increase of inflammation during this phase leads to the development of PD pathogenesis (Tansey et al. 2022). Inflammation is mediated by the production of cytokines and other chemical messengers. These are generally produced by the glial cells (Valenzuela-Arzeta et al. 2023). In PD, the dysfunction of blood-brain barrier (BBB) plays an important role in the degeneration of dopamine neurons. The neuroinflammatory response of PD is usually regulated by microglial activation and secretion of proinflammatory factors (T. W. Liu, C. M. Chen and Chang 2022). Microglial activation by various stimuli, changes its morphology from a resting state to a neurotoxic and a neuroprotective state (Kreutzberg 1996). On the one hand, the neurotoxic state enhances pro-inflammatory factors and promotes ROS production and dopaminergic neuron death. The neuroprotective state, on the other hand, regulates therapeutic characteristics by inhibiting inflammation and reducing dopaminergic neuron death (Rasheed et al. 2021). The activation of pro-inflammatory state in microglia is regulated by NOD-, LRR- and pyrin domain-containing protein 3 (NLRP3) inflammasome signaling (Tansey et al. 2022). In PD, a-syn triggers NLRP3 inflammasome in microglia, which leads to degradation of a-syn later on (Scheiblich et al. 2021). Inflammation also leads to increased oxidative stress, which plays a major role in the loss of dopaminergic neurons in the brain of PD patients (Dias, Junn and Mouradian 2013). In-vivo animal models have also demonstrated the loss of mitochondrial function upon inflammation (Hunter et al. 2007). Thus, a combination of inflammation, oxidative stress and mitochondrial dysfunction provide a cycle leading to the activation of microglia with the loss of dopaminergic neurons.

Neuroinflammation in PD is not confined to the innate immune system; rather, some populations of T-cells also contribute towards PD disease progression (Sommer et al. 2018). Studies on PD patient brains revealed the presence of a higher number of CD8+ T-cells, and a decrease in CD4+ T-cells (Saunders et al. 2012; Galiano-Landeira et al. 2020; Grotemeyer et al. 2022). Alterations in the B-cell and T-cell population under PD

pathology point towards a polarizing effect of adaptive immune cells, similar to the microglial polarization (DeMaio et al. 2022; R. Li et al. 2022). Some studies are even indicative of PD being an autoimmune disease, since autoreactive T-cells are activated in response to a-syn pathology (Sulzer et al. 2017). A lot of factors, like head injury, stress, and aging, could contribute to neuroinflammation. Inflammation in PD includes both the central and peripheral nervous systems, as changes in gut microbiome also generate inflammatory factors in the periphery, leading to an enhanced activation of cytokines and a-syn aggregation (Pajares et al. 2020). As inflammation is one of the major hallmarks of the disease pathology, targeting inflammatory pathways as a therapeutic approach to prevent the pathogenesis of PD would be beneficial (R. Kim et al. 2018; Pajares et al. 2020).

1.3.1.6 Mitochondrial dysfunction in PD

Mitochondrial dysfunction plays an important role in the pathogenesis of PD and complex I deficiency is the primary cause for the degeneration of neurons in PD (Moon and Paek 2015). The investigation of complex I deficiency in PD started after the discovery of 1-Methyl-4-phenyl-1,2,3,6-tetrahydropyridine (MPTP) compound. As stated earlier, MPTP crosses the blood-brain barrier and converts to MPP+ and is taken up selectively by the dopaminergic neurons, where it inhibits complex I, thereby decreasing ATP production and increasing reactive oxygen species (ROS) production, further altering mitochondrial proteins leading to consequences in the dopaminergic system (Moon and Paek 2015). Structural changes in complex I also results in a loss of apoptosis (Bose and Beal 2019). After this discovery, analysis of the brains of sporadic PD patients revealed deficits in several brain regions like substantia nigra and frontal cortex [reviewed in (Hauser and Hastings 2013)]. Apart from complex I, a decrease in the function of complex III and IV have also been reported in PD patients [reviewed in (Keane et al. 2011)]. On several occasions, mitochondria also undergo oxidative stress, which is damage caused to the cells and tissues, leading to ROS production, ultimately leading to cell death (S. Li et al. 2025). Brain samples of PD have been reported to have oxidative stress markers (Floor and Wetzel 1998). Thus, mitochondrial metabolic pathways provide measures to protect mitochondria from molecular damage.

Loss-of-function mutations in genes like Parkin, PTEN-induced putative kinase 1 (PINK1) and Protein deglycase (DJ-1) impairs mitochondrial quality control and leads to autosomal recessive form of PD (Hao, Giasson and Bonini 2010). Parkin is an E3 ubiquitin ligase and PINK1 and Parkin interact genetically to control mitochondrial quality, however the role of these two genes in mitophagy remains largely unknown. Parkin recruitment to mitochondria is regulated by PINK1 expression and mutations in PINK1/Parkin impair mitochondrial trafficking and the defective mitochondria could be cleared by autophagy (Deas, Wood and Plun-Favreau 2011). Cells lacks DJ-1 caused enhanced ROS production, leading to impairment of mitochondrial fusion (McCoy and Cookson 2011). These observations suggest that failure of the autophagic pathway leads to mitochondrial dysfunction and contributes to the pathogenesis of PD.

1.3.1.7 Epigenetic mechanisms underlying PD

Neuroinflammation causes dopaminergic neuron loss, triggering subsequent epigenetic modifications (Rasheed et al. 2021). Upon activation of neurotoxic microglia, inflammatory

factors and reactive oxygen species are produced, causing neuronal death. On the other hand, neuroprotective microglia inhibit neuroinflammation and produce anti-inflammatory factors (Rasheed et al. 2021). Neuroinflammation in PD is associated with various epigenetic modifications such as DNA/RNA methylation and histone acetylation. Histone 3 lysine 27 (H3K27) methylation is involved in regulating the M1 phase of microglia (Rasheed et al. 2021). Histone modifications like H3K27 acetylation and H3K27 methylation play opposing roles to each other. For PD patients, there is a higher level of histone acetylation in the dopaminergic neurons (Labbé, Lorenzo-Betancor and Ross 2016). DNA methylation is the most common epigenetic modification that is studied in pathological diseases (Miranda-Morales et al. 2017). Methylation in the SNCA gene is associated with the recruitment of various transcriptional factors in the vicinity of the CpG island, and is associated with an increased onset of PD (Wüllner et al. 2016). DNA methylation regulates the expression of inflammatory factors like TNF-α and thus modulates the phenotype of microglia (Rasheed et al. 2021). MicroRNAs (miRNAs) are a group of small non-coding RNAs that bind to the 3' untranslated region (3'UTR) of mRNAs, mediating post-transcriptional regulation. Dysregulation of microRNA is also associated with PD pathogenesis (Nies et al. 2021). These alterations in epigenetic profiles detected in different tissues could provide a path for epigenetic modulators that may be useful for PD therapeutics in the future (Song et al. 2023).

1.3.2 Huntington's disease (HD)

HD is another autosomal dominant inherited disease of the CNS, which is usually caused by a mutation in the huntingtin gene (Bates et al. 2015). This disease is usually inherited from generation to generation. Expansion of cytosine-adenine-guanine (CAG) repeats (trinucleotide repeat expansion) results in the mutation of the huntingtin gene, producing an abnormal mutated protein mHtt, leading to cell death in the brain (Bates et al. 2015). The onset of the disease depends on the length of the CAG repeat (Roos 2010). Motor, cognitive and psychiatric symptoms have been displayed by HD patients. The onset of the disease ranges between 30 and 50 years. Motor changes are usually involuntary and affects the daily routine of the person. The involuntary movements are called chorea (Roos 2010). Later, instability in walking, abnormalities in facial expression, difficulties in eating and speaking, sleeping problems, and weight loss are also associated with HD (Dickey and La Spada 2018).

1.3.2.1 Neuropathology of HD

HD is an autosomal dominant ND, which is mostly inherited through generations. It is caused by the gene HTT, located on the short arm of chromosome 4. Mutation of HTT leads to the expansion of CAG repeat, which enlarges the polyQ chain located on the N-terminus in HD patients (Macdonald 1993). This expansion of CAG repeat is responsible for causing either gain-of-function or loss-of-function of wild-type HTT (Cattaneo et al. 2001; W.-J. Huang, W.-W. Chen and Xia Zhang 2016; Duyao et al. 1993). A longer repeat of CAG leads to earlier onset of the disease and progression of the disease is faster (Walker 2007). The extended CAG stretch leads to the enlargement of the polyglutamine (polyQ) region within the HTT protein, which leads to misfolding of the proteins in the neurons (Rubinsztein and Carmichael 2003). This disrupts the normal physiological functions like mitochondrial respiration, transcription, and protein biogenesis (Imarisio et al. 2008).

The common pathology of this disease is the formation of intracellular aggregates in the affected neurons and death of neurons in the striatum (Rubinsztein and Carmichael 2003).

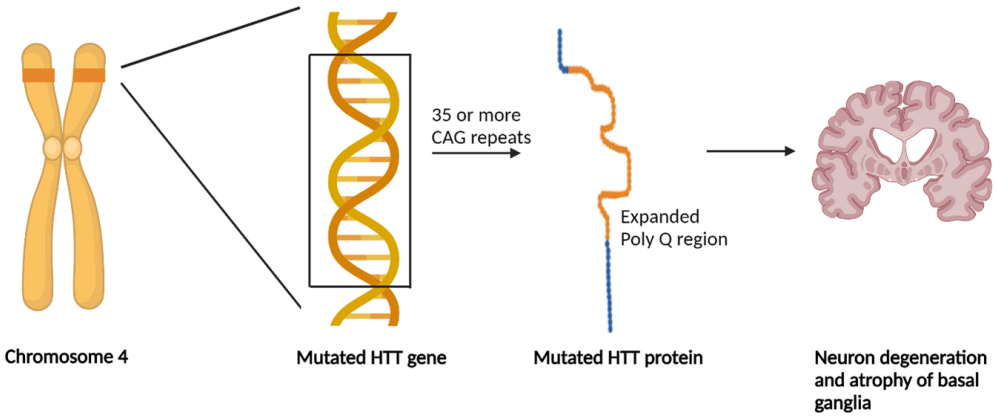

Figure 1.4: The correlation of CAG repeat and poly Q expansion in HD pathology. The trinucleotide repeat expansion is the primary cause of the pathogenesis of HD, leading to the expanded polyQ region and ultimately causing atrophy of the basal ganglia. This figure has been generated with BioRender.com.

Mutations in HTT cause disruptions in intracellular activities like mitochondrial dysfunction, protein degradation, and aberrations in transcription, ultimately leading to neuronal death (Valor 2015). Post-translational modifications like phosphorylation, SUMOlytion and acetylation could be altered by the mutation in HTT gene and could play an important part in the pathogenesis of HD (Ehrnhoefer, Sutton and Hayden 2011).

1.3.2.2 Huntington's disease animal models

HD is a disease with a trinucleotide repeat expansion (CAG) in exon 1 of the htt gene, leading to an abnormally long polyglutamine chain with the production of mhtt protein (Ramaswamy, McBride and Kordower 2007). Apart from the involuntary movement of the body, severe cognitive decline also happens in HD. Thus, animal models are used to study the disease pathogenesis and the associated changes in brain function. Animal models could be either genetic or non-genetic in the case of HD. Two key compounds, namely Quinolinic acid and Kainic acid, are used to induce cell death in animal models of HD. The cell death mechanism follows with the destruction of the mitochondrial complex (Ramaswamy, McBride and Kordower 2007).

Alternatively, genetic models provide a better insight into the disease onset and progression of HD. The most common mouse model is the R6/2 mouse model, that contain exon 1 of the human htt gene with 150 CAG repeats (Mangiarini et al. 1996). The R6/2 shows a robust pathological response to HD and also shows behavioural abnormalities from 5 weeks of age (Mangiarini et al. 1996; Kaye, Reisine and Finkbeiner 2021). The pathological expression at the age of 2-3 weeks clinically resembles the early signs of HD; however, since it has only exon 1, it limits the exploration of the involvement of other exons in HD pathogenesis (Mangiarini et al. 1996). A reduction in both brain weight and volume was reported in R6/2 mice, when compared with the wild-type controls (Davies et al. 1997). In contrast to R6/2 mice, other models exhibit higher expression levels of

the htt gene (Hodgson et al. 1999). There are studies conducted using knock-in mouse models of HD, where the CAG repeat expansion is present in the mouse genome and the endogenous mouse promoter regulates the expression of the mutant huntingtin (Menalled and Chesselet 2002). Transgenic mouse models containing YAC and BAC (Yeast Artificial Chromosome and Bacterial Artificial Chromosome) expressing full-length human htt protein have also been used in several studies (Farshim and Bates 2018). YAC transgenic mice with mhtt having 128 glutamines were successfully used for targeting therapeutics of HD (EJ et al. 2003), which displayed a progressive decline in cognition and motoric abilities (Menalled and Chesselet 2002; Van Raamsdonk et al. 2005). Other than these models, transgenic rat models have also contributed towards the understanding of the molecular pathogenesis of HD. A rat model with bacterial artificial chromosome (BAC) carrying full-length mhtt protein that replicates the disease pathogenesis to some extent (Yu-Taeger et al. 2012). The BAC HD rats displayed an early onset of motor deficits, reduced food intake, and displayed a higher number of huntingtin aggregates at the age of 12 months (Yu-Taeger et al. 2012). Since the identification of disease pathogenesis, a lot of genetic models have been developed to represent disease pathology and to identify the outcome of therapeutic strategies. One of the examples of therapeutics would be that of R6/2 mice, where higher doses of coenzyme Q10 improved motor deficiency and survival of the mice (Smith et al. 2006).

1.3.2.3 Etiology: Understanding the gene-environment axis of HD

HD is an autosomal dominant inherited disease, in which one copy of an expanded trinucleotide repeat of the gene is inherited by the next generation (Bates et al. 2015). It is caused by the htt gene, also known as IT15 gene (Schilling et al. 1995). The Htt gene is located on the short arm of chromosome 4 at 4p16.3 (Reiner, Dragatsis and Dietrich 2011). Htt containing a sequence of three DNA bases – cytosine-adenine-guanine (CAG) forms the trinucleotide repeat sequence, coding for the amino acid glutamine. So, the trinucleotide repeat forms a chain of glutamine known as the polyglutamine tract (polyQ) (Katsuno et al. 2008). If 36 or more glutamines are present, the protein alters its form to a mutant huntingtin form and leads to neuronal loss. Thus, HD pathogenesis is related to the number of CAG repeats present (Walker 2007). Juvenile HD usually occurs when the repeat counts are very large and it affects individuals around 20 years of age (Squitieri et al. 2005). Usually, paternal transmission is the most common modifier of HD. Other genetic modifiers, like the size of the CAG repeat and HD haplotypes, also contribute to CAG instability in HD. Glutamate receptor ionotropic kainate2, known as GLUR6 was the earliest genetic modifier that was reported in HD, containing a polymorphic TAA trinucleotide repeat in its 3' untranslated region (3' UTR) in early HD (SC et al. 2009; Reiner, Dragatsis and Dietrich 2011). Other polymorphisms like huntingtin-associated protein 1 (HAP1) and autophagy-related 7 homolog (Atg7) have also played a role in the onset of HD (Reiner, Dragatsis and Dietrich 2011). Post-translational modifications of HTT also play an important role in the pathogenesis of HD. HTT is usually prone to modifications by phosphorylation, SUMOylation, acetylation, and palmitoylation, and these modifications can be altered by mutations in the HTT gene and polyQ addition (Ehrnhoefer, Sutton and Hayden 2011).

Although HD is mainly genetic, environmental factors also contribute to the pathogenesis of this disease (Mo, Hannan and Renoir 2015). Maintaining a healthy and balanced diet and exercising regularly have boosted cognition, whereas high-stress levels and obesity

could contribute as potential modulators of HD (E. Dickson et al. 2022). These environmental modulators could affect protein interactions and other intracellular processes involving synaptic signal processing (Mo, Hannan and Renoir 2015).

Environmental enrichment studies have been conducted on rats that increased sensory stimulation and physical activity and improved synaptic and cognitive function, alleviating HD (Clifford et al. 2002). Increased physical activity has been beneficial for cardiovascular, immune, and metabolic systems. The R6/2 mouse model studies of HD have implicated that with chronic exercise, there is an improvement in the synaptic activity in the striatum (Cepeda et al. 2010). HD patients have undergone treatments with different motor rehabilitation exercises that improved their cognitive function and physical quality of life (Dawes et al. 2015; Novati, Nguyen and Schulze-Hentrich 2022). Similar to exercise, less stress delays the onset of progression of HD. Studies showed that HD patients display a higher level of stress scores compared to normal individuals [reviewed in (Mo, Hannan and Renoir 2015)]. Diet has played an important role in modulating HD. Diets with a high content of essential fatty acids slow disease progression (Clifford et al. 2002). It has been concluded that intermittent fasting improves blood glucose regulation, thus increasing the effects of neuroprotection (Duan et al. 2003). Higher dairy consumption has also been related to disease progression (Mo, Hannan and Renoir 2015).

1.3.2.4 Huntingtin in HD

Huntingtin is the protein coded by the Htt gene, a 348 kDa protein well conserved among vertebrates (Saudou and Humbert 2016). It forms a helical solenoid structure containing HEAT (Huntingtin, Elongation factor 3, PR65/A subunit of protein phosphatase 2A, and the lipid kinase TOR) (W. Li et al. 2006). The N-terminal region is the most studied one, as it contains the extended polyQ stretch (Saudou and Humbert 2016). It starts at amino acid 18 of Htt and is followed by a proline-rich domain (Schulte and Littleton 2011). It forms an alpha-helical structure and is important for vesicular trafficking (Atwal et al. 2007). This region functions as a nuclear export signal and is exposed towards posttranslational modifications like phosphorylation at serines 13 and 16, acetylation, sumoylation and ubiquitination at lysines 6, 9 and 15 (Atwal et al. 2007; Thompson et al. 2009; Steffan 2010; T. Maiuri and Truant 2013). An important step in the regulation of HD pathogenesis are the cleavage of full-length Htt protein releasing N-terminal (containing polyQ stretch) and C-terminal fragments, and these polyQ fragments have been visibly reported in HD patient brains too (Mende-Mueller et al. 2001; El-Daher et al. 2015). Huntingtin cleavage have been facilitated by caspases and calpains group of proteases (Y. J. Kim et al. 2001; Gafni and Ellerby 2002). The Htt gene that is widely expressed contains 67 exons and the CAG expansion happens in the first exon of the Htt gene (Elena-Real et al. 2023). It consists of two mRNA transcripts 10.3 kb and 13.7 kb (Lin et al. 1993; Saudou and Humbert 2016).

The hallmark of HD pathogenesis is the formation of insoluble Htt aggregates in the brain of HD patients (Wanker 2000). The aggregates were present as inclusion-like bodies in the nucleus (Roizin et al. 1974). R6/2 mice displayed a stronger aggregation pattern of Htt with Htt present as either round-shaped, fibrillar or granular (Davies et al. 1997). The localization of Htt aggregates were not confined to the nucleus only, but also to cytoplasm, dendrites, axons and synapses (Gutekunst et al. 1999). Neuropathologically,

the Htt aggregates observed in rodent models represent the HD aggregates present in patient brains (DiFiglia et al. 1997). BAC HD rats displayed nuclear accumulation of Htt more in the amygdala and cortex region of the brain and a higher number of aggregates could be seen with higher age (Yu-Taeger et al. 2012). EM48 immunohistochemistry stainings have been carried out to observe N-terminal aggregates of Htt in rodent brains (H. Li et al. 2001).

1.3.2.5 Elucidating the role of neuroinflammation in HD

Astrocytes and microglia play a pivotal role in neuroinflammation and HD pathogenesis (Palpagama et al. 2019), and accumulation of reactive microglia had been found in the brains of HD patients (Tai et al. 2007). Upon activation, microglia releases pro-inflammtory cytokines and causes inflammation in the CNS (Palpagama et al. 2019). Activation of microglia has also been linked to the accumulation of mHtt in the neurons, thus contributing towards HD pathology (Jansen et al. 2017). A number of different signalling pathways are activated in response to microglial activation, such as the NF- κB pathway, which plays a critical role in inflammation (Palpagama et al. 2019). mHTT gets accumulated in the microglia, which causes an increased infiltration of the inflammatory cytokines in the brain, leading to inflammation and tissue damage (Palpagama et al. 2019). Further, it has been postulated that microglia activation occurs at an earlier stage of HD, even before the initial symptoms appear in HD (Tai et al. 2007), and thus sheds more light on the development of the disease at later stages. HD disease patients showed an increase in the levels of IL-6 at a very early stage of diagnosis (Björkqvist et al. 2008). Cerebrospinal fluid from HD patients shows the upregulation of pro-inflammatory factors like IL-6, IL-8, and TNF-α (tumor necrosis factor). Also, the presence of mHtt has been linked to oxidative stress in HD. All these factors indicate that the expression of mHtt produces cell-autonomous pro-inflammatory activation of microglia leading to neuronal degeneration (Crotti and Glass 2015).

1.3.2.6 Epigenetic mechanisms underlying HD

Transcriptional dysregulation plays an important role in HD pathogenesis (Seredenina and Luthi-Carter 2012). Alteration in the DNA methylation in the promoter region of neuronal genes has been reported in HD patients, which regulates the expression of mHTT (Ng et al. 2013). Changes in DNA methylation also alters transcriptional levels and is associated with post-transcriptional histone modifications (J. Lee et al. 2013). Changes in H3K9ac, H3K27ac, H3K4me3, H3K9me3 and H3K27me3 have been identified in HD patients (Hyeon, A. H. Kim and Yano 2021). The role of histone acetylation has gained a lot of attention during recent years, and was found to be altered in HD (Steffan et al. 2001; Francelle et al. 2017). Alterations in the activity of microRNAs can affect gene expression level. Reports of dysregulation of microRNAs in HD are common and are used as a marker for diagnosis of the disease (Dong and Cong 2021).

1.3.2.7 Microglia contributing to the pathology of PD and HD

Detailed insights into the role of microglia revealed its importance in ND like Alzheimer's, Parkinson's and Huntington's diseases. As described earlier (in section 1.3.1.5), the connection between microglia and neuroinflammation has already been established in

PD. Chronic inflammation also leads to neuronal death and that causes further release of cytokines (Kannarkat, Boss and Tansey 2013). Neuronal death induces inflammation by releasing apoptotic factors in the CNS. The dopaminergic neurons are sensitive to the changes in the CNS and release of cytokines like TNF-α and IFN-γ (Kannarkat, Boss and Tansey 2013). Increased levels of cytokines like TNF-α, IFN-γ, IL-6 and IL-1β have been associated with the activation of innate immune cells. The release of IL-1β from microglia is associated with the dopaminergic neuronal loss (Long-Smith, Sullivan and Nolan 2009).

On one hand, dopaminergic neurons are more prone to inflammation in PD, on the other hand, there is an evidence for the activation of microglia occurring at an earlier stage. In section 1.3.2.5, neuroinflammation in HD is mainly mediated by the microglia (Palpagama et al. 2019). Cytokines like IL-4 and IL-10 are mainly released at the later stages of the disease (Palpagama et al. 2019). The protein mutant huntingtin is also expressed in microglia and thus may be the reason for causing inflammation in the CNS (Ellrichmann et al. 2013). Other than microglia, reactive astrocytes also play an important role in the pathogenesis of HD (Palpagama et al. 2019). Over-active microglia is seen as the hallmark of HD, whereas suppressing the release of inflammatory cytokines resulted in alleviating the disease (Yang et al. 2017).

1.4 Stimulating the immune responses

1.4.1 How lipopolysaccharide (LPS) is involved in shaping immune responses

Bacterial lipopolysaccharide (LPS) is an endotoxin, belonging to the Gram-negative bacteria group. It is recognized by Toll-like receptor 4 (TLR4) and serves as an important stimulus for inducing inflammation in the CNS (Zhao et al. 2019). Upon stimulating the neuronal cells, it releases a vast number of cytokines and could act as a potential immune modulator for the CNS. Peripheral stimulation of the LPS can drive brain pathology. It crosses the BBB, releasing components in both blood and brain and thus activating microglia and causing neuroinflammation (Guy C. Brown 2019). The effect of LPS on innate immune cells is usually dependent on the dosage of administration. Immune tolerance is characterized by the prolonged exposure of LPS of innate immune cells and in this way, LPS stands as one of the best examples in inducing immune memory by peripheral stimulation (Hamon and Quintin 2016). Further, microglia change their states like M1 and M2 depending on the strength and duration of LPS (M. C. Morris, Gilliam and L. Li 2014). For AD, it was reported that on induction of different doses of LPS, microglia switched between their states, and this helped the researchers to identify the pathology of AD better (Wendeln et al. 2018).

1.4.2 The role of High-fat diet (HFD) in inducing peripheral immune memory

Unhealthy lifestyle, unbalanced diets, lack of sleep, and less exercise are potential triggers of inflammation (E. Kip and L. C. Parr-Brownlie 2023). Environmental triggers, such as a

high-fat diet (HFD), food enriched with a higher content of fatty acids, cause peripheral immune training, leading to long-lasting alterations in immune responses (Christ et al. 2018). The HFD contains excess saturated fatty acids that affect the energy and metabolism of an individual, triggering neuroinflammation. Consumption of these fatty-rich diets can alter the gut microbiome, affecting the gut-brain axis (Butler 2021). In addition to responding to peripheral stimulation, microglial phenotype can be altered by HFD. Earlier research has confirmed that HFD has the capacity to activate TLR4, similarly as that of LPS and in turn, enhances the recruitment of innate immune cells by microglia. A diet-induced inflammatory response activates the microglia and increases the production of the pro-inflammatory cytokines in the CNS (Butler 2021). Introducing HFD to the diet also leads to epigenetic reprogramming of the microglia. Sequencing analyses of disease-associated models have reported certain epigenetic changes associated with HFD feeding and long-term transcriptomic reprogramming, and thus HFD could induce an 'immune memory' in the myeloid cells similar to LPS (Christ et al. 2018).

1.4.3 LPS and HFD-induced inflammation in PD and HD models

In PD animal models, induction of LPS leads to the death of dopamine neurons in the substantia nigra, which further leads to the increase of cytokine level (M. Liu and Bing 2011) associated with mitochondrial dysfunction. LPS induction also stimulates reactive oxygen species (ROS) and nitric oxide synthase (iNOS) production in excess, which is harmful to the body (Batista et al. 2019). In comparison to PD, studies on the impact of LPS on HD are rare; however, reports of microglial alterations induced by LPS have been described. Repeated dosage of LPS delayed the progression of HD in R6/2 mice (S. W. Lee et al. 2018).

On the contrary, HFD based experiments and its effect on the immune memory have not been extensively studied. In PD, HFD-induced obesity affects motor function, leading to cognitive decline (Jang et al. 2017). It increases the release of neurotoxins in the brain and also depletes dopamine neurons in the substantia nigra. An increase in the number of saturated fatty acids has been associated with the risk of developing PD (Hantikainen et al. 2022). Similar to PD, HFD also acts as a potential trigger for the pathology of HD, as studies have reported the accumulation of polyunsaturated fatty acids in the brains of HD patients (Block et al. 2010). Thus, HD is characterized by impaired insulin secretion and excessive weight loss. On the contrary, some studies have shown fatty diet as a beneficial factor for HD (Ruskin et al. 2011).

1.4.4 LPS and HFD-induced pathological response in PD and HD models

It has been often reported that peripheral stimulation of immune cells with an endotoxin like LPS promotes misfolded protein aggregation in the brain, contributing to ND (G. C. Brown, Camacho and Williams-Gray 2023). For the Alzheimer's mouse model, one dose of LPS increased the deposition of amyloid beta plaques in the brain, while repeated doses of LPS alleviated this effect (Wendeln et al. 2018). Histopathological stainings revealed LPS-induced microglial activation in the postmortem brains of PD patients (Halliday

and Stevens 2011). In a A53T PD mouse model, delayed degeneration of dopaminergic neurons was observed after moderate doses of LPS injections (Gao et al. 2011). After 5 months of LPS injections, an increase in accumulation of a-syn could be observed in the brain. BAC a-syn rats also display strong pathological aggregation in the brain with an early microglial activation (Krashia et al. 2019). On the contrary, studies of pathological changes with LPS in HD disease models are not that common. Repeated doses of LPS leading to immune activation can alleviate HD pathology (S. W. Lee et al. 2018).

A30P mice displaying human-like PD symptoms were exposed to HFD for 4 months, and pathological aggregation of phosphorylated a-syn could be visible in the mice brains (Kahle et al. 2001; Rotermund et al. 2014). While comparing with the control mice, no Lewy-body pathology could be observed as was in the case for HFD-fed mice. HFD consumption has led to pre-mature a-syn pathology in A30P mice brains (Rotermund et al. 2014). HFD has also led to the loss of dopaminergic neurons in C57BL/6 mice, one of the pathological hallmarks of PD (Bousquet et al. 2012). In other animal models of PD, it has been seen that the consumption of fatty foods for a long time resulted in the depletion of glial cells in the brain (Chou et al. 2022). Ketogenic diets rich in high-fat foods have shown a neuroprotective effect on the R6/2 HD mice model and have led to the improvement in motoric functions (Ruskin et al. 2011). Essential fatty acids have been shown to protect motor deficits in R6/1 mice (Clifford et al. 2002). BACHD mouse model was subjected to a ketogenic diet for three months, which improved their motor skills and delayed the disease progression subsequently (Whittaker et al. 2022).

1.5 Epigenetic reprogramming in health and disease

Epigenetic reprogramming is a process that does not alter the DNA sequence but will remodel the epigenetic marks (F. Santos and Dean 2004; Tang and Ho 2007). This reprogramming involves DNA methylations, histone modifications and regulation of non-coding RNA (Tang and Ho 2007). A lot of factors affect epigenetic reprogramming like dietary factors (HFD), high dairy intake, heavy metals and pesticides (Tang and Ho 2007). Epigenetic changes are associated with the activation of the innate immune cells (M. Huang et al. 2023). Inhibition of certain epigenetic pathways could act as a beneficial target for treatment (Dominguez-Andres and Netea 2019). Subsequent changes in the gene transcriptional level happens once the microglia is 'primed'. Increased transcription of inflammatory genes was seen with immune training, whereas tolerance display reduced transcriptional levels (Xiaoming Zhang et al. 2021).

Trained immunity has the ability to produce a stronger transcriptional response when stimulated, as shown in Figure 1.5. Innate immune memory is associated with epigenetic reprogramming at the level of chromatin organization. When stimulated, the innate immune cells develop an 'epigenetic scar', causing long-term changes at the gene level. Further, with acute stimulation of the innate immune cells, enhanced cytokine production happens, accompanied by the unfolding of chromatin and enhanced gene expression. Epigenetic marks accompanying trained immunity are histone 3 lysine 27 acetylation (H3K27ac), histone 3 lysine 4 methylation (H3K4me1) and histone 3 lysine 4 trimethylation (H3K4me3) (Netea, Dominguez-Andres et al. 2020). Studies have also reported that DNA methylation patterns discriminate between cells undergoing trained immunity and cells

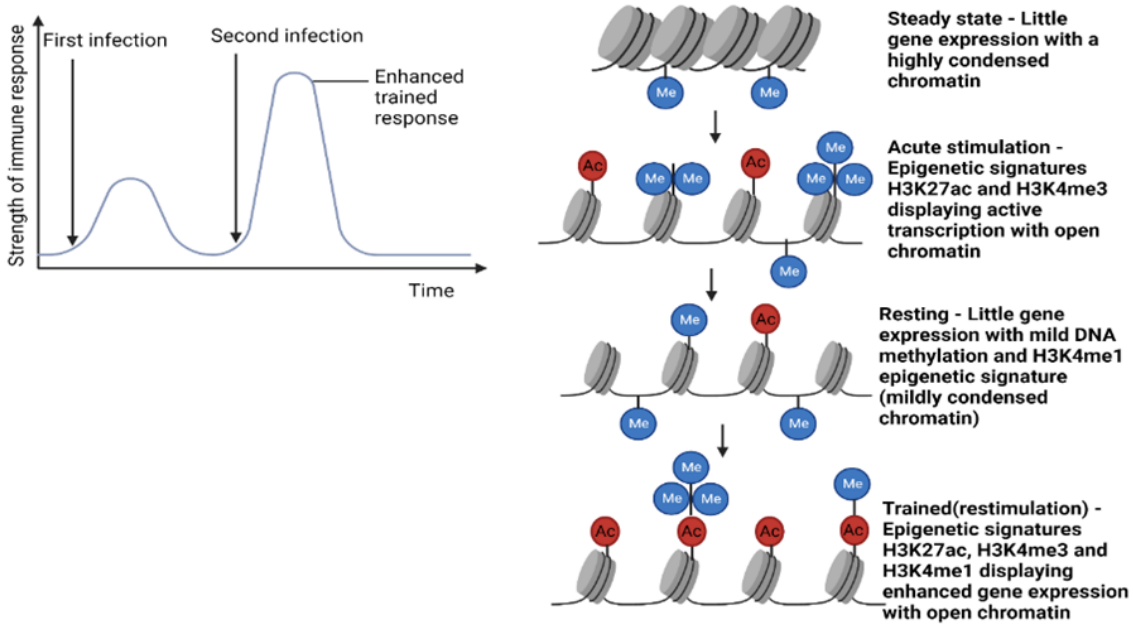

Figure 1.5: Epigenetic modifications in innate immune cells.
Induction of trained immunity is accompanied by epigenetic reprogramming of the innate immune cells. When the chromatin is in an unstimulated or steady state, there are different chromatin marks and lower gene expression. Upon initial stimulation, chromatin acquires an open state, assisted by the deposition of chromatin marks and a higher expression of genes. Enhanced recruitment of gene expression occurs after the second stimulus (Netea, Dominguez-Andres et al. 2020). This figure has been generated by BioRender.com.

that are not. Example has been cited for the Bacillus Calmette–Guérin (BCG) vaccine against tuberculosis. There was a loss of DNA methylation in patients undergoing trained immunity after vaccination (Verma et al. 2017). Thus, inhibiting trained immunity and regulating epigenetic mechanisms could be of clinical relevance for treating ND.

1.6 Research Questions

1.6.1 How is immune memory linked to the pathology of Parkinson's and Huntington's diseases?

Various research works have identified LPS as a stimulator of immune memory, which has been discussed above in detail. LPS-activated microglia, which resulted in a switch between microglial phenotypes, causing the release of either pro-inflammatory cytokines or anti-inflammatory cytokines, has been demonstrated in an AD mice model (Wendeln et al. 2018). Further, peripheral stimuli modulated neuropathology in the AD mice model. Previously, research has pointed to the correlation between alpha-synuclein aggregates and the activation of both innate and adaptive immune responses in Parkinson's disease (B. Zhu et al. 2022). Also, peripheral stimulation delays or prevents the onset of HD, indicating that the severity of HD are also associated with the impairment of the immune system (S. W. Lee et al. 2018). The brain's immune cells develop an immunological

memory function, and it would be beneficial to know its impact on the disease models of BAC SNCA and BAC HD, which have not been discussed before. Additionally, the importance of LPS and HFD in triggering pathological responses in these rat models has been highlighted.

1.6.2 Does LPS and HFD act as modifiers of neuropathology?

Myeloid cell plasticity is largely dependent on the mechanism of innate immune memory. The immune memory is usually triggered by the environmental stimuli (Wendeln et al. 2018). HFD has also been shown to accelerate amyloid beta pathology in an AD mice model (Maesako et al. 2013). The impact of LPS and HFD on neuropathology in BAC SNCA and BAC HD disease models has not been demonstrated yet. Thus, it could be beneficial to understand if the immune memory response triggered with different doses of LPS and HFD could play a role in altering neuropathology in our disease models. Examining changes in neuropathology could offer a pathway for in-depth investigation into the neurotoxic or neuroprotective effects of microglia. Understanding the mechanism by which various treatments trigger the buildup of distinct types of protein aggregates, including monomeric and oligomeric forms, in these disease models can provide valuable insights. Additionally, comparing these protein aggregates with the neuropathology would provide more insights into the protein expression levels in these disease models and its associated post-translational modifications, if any.

1.6.3 Conclusions and relevance to the present study

The first evidence of innate immune training and tolerance in microglia and the link to pathology was provided by Wendeln et al., concluding that training promotes and tolerance reduces neuropathology (Wendeln et al. 2018). The influence of microglial immune memory activated by LPS and HFD on the pathogenesis of BAC SNCA and BAC HD rat models is not yet fully understood. Since immune memory is a hallmark of neuropathology, exploring inflammatory processes in other NDs like Parkinson's and Huntington's would pave the way to identify epigenetic signatures that could offer future potential approaches to treat age-associated NDs.

1.7 Future directions

Targeting dysregulated immune responses for therapeutic purposes is a key area of ongoing scientific research in today's world (Mulder et al. 2019). Debates have been going on about whether producing drugs that target epigenetic pathways would prove beneficial in treating diseases (Rodriguez, Suarez-Alvarez and Lopez-Larrea 2019). Immunotherapies like reversing the effects of trained immunity to rebalance the myeloid state from a pro-inflammatory to an anti-inflammatory state have been studied extensively; for example, using a mechanistic target of rapamycin (mTOR) inhibitor inhibits trained immunity. Trained immunity can also be used by inhibiting epigenetic modulators for DNA methylation and histone modifications (Netea, Dominguez-Andres et al. 2020). Since epigenetics also plays a crucial role in regulating macrophage phenotypes, epigenetic

drugs that target the activation of the innate immune system could be associated with treating ND, but it could come with its own disadvantages as epigenetic drugs are not cell-specific (Rodriguez, Suarez-Alvarez and Lopez-Larrea 2019).

1.8 Aim of the thesis

Neurodegenerative diseases like PD and HD have no effective treatments to date. Both genetic and environmental factors contribute towards the progression of the diseases. Studies have reported that inflammatory processes play a role in ND. It is crucial to understand how the brain's immune system impacts neuropathology and how environmental factors pose as risk factors for ND. With respect to the emerging role of innate immune memory in microglia, BAC SNCA and BAC HD rats have been used in this project -

- to investigate how immune memory is induced in the brain through LPS and HFD
- to understand how microglia immune memory shapes neuropathology in these disease models
- to check if there are additional microglial phenotypes that play a role in pathology

This could assess a broader reach of the knowledge of microglial reprogramming in NDs.

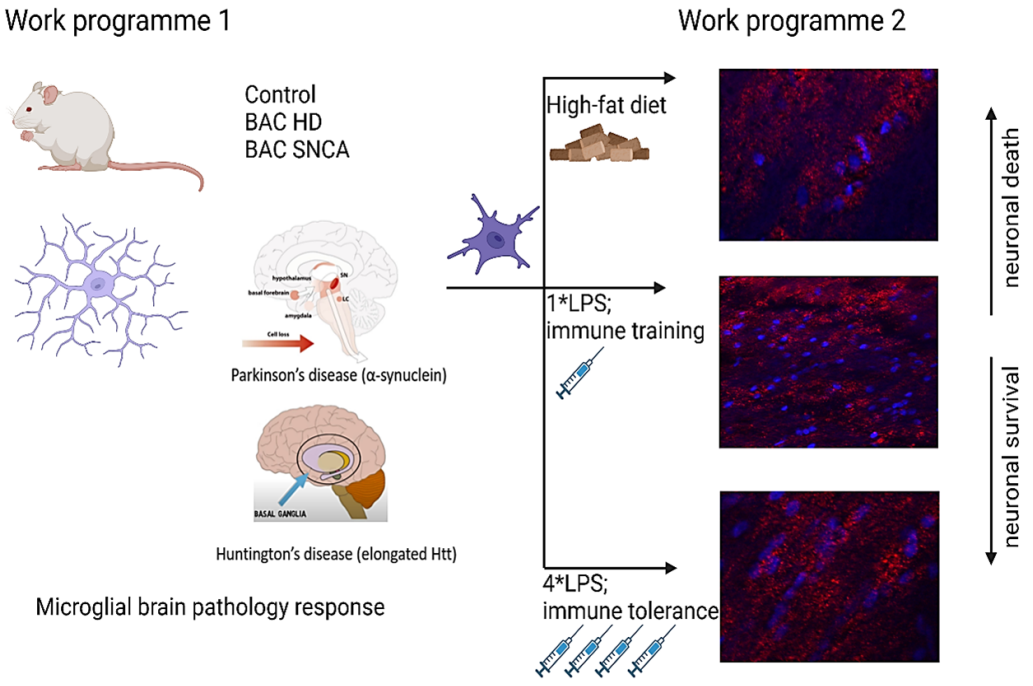

Figure 1.6: Overview of the project.
The above figure describes the overall workflow. This figure has been generated by BioRender.com.

Chapter 2

Materials and Methods

2.1 Study Design

2.1.1 Introduction to the rat models of PD and HD

Two well-characterized rat models of PD (Nuber et al. 2013) and HD (Yu-Taeger et al. 2012), developed at the Institute of Medical Genetics and Applied Genomics, Tübingen, were set up for 3 months and 9 months' timeline. Both rat models were generated using a bacterial artificial chromosome (BAC). BAC SNCA carried the full-length human SNCA gene that over-expressed alpha-synuclein. Over-expression of alpha-synuclein lead to truncated C-terminal fragments of alpha-synuclein and production of insoluble alpha-synuclein (Nuber et al. 2013). With increasing age, BAC SNCA rats showed an impairment in locomotion, novelty-seeking, and avoidance, associated with olfactory bulb deficits. BAC SNCA overexpression leads to the loss of dopamine neurons in the brain. BAC HD rats containing full-length HTT with 97 CAA/CAG repeats show early and progressive motor-deficit symptoms, with additional anxiety symptoms (Yu-Taeger et al. 2012). Accumulation of mHTT occurs earlier and is more common in the cortex region of the brain. For HD, stability of CAG repeats is of utmost importance, since the onset of the disease is inversely correlated with the number of CAG repeats.
Only male rats were used in the experiments. Rats were group-housed with mixed genotypes (four rats per cage with two transgenic and two wild-type rats respectively), maintaining a standard light-dark cycle (12h light/12h dark), having a constant temperature-humidity room with free access to both food and water. The care of animals was undertaken according to the local Animal Welfare Committee in Tübingen.

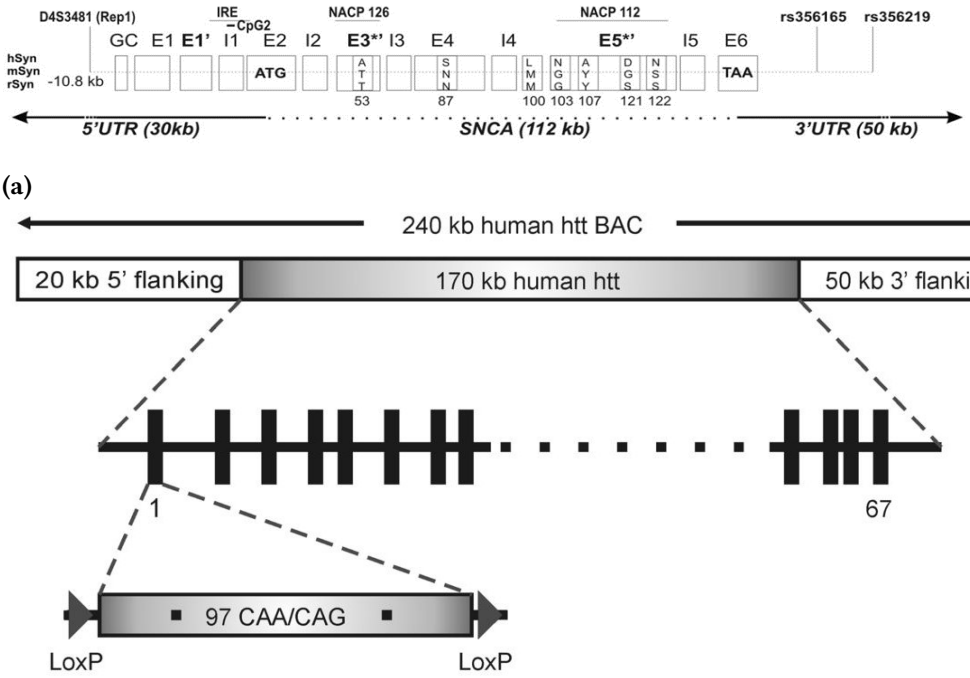

Figure 2.1: Generation of (a) BAC SNCA and (b) BAC HD rats. (a) Schematic representation of the human alpha-synuclein gene structure which has been used for generating BAC SNCA PD rats, including all introns, exons and other regulatory regions (Nuber et al. 2013). (b) Representation of the BAC HD construct with the entire 170 kb region of the HTT gene with 20 kb upstream and 50 kb downstream sequences, and including 97 CAA/CAG trinucleotide repeats of the endogenous HTT gene (Yu-Taeger et al. 2012).

2.1.2 Ethical Approval

All procedures strictly adhered to international standards for the care and use of laboratory animals and were approved by the local Animal Welfare and Ethics committee of the Country Commission Tübingen, Germany (TVA HG 2/19).

2.1.3 Breeding strategies and preparation of the cohorts

Two sets of cohorts were set up for 3-month and 9-month time period, respectively. For PD, BAC SNCA homozygous rats were considered for the study, since the expression of SNCA gene is stronger in homozygous rats. Firstly, heterozygous male and female rats were bred to produce 50% heterozygous, 25% homozygous and 25% wild-type animals. Then, homozygous male and female rats were bred to produce homozygous offspring (F1 generation). Thus, one homozygous/wild-type male rat was housed with two homozygous/wild-type female rats to produce homozygous/wild-type rats simultaneously. 5 sets and 8 sets of each breeding pair for both transgenic and wild-type rats were set up for the BAC SNCA 3-month and 9-month cohorts, respectively.

For BAC HD, TG5 rat line was considered and only heterozygous rats were considered for the study. One heterozygous male rat and two WT female rats were bred to produce

50% heterozygous and 50% wild-type animals. 8 sets and 14 sets of breeding pairs of TG5 males and wild-type females were set up for the BAC HD 3-month and 9-month cohorts, respectively. The wild-type female rats used for the BAC HD breeding were ordered from Charles River Laboratories, Wilmington, USA.

2.2 Determination of the respective genotypes

2.2.1 Isolation of genomic DNA

The animal's genomic DNA was isolated by taking the ear biopsy from the animal and by using the Roche High Pure PCR Template Preparation Kit (Roche Applied Science, Mannheim, Germany). The appropriate buffers, filters and the corresponding protocol were provided with the Kit. The ear biopsy tissues were digested with proteinase K overnight in a water bath at 55°C in Eppendorf tubes with 40 µl of Proteinase K and 200 µl of lysis buffer. On the next day, isopropanol and binding buffer were added to the samples and then vortexed for 5 seconds so the tissue dissolved well, and finally centrifuged at 13,000×g for 5 minutes. The supernatant was filtered through the High Pure Filter Tube and the DNA was then washed with the inhibitor removal buffer to prevent DNA loss during washing steps, and finally the DNA was washed with washing buffer twice. These two steps were coupled with centrifugation at 8000×g for one minute. The remaining excess washing buffer was removed by an additional centrifugation step of 13,000×g for 10 seconds. DNA was then eluted with 200 µl of elution buffer (pre-warmed at 70°C) and then stored at 4°C. For longer storage, DNA should be stored at -20°C.

2.2.2 Polymerase Chain Reaction (PCR)

PCR amplifies a specific DNA sample and produces millions of copies of it using the polymerase chain reaction. It requires a DNA template and a free 3'-OH, which are sequence-specific primers. For BAC SNCA, the PCR reaction involves denaturation by heating at 94°C for 5 minutes (for breaking down the double-stranded DNA into single strands), annealing by varying temperature and time, since it depends on the length and GC content of primers (for the primers to get attached to each original strand for new strand synthesis), and extension at 72°C for 10 minutes (for extension of the new DNA strands and the temperature may vary depending on the polymerase used). The number of PCR cycles used in this case was 35. For BAC HD, HTT comprises 67 exons. For genotyping, primers are used specifically against exons 1 and 67 to interpret the complete expression of the gene. Here, the denaturation step is shorter (94°C for 30 seconds), the annealing temperature, as usual, depends on the length and GC content of primers and extension remains at 68°C for 5 minutes. The number of cycles for exon 1 was 30 and for exon 67 was 35. Usually, a positive interpretation of the DNA present for exon 1 confirms the presence of HTT gene strongly. Transgenic and wild-type animals were subjected to PCR by Taq DNA polymerase (Taq from Qiagen, Hilden, North Rhine-Westphalia, Germany for BAC SNCA PCR and NEB OneTaq-Pol from New England BioLabs, Ipswich, USA for BAC HD PCR). The primers (100 µM) designed to amplify the corresponding DNA fragment of BAC SNCA and BAC HD were designed by Metabion, Martinsried, Germany and are listed below.

Table 2.1: Rat PCR genotyping primers

Transgene	Primer sequence	DNA strand direction	Amplicon size	Annealing temp.
hSNCA	ATT CCC TGA AGC AAC ACT GCC A	Forward	1048 bp	55°C
hSNCA	GAC ACA TGC AGC TTA GCA CTC TG	Reverse	1048 bp	55°C
Exon 1	ATG GCG ACC CTG GAA AAG CTG	Forward	200 & 500 bp	57°C
Exon 1	AGG TCG GTG CAG AGG CTC CTC	Reverse	200 & 500 bp	57°C
Exon 67	TGT GAT TAA TTT GGT TGT CAA GTT TT	Forward	200 bp	47°C
Exon 67	AGC TGG AAA CAT CAC CTA CAT AGA	Reverse	200 bp	47°C

25 µl of the PCR reaction was prepared which consisted of 10 µM/mM of primer mix (Metabion, Martinsried, Germany), 10 mM dNTP mix (Roche), Taq DNA polymerase, 1x standard or GC reaction buffer (CoralLoad Qiagen for BAC SNCA and OneTaq for BAC HD), 100 pg genomic DNA, and Ampuwa water (Ampuwa, Fresenius Kabi, Germany) to adjust to the volume of 25 µl. Reaction was either performed in small PCR tubes (0.2 ml 8 strip pieces, StarLabs, USA), or in a 96-well PCR plate (96x0.2 ml half-skirted, natural plates, NerbePlus, Winsen, Germany). After the PCR reaction was done, amplicons were visualized using 1.5% agarose gel which was prepared using LE Agarose powder (Lonza, Basel, Switzerland) and 1xTBE buffer (Tris/Borate/EDTA) containing ethidium bromide (1% 10mg/ml Carl Roth GmbH, Karlsruhe, Germany) and the samples were run for 1.5 hours at 120 V. DNA ladder (ThermoScientific Gene Ruler DNA Ladder Mix 0.1 µg/µl) was used to determine the size of the DNA obtained.

2.2.3 Quantitative PCR genotyping (qPCR)

Homozygosity and heterozygosity of BAC SNCA samples were determined using the qPCR method on a LightCycler 2.0 (Roche). For qPCR detection, the dye FastStart DNA MasterPlus SYBR Green (Roche) was used to generate fluorescent signals upon binding to double-stranded DNA. All the transgene signals obtained from PCR were considered for qPCR genotyping. The DNA concentrations of individual samples were measured by Nanodrop Cuvette (Eppendorf G1.0) on Eppendorf BioPhotometer. For good DNA concentrations, the ratio A260/A280 should be between 1.7-2.0. Usually, the DNA concentration depends on the tissue and DNA isolation. According to the concentration of DNA obtained, samples were diluted to 10 ng/µl with Ampuwa water. Firstly, five standard solutions were prepared and they were diluted in a ratio of 1:5.

After that, master mixes for both the reference gene (beta-actin, bact) and the target gene (hSNCA) were prepared, containing each primer set (1:20 dilution) for bact and SNCA gene, 1 x SYBR Green Mix (QuantiNova/QuantiTect, Qiagen), and Ampuwa water. For the final solution, 8 µl of the master mix and 2 µl of DNA were pipetted in each well of a 96-well or a 384-well reaction qPCR plate (LightCycler 480 Multiwell Plate 384, white, Roche). The reaction plate was divided equally into two sides, where on the left side, the reaction mixture for SNCA was pipetted and on the right side, the reaction mixture for beta-actin was pipetted. The standards, the samples and the controls were pipetted into the plate in triplicates to compare the relative differences between them. The plate was

sealed and was centrifuged at 900 rpm for 2 minutes and then the plate was run on a Light cycler according to the template provided by Roche.

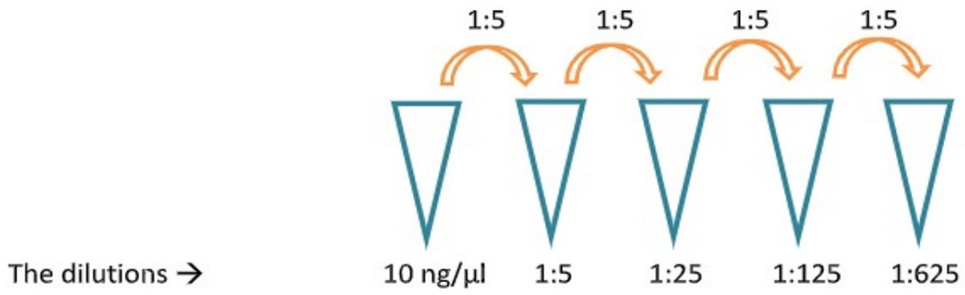

Figure 2.2: qPCR dilution scheme. The above illustration has been created by Dr. Zinah Wassouf and her qPCR protocol has been used as a reference. The first standard was a mixture of the samples and then the rest of the standards were diluted in a ratio of 1:5 with Ampuwa water.

The efficiency of the curve is based on the slope of the standard samples, and it should be between 1.6 and 2.0 (in %, it should be between 90% and 110%). Theoretically, efficiency is calculated as $E = 10 - (1/slope)$−1, and it depends on the primers, assay performance, reagents used, and their concentrations (David Svec, 2015). The quantification was performed by measuring the Cp (Crossing point) values, which were determined from the amplification of fluorescence signals. The mean of the triplicate Cp values was calculated, and then ΔCp was calculated by subtracting the Cp of the gene of interest from the Cp value of the reference beta-actin gene. The ΔΔCp was determined by subtracting ΔCp of the sample from the ΔCp of the heterozygous animals. Then, the E^{Cp} value of each sample was calculated, and the final value of the homozygosity/heterozygosity would be $E^{Cp}(hSNCA)/E^{Cp}(bact)$. The values of the heterozygous animals would be 1.00 and for the homozygous animals would range from 1.70-2.30. This helped us to distinguish between wildtype (if any), heterozygous, and homozygous animals. The specificity of the qPCR reaction would depend on the DNA length, the GC content of the primers, and the melting curve. The primers (100 µM) for the beta-actin and SNCA genes, designed by Metabion, Martinsried, Germany, are listed below.

Table 2.2: Rat qPCR genotyping primers

Transgene	Primer sequence	DNA strand direction	Annealing temp.
hSNCA qPCR	CCG CTC GAG CGG TAG GAC CGC TTG TTT TAG AC	Forward	52°C
hSNCA qPCR	CCT CTT TCC ACG CCA CTA TC	Reverse	52°C
bact qPCR	AGC CAT GTA CGT AGC CAT CCA	Forward	53°C
bact qPCR	TCT CCG GAG TCC ATC ACA ATG	Reverse	53°C

2.3 Experimental set-up

2.3.1 Preparation of the experimental groups

Two experimental groups of BAC SNCA and BAC HD rats were set up for 3 months and 9 months time-line. Animals were randomly assigned into 1×LPS, 2×LPS, 4×LPS, standard group (PBS) and high-fat diet (HFD) group. A total of 50 animals were considered for the 3-month cohort and for the 9-month cohort, 96 animals were used. Breedings for the 3-month and 9-month cohorts were set up, keeping in mind the number of experimental animals to be used. Depending on the injections they received, the animals were later sacrificed for microglia isolation.

2.3.2 Peripheral immune stimulation

As stated earlier, LPS stands as one of the best examples for stimulating peripheral immune stimulation (Hamon and Quintin 2016). LPS (Lipopolysaccharide from Salmonella typhimurium, L6511, Sigma-Aldrich) solution was prepared in DZNE, Tübingen, and was injected intraperitoneally (i.p.) in 3-month-old rats in treatment groups of 1×LPS, 2×LPS and 4×LPS with a daily dose of 500 µg per kg body weight. For the 3-month-old cohort, both BAC SNCA and BAC HD rats received either a single LPS injection (1xLPS), two LPS injections on two consecutive days (2×LPS), or four LPS injections on four consecutive days (4×LPS). For comparison, rats received 1×, 2× and 4× phosphate-buffered saline (PBS). For long-term cohort (9-month-old rats), the rats received a single LPS injection followed by three PBS injections on three consecutive days (1×LPS) or four LPS injections on four consecutive days (4×LPS). For comparison, 4×PBS injections on four consecutive days were injected into the rats. Along with LPS, rats received HFD at the age of two months for 30 days (TD 88137: Fat % 21.3, Sugars % 34.0, Cholesterol mg/kg 1972.4). To monitor the weight changes with the treatment, rats were weighed constantly before and after the treatment, and further changes in their behavior with the treatment were noted down accordingly.

2.3.3 Tissue preparation

Rats were sacrificed by administering anesthesia with xylazine and ketamine (20 mg/kg and 750 mg/kg, respectively) at the given time points of 3 months and 9 months. After the anesthesia, the rats were perfused with ice-cold PBS through the left ventricle, and blood samples were drawn from the right ventricle for cytokine analysis. The blood samples were then centrifuged at 2000 rcf for 10 minutes at room temperature, and the serum collected was stored at -80°C for Enzyme-linked immunosorbent assay (ELISA) studies. The brain was isolated from the rat and was cut from the middle in two hemispheres; one hemisphere was used for microglia isolation, and the other was stored in 4% paraformaldehyde for further analysis in immunostaining studies. The half-intact hemisphere with the cerebellum and brain stem was kept in a 50 ml Falcon tube with 15 ml 4% PFA for 24 hours at 4°C. The brain was then transferred to a falcon tube containing 30% sucrose and was stored for 48 hours until the brain sank to the bottom of the tube. The brain was frozen in 2-methylbutane, dried, and stored at -80°C for sectioning later.

2.3.4 Microglia isolation with Fluorescence-activated cell sorting (FACS)

For the microglia isolation, from the half-intact hemisphere, olfactory bulb, cortex, striatum and hippocampus were collected. The hypothalamus was taken out and stored in a 2 ml collection tube for further studies. The brain was dissected in 15 mM ice-cold Hank's buffered salt solution (HBSS) with 0.54% D-glucose with 0.1 mg/ml DNAse I (Sigma). The minced tissue was homogenized in 7 ml and 5 ml glass Dounce homogenizers. Once thoroughly homogenized, three aliquots of brain homogenates were collected from the surface and stored at -80°C for ELISA and cytokine analysis. The homogenate solution was filtered through a 200 µm cell strainer and was centrifuged at 300 rcf for 10 minutes at 4°C without brake. The brain homogenates then underwent Percoll density gradient centrifugation, where the cells were resuspended in 70% Percoll solution and underlaid with 37% and 30% isotonic Percoll solution. The pellet was centrifuged at 800 rcf for 30 minutes at 4°C without brake. After carefully removing all the myelin from the gradient, the cells lying at the interphase of 37% and 70% Percoll layer were transferred to a new 15 ml Falcon tube and washed with FACS buffer containing HBSS, 2% FCS buffer, 10 mM EDTA and 0.5M HEPES. The cells were then resuspended in FACS buffer with Fc block (1:400, 553141 BD Biosciences) for blocking the Fc receptors and Zombie Violet (1:400, BioLegend) for dead-cell detection. It was incubated for 10 minutes on ice in the dark, followed by 15 minutes of incubation at 4°C with anti-rat CD11b/c Alexa Fluor 647 (1:100, 101234 BioLegend) and anti-rat CD45 Alexa Fluor 488 (1:100, 103128 BioLegend). After washing with FACS buffer and discarding the supernatant, the cells were loaded on the FACS machine (Sony SH800) for microglia sorting. The sorted microglia were further used for bulk-RNA sequencing, single-cell RNA, single-cell ATAC sequencing, and ChIP sequencing.

2.3.5 Tissue lysate

Proteins were lysed from brain homogenates, which were prepared during microglia isolation. The raw brain homogenates were centrifuged at 100xg for 1 minute at 4°C, and the supernatants were transferred to new 0.5 ml Eppendorf tubes. For some experiments, the raw brain homogenates were considered and for some, the supernatants were considered for TR-FRET, Filter-Trap and Western blotting. Protein concentration was determined by Bradford assay (Bradford reagent, Bio-Rad Laboratories, USA) through Gen 5 3.11 (Microplate Reader and Imager Software) at 595 nm wavelength. For BAC HD, the samples were diluted to 4 µg/µl with dilution buffer PBS with Tween-20 (0.5% PBST with proteinase inhibitor) in a 96-well transparent plate (96-well Conical Btm Natural RNase/DNase Free-Sterile ThermoScientific, 249946) sealed with a transparent foil (96-well Cap Natural Radiation Sterilized ThermoScientific, 276000). For BAC SNCA, the same procedure was followed, but the samples were diluted to 2 µg/µl with PBST.

2.3.6 Western blotting

To quantify the protein levels for genotype and treatment, Western blotting of the tissue lysates was performed with supernatants and brain homogenates (diluted with PBST). For sample lysis, 50X complete EDTA diluted with 2 ml of Milli Q water and protease

inhibitors was considered as a lysis buffer (cOmplete™, Roche, Basel, Switzerland). 20-25 µg of protein was mixed with the lysis buffer, along with 4x LDS buffer (1 M Tris Base pH 8.5, 2 mM EDTA, 8% LDS, 40% glycerol, 0.075% CBB G, 0.025% phenol red) and 1 M DTT. The samples were briefly centrifuged and heat-denatured at 70°C and 600 rpm for 10 minutes in a thermo shaker.

Western blotting was performed using the standard protocol. Proteins were separated electrophoretically using either a homemade 12% SDS-PAGE gel (Bio-Rad Laboratories, USA) (Table 2.3) or 10% Bis-Tris gels/7% NuPAGE® Tris-Acetate gradient gels (Thermo Fisher Scientific). Gels were run with either MES buffer (50 mM MES, 50 mM Tris-base pH 7.3, 0.1% SDS, 1 mM EDTA) or MOPS buffer (50 mM MOPS, 50 mM Tris-Base pH 7.7, 0.1% SDS, 1 mM EDTA) at a voltage of 120 V for one hour. Gel percentage usually depends on the size of the protein, that is, 4-40 kDa – 20%, 12-45 kDa – 15%, 10-70 kDa – 12.5%, 15-100 kDa – 10%, 25-200 kDa – 8%. The proteins were further transferred to a 0.2 µm nitrocellulose membrane (Amersham™ Protran™ Premium 0.2 µm, GE Healthcare, 10600004) using transfer buffer (containing 25 mM Bicine, 25 mM Bis–Tris pH 7.2, 1 mM EDTA) with 15% methanol and was run at 80 V for 2 hours. After transfer, the membrane was blocked with 5% skim milk powder (Merck Millipore) in TBS for 1 hour at room temperature and then incubated with respective primary antibodies diluted in TBST (TBS containing 0.1% Tween-20 and 0.02% sodium azide) at 4°C, and kept overnight. For detection, the membranes were incubated with secondary IRDye® antibodies (LI-COR Biosciences, Bad Homburg, Germany) for 1 hour at room temperature and visualized with a LI-COR Odyssey® Fc (LI-COR Biosciences, Bad Homburg, Germany) and the images obtained were quantified with the loading control using Image Studio 5.2 software (LI-COR Biosciences). For detecting autophagy and inflammatory markers like LC3, p62, Cox2, and beta-arrestin 1, 30 µg of protein was considered because of the lower expression of the proteins.

Table 2.3: Western blot gel composition.
Bis-Tris Gel Recipes (adapted from Tim Corson, PhD, Indiana University School of Medicine)

Resolving gel (1 gel-5 ml)	**8%**	**10%**	**12%**	**15%**	**Stacking gel (2 gels-5 ml)**	**6%**
3.5x buffer, mL	1.42	1.42	1.42	1.42	3.5x buffer, mL	1.42
30% acrylamide, mL	1.34	1.67	2	2.5	30% acrylamide, mL	1
H2O, mL	2.24	1.91	1.58	1.08	H2O, mL	2.58
10% APS, µL	30	30	30	30	10% APS, µL	30
TEMED, µL	4	4	4	4	TEMED, µL	4

3.5x buffer: 52.32 g Bis-Tris in 200 ml H2O pH 6.5-6.8 with HCl
APS and **TEMED** are used at equimolar concentrations (ca. 5mM)

2.3.7 Filter retardation assay

For the detection of SDS-insoluble alpha-synuclein and huntingtin, the diluted supernatants (for BAC HD) and the brain homogenates (for BAC SNCA) were considered after the measurement of the protein concentrations by Bradford assay. 10-20 µg of protein from brain homogenates/supernatants were taken and diluted in DPBS with 2% SDS and 50 mM DTT (Dithiothreitol). The samples were heat denatured for 5 minutes at 95°C and then cooled down at room temperature before running the assay to avoid precipitation of SDS. 0.45 µm nitrocellulose membrane (Amersham™ Protran™, GE Healthcare, 10600002, 300 mm*4m) and 3MM Whatman paper (GE Healthcare Life Sciences GmbH, 46*57 cm) was placed in the Minifold II Slot Blot System (Schleicher and Schuell) and the membrane was equilibrated with 0.1% SDS in DPBS. 100 µl of the diluted protein was passed through the membrane under vacuum and then washed with DPBS. The membrane was taken out and rinsed with TBS once (Tris-buffered saline, 10 mM Tris pH 7.5, 150 mM NaCl), before blocking it with 5% skim milk powder (Merck Millipore) in TBS for 1 hour at room temperature. Membranes were incubated according to the standard immunodetection protocol as described in the 'Western blotting' section.

The complete list of antibodies that have been used for Western blotting and Filter retardation assay has been listed in Table 2.4.

2.3.8 TR-FRET

Time-resolved fluorescence energy transfer (TR-FRET) was performed for the detection of soluble and aggregated huntingtin and was performed as previously described and established (Baldo et al. 2012; Clemens et al. 2015; Singer et al. 2021). The supernatants were measured in 384-well microtiter plates (PerkinElmer, USA) and the amount of huntingtin was detected by a combination of fluorophore-labeled antibodies anti-HTT BKP1 labelled with the Tb (donor) fluorophore (Wellington et al. 2002) and anti-polyglutamine antibody MW1 labelled with d2 (acceptor) fluorophore (J. Ko, Ou and Patterson 2001) in a ratio of 1:10 (Clemens et al. 2015; Singer et al. 2021). The resulting signals were read with an EnVision Multimode Plate Reader (PerkinElmer, USA) and were detected at 620 nm and 665 nm, respectively.

2.3.9 Tissue Sectioning

As stated earlier in Section 2.3.3, tissue preparation involved storing one half of the brain for immunostaining studies. Tissue was primarily placed on dry ice. The microtome blade was attached in a straight manner, and the sections were then cut sagitally at 25 µm thickness with a microtome (Leica SM2000R). While cutting, it was ensured that the brain was completely covered in dry ice and was straight. The cut brain sections were stored in TCS buffer (Tissue Culture Supernatant containing PBS, glycerol and ethylene glycol) in a 12-well plate (Costar® 12-well Clear TC-treated Multiple Well Plates, Bulk Pack, Sterile, Ref. 3512) at -20°C, and were used for immunohistochemistry (IHC) and immunofluorescence (IF).

Table 2.4: List of antibodies and staining conditions.

Antibody	Epitope	Company	Species	Concentration	Application
Anti-alpha synuclein (Clone: mc42) (mouse + human)	NAC domain	BD Biosciences (BDB610786)	Mouse	1:1000	FT,WB, IF
Anti-alpha synuclein (human, 15G7)	C-terminus	Enzo Life Science (ALX-804-258-L001)	Rat	1:100	WB, IHC
Recombinant anti-alpha-synuclein (phospho S129)	monoclonal	Abcam (ab51253)	Rabbit	1:500	IF
Anti-beta actin (clone: AC15)	monoclonal	Sigma Aldrich (A5441)	Mouse	1:2500	WB
Lactate dehydrogenase	monoclonal	Proteintech (66425-1-Ig)	Mouse	1:5000	WB
Cyclooxygenase 2	polyclonal	Proteintech (27308-1-AP)	Rabbit	1:2000	WB
MitoProfile total OXPHOS	—————	Abcam (ab 110413)	Mouse	1:2000	WB
Anti-VDAC 1	polyclonal	Millipore (ab 10527)	Rabbit	1:5000	WB
Anti-Citrate synthetase	polyclonal	Abcam (ab 96600)	Rabbit	1:1000	WB
Anti-dnm1l (Drp1)	polyclonal	Novus Biologicals (NB1100-55237)	Rabbit	1:1000	WB
Anti-OPA1 (clone: 1E8-1D9)	monoclonal	Novus Biologicals (NBP1-71656)	Mouse	1:1000	WB
LC3	polyclonal	Cell Signaling (2775S)	Rabbit	1:500	WB
p62 (clone: 2C11)	monoclonal	Abcam (ab 56416)	Mouse	1:1000	WB
Anti-Huntingtin (clone: 1HU-4C8)	monoclonal	Merck Millipore (MAB2166)	Mouse	1:1000	FT,WB
Huntingtin antibody	monoclonal	ThermoFisher Scientific (BSM-54305R)	Rabbit	1:1000	WB
Anti-Huntingtin (clone: mEM48)	monoclonal	Merck Millipore (MAB5374)	Mouse	1:500	IHC
IRDye goat anti-mouse 800CW	—————	LICOR Biosciences	————	1:5000	WB
IRDye goat anti-rabbit 800 CW	—————	LICOR Biosciences	————	1:5000	WB

2.3.10 Immunohistochemistry

Only the 9-month cohort was considered for IHC and IF, since older rats display a higher amount of aggregates in the brain than the young rats. The protocol for IHC for BAC HD 9m was earlier established (Yu-Taeger et al. 2012). Free-floating staining was performed in a 12-well plate and initially, the sections were washed with PBS and blocked with 0.5% sodium borohydride (NaBH4) to reduce the formalin-induced autofluorescence. After washing with PBS and 0.4% TBST, sections were incubated with the primary antibody in TBST overnight at 4°C (EM48 1:1000, MAB5374; Millipore Bioscience Research Reagents), followed by incubation with biotinylated goat anti-mouse IgG secondary antibody (1:1000, BA-9200; Vector Laboratories) for 1 hour at room temperature. After washing with 0.4% TBST, sections were treated with an avidin-biotin–peroxidase complex (Vector Laboratories, Vectastain Kit, 1:400) for 1 hour. After further washing steps with 0.4% TBST and TI buffer (0.5 M Tris, 0.5 M Imidazole with a pH of 7.2, stored away from light), sections were again incubated with an avidin-biotin–peroxidase complex (Vector Laboratories, Vectastain Kit, 1:400) for an hour for signal amplification, and then incubated

with DAB-H2O2 (0.01% DAB, 3,3′-Diaminobenzidine and 0.001% H2O2) until a brown color signal intensity has developed. The sections were mounted on slides (SuperFrost® + Objektträger, white, Art. Nr. 03-0060, R. Langenbrinck GmbH, Labor-und Medzintechnik) the next day after ethanol washing and sealed with a cover-slip (24*40mm, 100 beckglässer, Art. Nr. 190002440 iDL). After mounting, dehydration of the sections was done and is described in Table 2.5 below. Images were taken using an Axioplan 2 Microscope (Carl Zeiss Microscopy, Jena, Germany) equipped with an AxioCam MRm. Images were acquired using Zeiss imaging software (AxioVision-6; Zeiss). 6 animals per group were photographed under the microscope, and the images were analysed and quantified using Image J (National Institutes of Health, USA).

For detecting human alpha-synuclein, BAC SNCA 9-month-old cohort sections were considered and stained as described previously (Nuber, Harmuth et al. 2013). Sections were mounted on slides (SuperFrost® + Objektträger, white, Art. Nr. 03-0060, R. Langenbrinck GmbH, Labor-und Medzintechnik), and the antigen retrieval step was performed with 10 mM sodium citrate pH 6.0 to enable specific binding of the primary antibody. After treating the slides with H2O2 (0.3% in PBS) for 20 minutes and subsequently blocking (5% normal serum, 0.3% Triton X-100 in PBS) for 1 hour, sections were incubated with anti-human alpha-synuclein overnight at 4°C with 5% normal serum and PBS (15G7, 1:50, Enzo Life Science, ALX-804-258-L001). After washing with PBS, sections were incubated with biotinylated goat anti-rat IgG secondary antibody (1:200 in PBS, Vector) for 1 hour at room temperature. Sections were then exposed to avidin-biotin–peroxidase complex (Vector Laboratories, Vectastain Kit, 1:400) for an hour before visualizing them with DAB and H2O2 (0.01% DAB, 0.001% H2O2). After ethanol washing, sections were sealed with a cover slip (24*40mm, 100 beckglässer, Art. Nr. 190002440 iDL), and images were taken as described before for BAC HD. Images were analyzed by Image J.

Table 2.5: Section dehydration

Buffer	Time
70% ethanol	2 minutes
80% ethanol	1 minute
96% ethanol	1 minute
96% ethanol	2 minutes
100% ethanol	2 minutes
100% ethanol	2 minutes
Xylene	2 minutes
Xylene	2 minutes
Xylene	8 minutes

2.3.11 Immunofluorescence

Immunofluorescence stainings were performed for total and phosphorylated alpha-synuclein for BAC SNCA 9-month-old cohort. Sections were mounted on slides (SuperFrost® + Objektträger, white, Art. Nr. 03-0060, R. Langenbrinck GmbH, Labor-und Medzintechnik), and applied PapPen (A-PAPPEN LO+2008 2009P, Daido Sangyo Co., Japan) around sections so that the sections are covered in buffers. After washing in TBS buffer (24 g Tris + 88 g NaCl in 900 ml of water, pH 7.6), the antigen retrieval step was performed in the microwave for 30 minutes at 90°C. After cooling, sections were blocked in 5% normal serum, 0.3% Triton X-100 in PBS and 0.3 M glycine (pH 3.0) for one hour. Sections were further washed in TBS and incubated with primary antibodies (phosphorylated anti-alpha synuclein, phosphor-serine 129, ab51253, Rabbit monoclonal antibody to alpha-synuclein, EP1536Y or Purified Mouse anti-alpha-synuclein, Cat. 610787 BD Biosciences) at 4°C overnight, followed by fluorescent secondary antibody incubation (Alexa Fluor™ Plus 555, Goat anti-mouse IgG (H+L), Invitrogen, Ref. A21424, Lot 2291626 or Alexa Fluor™ 555, Goat anti-rabbit IgG (H+L) highly cross-adsorbed, Invitrogen, Ref. A32732, Lot 319533). For quantifying phosphorylated a-syn, fluorescence images were visualized as described in the section 'Immunohistochemistry', and different regions of the brain were photographed from each animal. In total, six animals per group were considered, and images were analyzed and quantified (for phosphorylated alpha-synuclein) using Image J.

2.3.12 Quantification of stained phosphorylated alpha-synuclein aggregates

As stated earlier, six animals per group (both genotype and treatment), with three slices per animal, were photographed. Brain regions of the cortex, striatum, and cortex striatum junction were taken into account since PD aggregates are mostly displayed in the striatum, with some expression in the cortex, too (Srinivasan et al. 2021). Pictures were taken using a 40X objective with an adjusted focus, keeping the exposure time constant for all images for quantification purposes. The Zeiss Apotome was used to achieve better axial resolution. For apotome acquisition, optional sectioning was performed with a high grid and a medium filter. Pictures were saved as high-quality color TIFF files and analyzed using ImageJ.

Acquired images were split into blue and red channels, and the red channel was further considered for the quantification of aggregates. To increase the reproducibility of the counting, a pre-determined lower and upper threshold was set on a positive transgenic animal and compared with the wild-type and negative controls to check if most of the unwanted background signal has been eliminated (lower threshold – 130, upper threshold – 255). For analyzing the particles, the size of the particles were set in different sizes - small (2–10 pixel^2), intermediate (10–30 pixel^2), and large (30–70 or 60–110 pixel^2, keeping in mind to eliminate small particles formed by secondary antibody accumulation. Circularity thresholds were set between 0.2–1.00 or 0.3–1.00 to ensure accurate identification of aggregate morphology. Multiple size ranges were used to assess the distribution and morphological characteristics of pS129 aggregates in the striatum. Finally, with the 'Analyze Particles' function, the number, size, and area of phospho-serine 129 were calculated in each image. Quantification was performed by taking the average of the

counts and the summation of the area of phospho-serine 129 from each section. Further, correlation analysis was performed to compare the correlation between the total area and the size of the aggregates. The quantified numbers were then plotted in GraphPad Prism 6.00 software (GraphPad Software Inc., La Jolla, CA, USA).

2.3.13 Statistical analysis of imaging and protein aggregates

Data are presented as mean ± SEM. Statistical analysis was conducted using GraphPad Prism 6.00 software (GraphPad Software Inc., La Jolla, CA, USA). Statistical significance of data-sets were evaluated using one-way ANOVA with Dunnett statistical hypothesis testing and one-sample t-test. Significance was considered when p-value ≤ 0.05. Statistical outliers were determined by Grubbs' outlier test (alpha = 0.2) and were excluded from the analysis thereafter.

Chapter 3

Results

3.1 Generation of transgenic and wild-type rats

Homozygous and wild-type male rats were considered from BAC SNCA, and heterozygous and wild-type male rats were considered from the BAC HD breeding cohorts for our experiments. The breeding plan is described in Section 2.1.3. Rats were genotyped using genomic DNA isolated from the ear biopsies, and corresponding genotyping was performed for both cohorts. Since, for BAC SNCA, homozygous rats were considered, an additional qPCR step was performed.

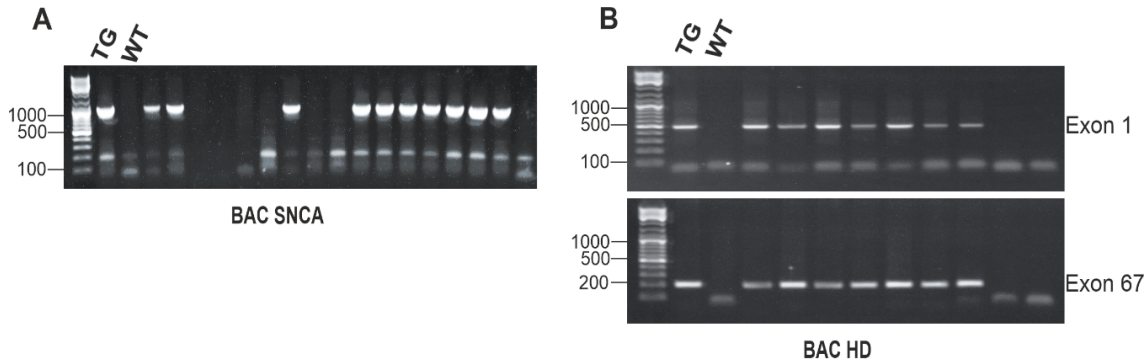

Figure 3.1: The genotype of both the cohorts was confirmed by PCR.
A. BAC SNCA genotyping shows the difference between a transgenic and a wild-type animal. **B.** BAC HD genotyping using exon 1 and exon 67 verified the transgenic animal.

As seen in Figure 3.1, animal genotyping was performed with PCR using primer-specific pairs for BAC SNCA and BAC HD, and the amplified PCR products were visualised with gel electrophoresis on a 1.5% agarose gel. Specific primer pair for BAC SNCA generated amplicons migrating at 1000 base pair. Primer pairs for exon 1 and exon 67 of BAC HD generated amplicons at 500 and 200 base pairs, respectively. If both exon 1 and exon 67 showed DNA amplicons, it confirmed a transgenic animal for BAC HD. The DNA-specific lanes have been marked by transgene (TG) and wild-type (WT). The presence of a DNA amplicon in the PCR indicated a TG animal (Fig. 3.1). Primer dimer accumulation could also be seen at the bottom of the gels.

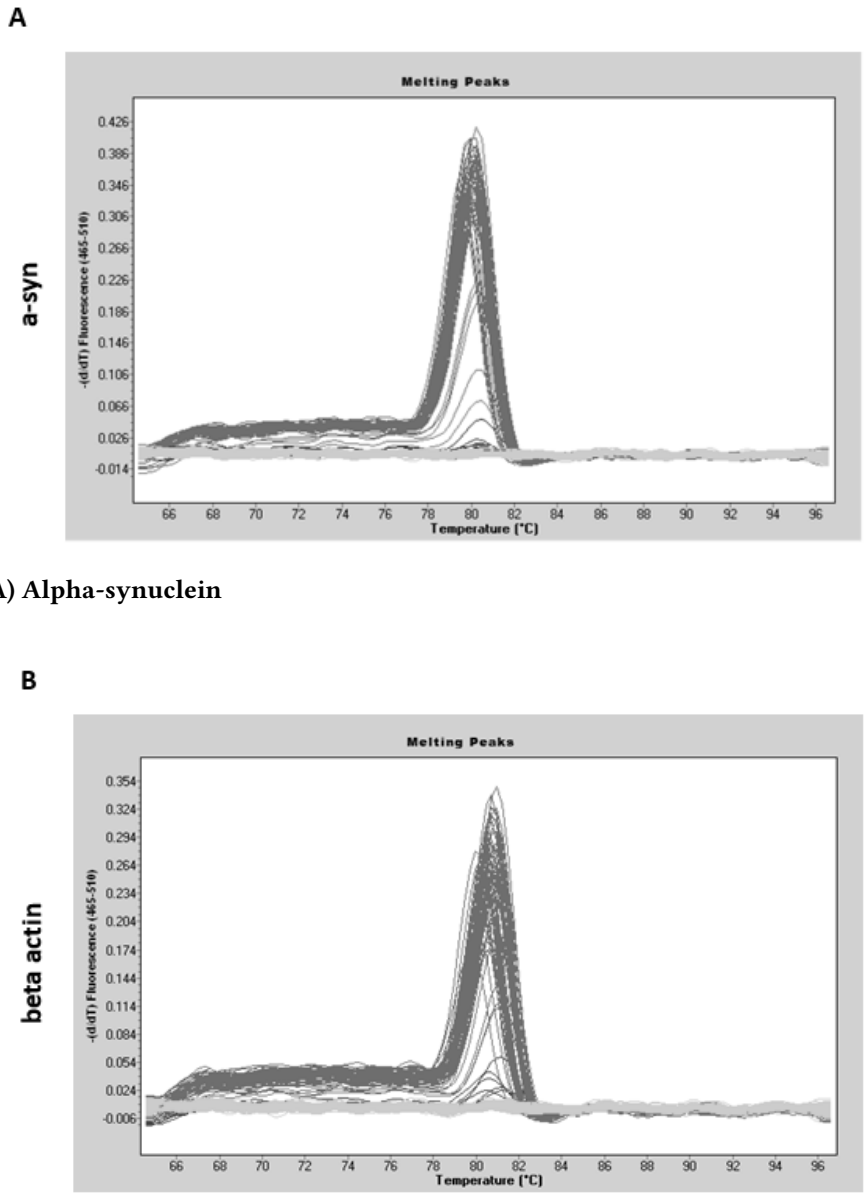

(A) Alpha-synuclein

(B) Beta actin

Figure 3.2: Specificity of the qPCR reaction was analyzed using the melting curves.

For BAC SNCA, the gene is strongly expressed in homozygous animals. Homozygosity and heterozygosity of BAC SNCA animals could then be further determined by qPCR. The melting curves were checked with each primer pair, and further, the Cp values were generated as described under Section 2.2.3. The melting curve usually depicts the dissociation characteristics of double-stranded DNA during heating. For each pair of primers and each sample, only one melting curve was present, suggesting the presence of one DNA amplicon (Fig. 3.2), and further, the quantification of qPCR by which the homozygosity of the animals was determined is shown in Fig. 3.3.

A

Het, Hom, WT?		
Sample	NRQ	
homozygous	1.51	
heterozygous	1.00	
wildtype	0.00	
water	0.00	
ES 1.01	0.64	het
ES 1.02	1.48	homo
ES 1.03	1.21	homo
ES 1.04	1.12	homo
ES 1.10	1.29	homo

B

Het, Hom, WT?		
Sample	NRQ	
homozygous	1.98	
heterozygous	1.00	
wildtype	0.00	
water	0.00	
ES 1.30	1.92	homo
ES 1.31	2.02	homo
ES 1.32	0.71	het
ES 1.33	0.81	het
ES 1.34	1.07	het

C

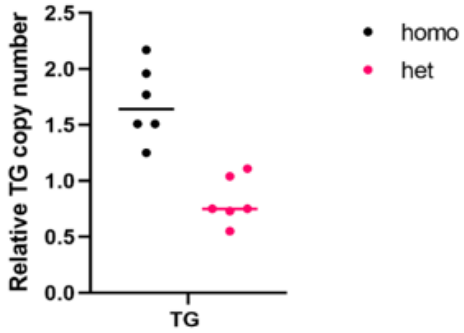

Figure 3.3: Quantification of qPCR.
A,B. Examples of the calculated Cp values from two qPCR results show the differences between homozygous and heterozygous animals for the BAC SNCA cohort, calculated by Efficiency = $E^{Cp}(hSNCA)/E^{Cp}(bact)$. The NRQ in the table above represents normalised relative quantities, reflecting which samples are homozygous, heterozygous or wild type animals. **C.** The graph depicting the relative transgene copy numbers has been generated, with six animals represented in each group. Moreover, only the homozygous animals were included in the experimental cohort.

3.2 Exposing the rats to environmental insults

As described earlier under Section 2.3.2, PD and HD rats were exposed to different doses of LPS and HFD in both 3-month-old and 9-month-old cohorts. A detailed experimental workflow has been provided below (Fig. 3.4).

As depicted in Figure 3.4, BAC SNCA and BAC HD rats, containing full-length alpha-synuclein and mutant human HTT rats, respectively, were used for the study. Rats were randomly distributed in experimental groups of HFD, control PBS, 1×LPS, 2×LPS, and 4×LPS. Some rats received HFD for one month at the age of two months to induce immune memory. Rats that were fed HFD were administered PBS injections at the age of three months, subsequent to the HFD treatment. For the 3-month-old cohort, some rats received a single LPS dose (1×LPS), two LPS doses on two consecutive days (2×LPS), or four LPS doses on four consecutive days (4×LPS). For comparison, some rats received PBS injections either on a single day (1×PBS), on two consecutive days (2×PBS), or four

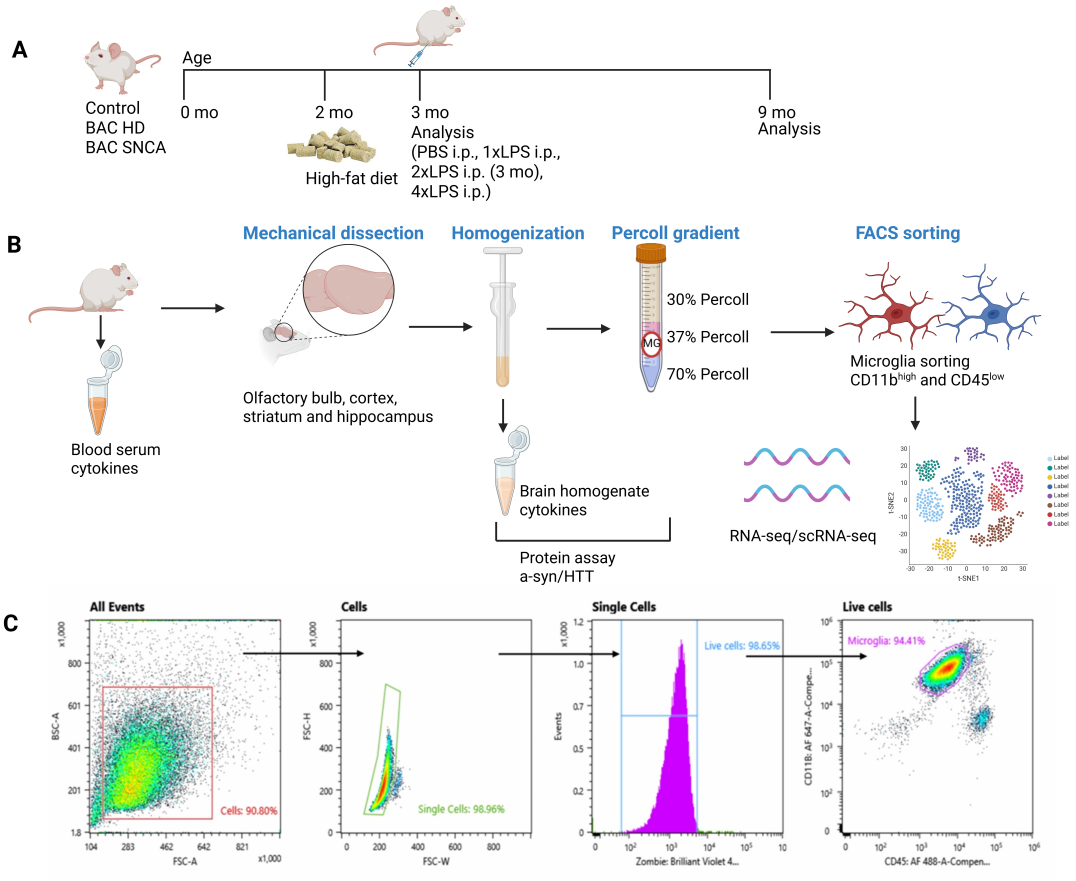

Figure 3.4: Research methodology.

A. Experimental workflow. **B.** Microglia isolation and associated techniques. **C.** Microglia sorting strategy used in this study with markers CD11b^{high} and CD45^{low} (P. Liu 2022), generated by BioRender.com.

consecutive days (4×PBS) at the age of three months. For the 9-month-old cohort, rats received either four LPS doses on four straight days (4×LPS), a single LPS dose followed by vehicle doses on three consecutive days (1×LPS), or four vehicle doses on four consecutive days (4×PBS). The 9-month-old cohort was then kept for more than six months to observe the effects of immune memory in the long-term cohort. After the injections, analysis was performed at the ages of three months and nine months. For the microglia isolation, one half of the brain was used for isolation, and the other was used for immunofluorescence and immunohistochemistry studies. The blood and brain serum cytokines were used for ELISA study, and the remaining brain homogenates were used for protein assays like Western blotting and Filter retardsation assay. The microglia isolated was then divided into bulk-RNA, single-cell RNA, single-cell ATAC and ChIP sequencing analysis.

3.3 The effect of LPS and HFD on the body weight of the rats

Rats receiving LPS and HFD were monitored constantly in terms of their behaviour and weight. It has been studied extensively that sickness behaviour occurs in response to

inflammatory processes (Mazuco et al. 2019), and this behaviour in animals is usually associated with less physical activities, decrease in social and sexual activities, feeling of tiredness, less feeding and exploration. HFD has been shown to induce weight gain and decrease motoric activity in C57BL/6J mice (Han et al. 2020). For our cohorts, with higher doses of LPS (4xLPS), the rats looked more tired, and their weight loss is apparent in the figure below. For the HFD, after four to five weeks, the rats gained considerable body weight. Due to obesity, some rats even fell sick and were excluded from the study later on. The observed differences in the LPS and HFD doses in rats were then compared with the cytokine analysis to determine how the cytokine level changes with each treatment. The weight curves for both BAC SNCA and BAC HD rats are plotted below (Fig. 3.5).

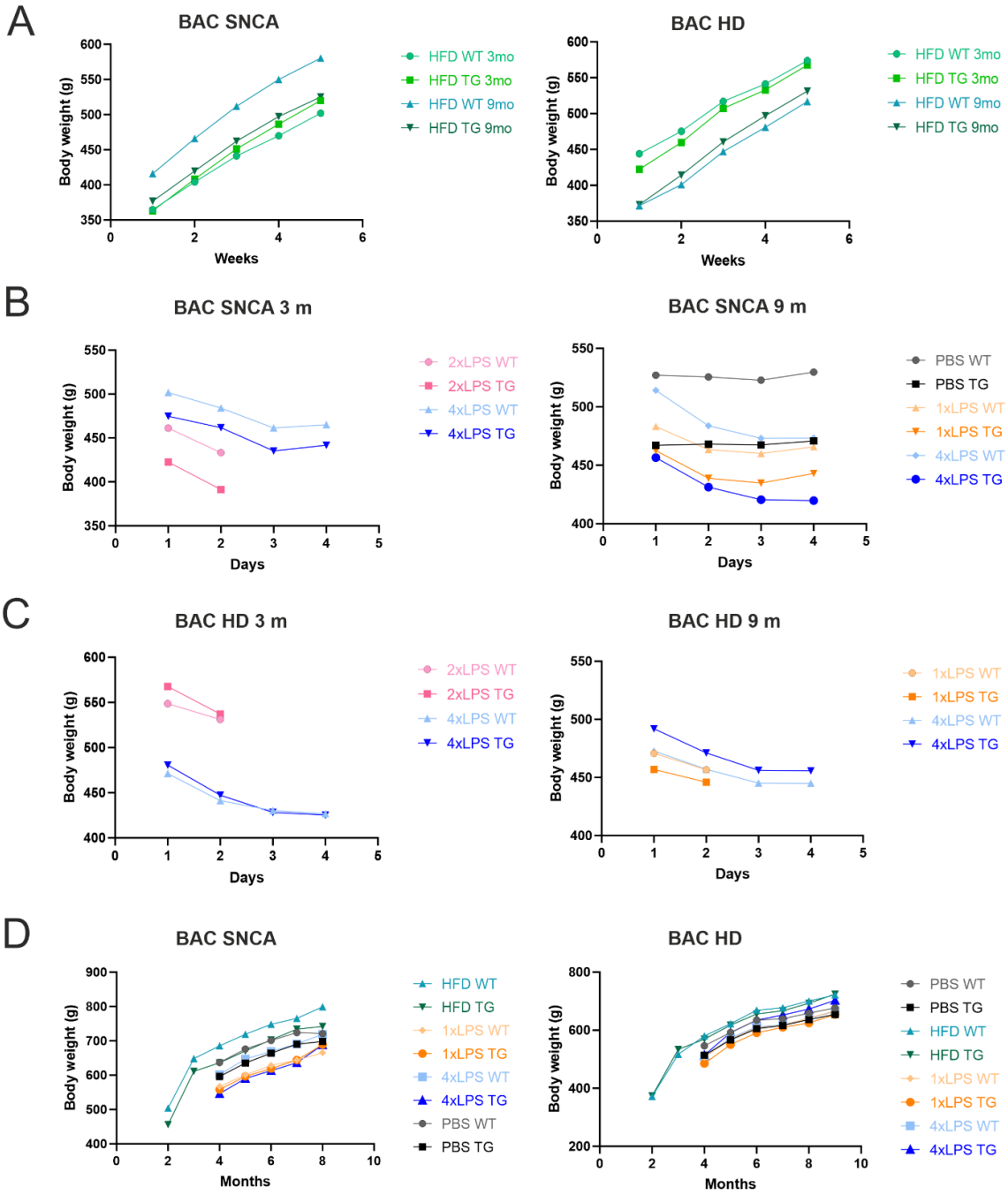

Figure 3.5: The changes in the body weight of BAC SNCA and BAC HD rats with LPS and HFD.

Figure 3.5: A. The weight graphs show fluctuations in BAC SNCA and BAC HD rat cohorts aged 3 and 9 months with HFD. BAC SNCA TG rats at 3 months exhibited a 43% weight increase between one and five weeks, and 39% at 9 months. BAC HD TG rats showed a 34% increase at 3 months and 42% at 9 months. The study included the following numbers of animals: for BAC SNCA (HFD – 6 TG & 6 wild-type (WT) for the 3-month cohort, HFD – 12 TG & 12 WT for the 9-month cohort), and for BAC HD (HFD – 6 TG & 6 WT for both the 3-month and 9-month cohorts). **B.** Weight graphs of BAC SNCA 3 months and 9 months cohort representing the differences in the LPS treatment groups with the control group (PBS). At 3 months, BAC SNCA TG rats showed a 7% weight decrease after both 2xLPS and 4xLPS. For the long-term cohort, the comparisons were made between the control group and the LPS injections received each day. In the 9 months group, the 1xLPS group received one LPS injection on a single day, followed by 3xPBS injections, and the 4xLPS group received four LPS injections on four consecutive days. It was observed that 1xLPS TG and 4xLPS TG exhibited a decrease of 5% and 7% when compared with the PBS TG group. The number of animals considered were – BAC SNCA 3 months cohort (2xLPS – 5 TG & 5 WT, 4xLPS – 6 TG & 5 WT) and BAC SNCA 9 months cohort (PBS – 12 TG & 12 WT, 1xLPS – 12 TG & 12 WT, 4xLPS – 12 TG & 12 WT). **C.** Weight graphs of BAC HD 3 months and 9 months cohort representing the differences in the LPS treatment groups. TG rats at 3 months showed a 5% decrease after 2xLPS and 11% after 4xLPS. In the 9-month cohort, TG rats exhibited 2% and 7% decreases after 1xLPS and 4xLPS. For these graphs, the number of animals taken into account was – BAC HD 3 months cohort (2xLPS – 6 TG & 6 WT and 4xLPS – 6 TG & 6 WT) and BAC HD 9 months cohort (1xLPS – 12 TG & 11 WT, 4xLPS – 11 TG & 12 WT). **D.** Some of the rats that received injections at the age of 3 months were kept longer to see the long-term effects of immune memory, and their weight changes were constantly monitored every month. Long-term monitoring at 9 months showed weight increases in BAC SNCA TG rats (17% with PBS, 44% with HFD, 23% with 1xLPS, and 26% with 4xLPS) and BAC HD TG rats (27% with PBS, 61% with HFD, 34% with 1xLPS, and 36% with 4xLPS). Both cohorts displayed the highest weight change with the HFD group. During the span of six months, some animals became sick, resulting in a lower number of animals being taken into account for specific groups, which include – BAC SNCA (1xLPS – 12 TG & 12 WT, 4xLPS – 12 TG & 12 WT, PBS – 12 TG & 12 WT, and HFD – 9 TG & 9 WT) and BAC HD (1xLPS – 12 TG & 11 WT, 4xLPS – 11 TG & 12 WT, PBS – 11 TG & 11 WT, and HFD – 12 TG & 12 WT). These changes in body weight in the rats might be associated with the sickness behaviour that was observed in the rats, resulting in further alterations in the cytokine level in blood and brain (P. Liu 2022).

3.4 Neuropathology of rats over-expressing alpha-synuclein

3.4.1 Human alpha-synuclein expression throughout the brain of BAC SNCA rats

For the generation of the BAC SNCA transgenic rat, a bacterial artificial chromosome (BAC) construct was used, containing all the coding regions, intronic regions, and human regulatory promoter elements that led to alpha-synuclein (a-syn) induced pathology in the brain (Nuber et al. 2013). To investigate the pathological differences between a TG and a WT animal, human a-syn expression was detected with a human-specific antibody 15G7 using the IHC method. This antibody was of particular interest since the TG animal will also express the human alpha-synuclein in addition to the endogenous signal, and

thus, this will be helpful to confirm the genotypes of the animal.

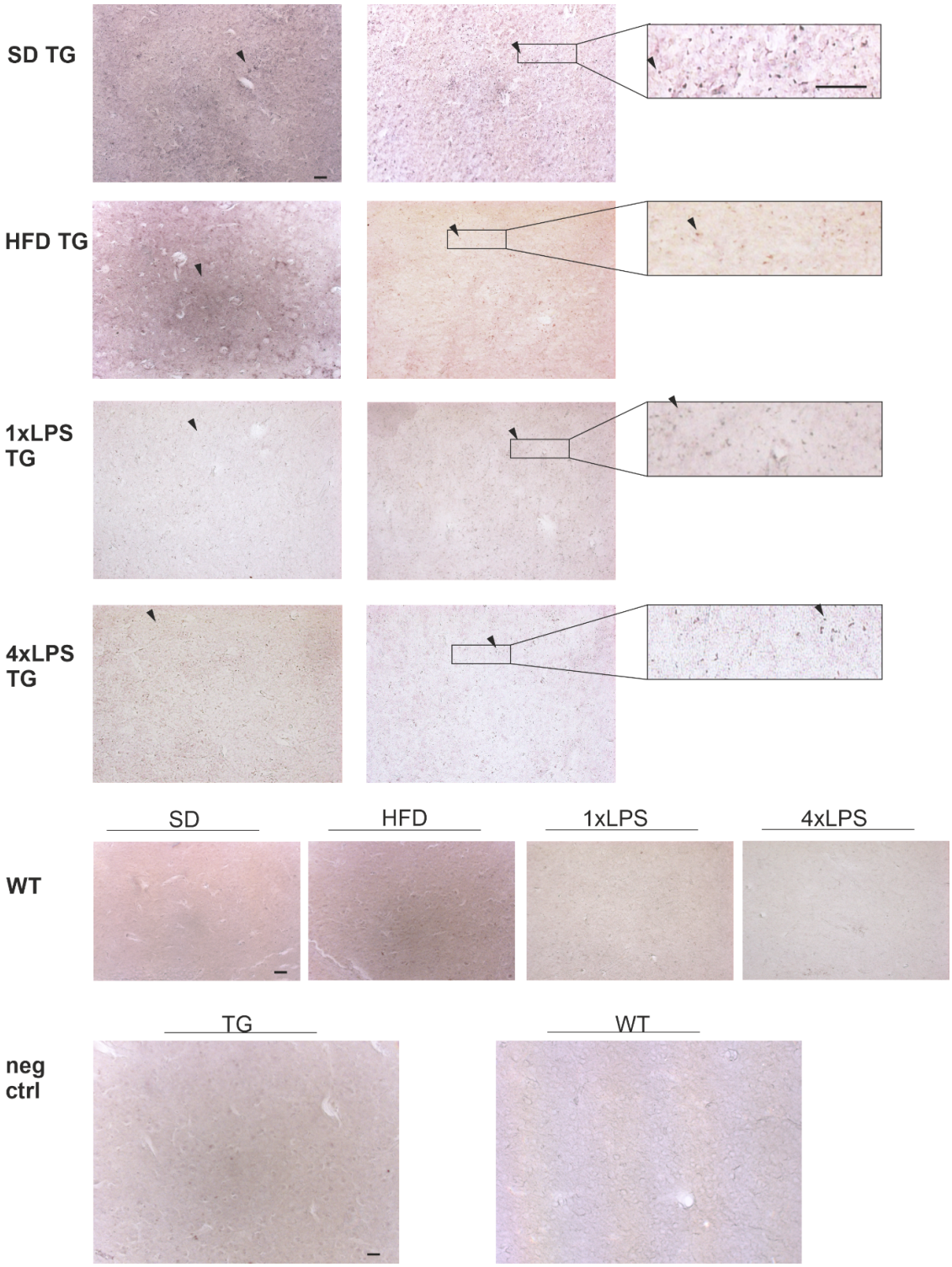

Figure 3.6: Neuropathological staining of human a-syn in BAC SNCA 9-month-old rats. There have been considerable differences between the WT and TG groups, confirming the genotype-dependent differences between the groups. Zoomed-in images of the staining with the scale bar have been provided. Sagittal sections of BAC SNCA were stained with human synuclein 15G7 and were detected with DAB staining. The arrowheads indicate the positive accumulation of a-syn granules in the intra-cellular and nuclear region of the cortex. Magnification = 20X, Scale bar =20 µm.

Since an increased number of a-syn aggregates are present with increasing age, 9-month-old rats were stained with 15G7 for detecting human a-syn, and the region examined was the cortex in the forebrain. Depositions of human a-syn in granular form were found in the intracellular and intranuclear regions of the cortex (Fig. 3.6). This helped confirm the genotypes of all the animals present in the 9-month-old cohort, reflecting human-specific staining of a-syn as described earlier (Nuber et al. 2013).

3.4.2 Accumulation of phosphorylated a-synuclein aggregates in the brain of BAC SNCA rats

For investigating total a-syn (human + rodent a-syn) and phosphorylated a-syn on Parkinson's BAC SNCA rats, 9-month-old rats were subjected to immunofluorescence stainings. Additionally, nuclei were stained with DAPI to check the intranuclear accumulations of a-syn in the brains of BAC SNCA rats. Phosphorylated a-syn was specifically checked since phosphorylation at Serine 129 is very common in synucleinopathy and is an important post-translational modification of a-syn as stated earlier in Section 1.3.1.4. Phospho-serine 129 has been identified as the dominant modification that has been pathologically found in PD disease brains (Anderson et al. 2006; Ghanem et al. 2022). To better understand the pathology of BAC SNCA rats, phosphorylated a-syn was included in our staining, which could also provide insight into how the treatments influence the pathology at 9 months of age.

For detecting total a-syn, an antibody specific to both humans and rats was used (Anti-alpha synuclein, mc42, BD Biosciences), and for detecting phosphorylated a-syn, an antibody specific for the detection of phosphorylated serine 129 was used (EP1536Y, Abcam). Expression of total a-syn was spread throughout the cortex and striatum region in 9-month-old BAC SNCA rats and. The positive spread of total a-syn in the TG animals was associated with the inclusion formation around the cell body and was observed in all the treatment groups without any visible differences (Fig. 3.7A)

Phospho-serine 129 stainings showed a granulated deposition of a-syn in the TG brains at the age of 9 months. Studies have earlier concluded that the striatum region shows higher deposition for PD aggregates (Duda et al. 2002). Thus, cortex, striatum, and cortex-striatum junction regions were explored for phospho-serine 129 deposits, and cytoplasmic accumulations of phospho-serine 129 were detected. Staining with DAPI revealed the formation of aggregates in the perinuclear region in BAC SNCA rats (Fig. 3.7B). Striatum displayed a higher number of phosphorylated a-syn, as stated earlier in the study. While there was a certain variability visible between the samples, there was a higher deposition of signal in HFD TG and 1xLPS TG, and thus a quantification of the number of aggregates was necessary to understand how the treatments affected the pathological aggregation of phosphorylated a-syn.

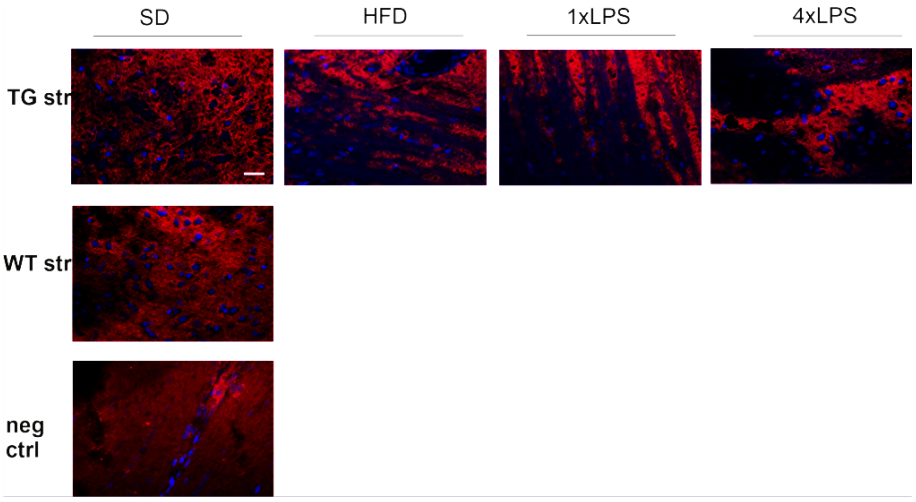

(A) Total alpha-synuclein

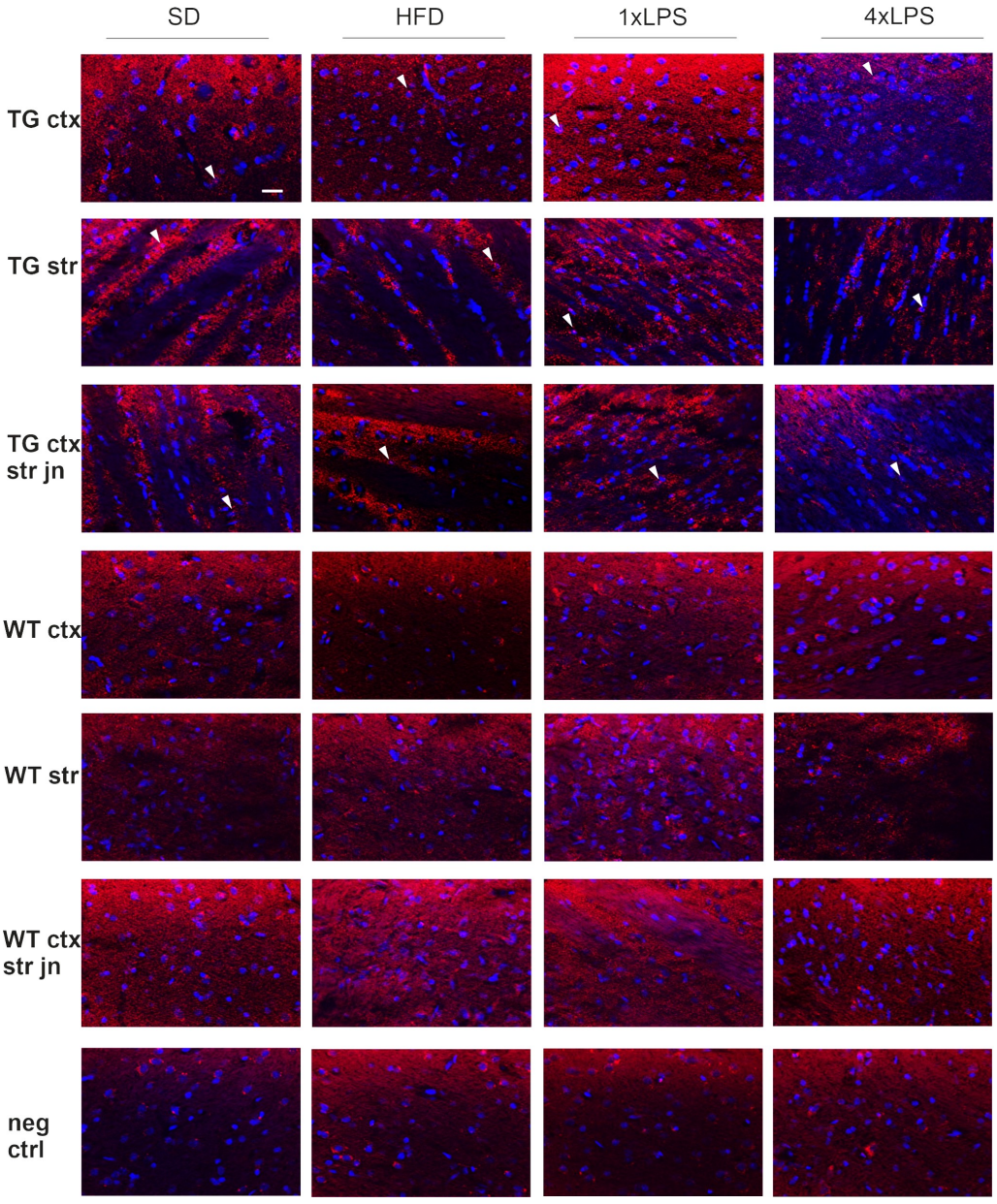

(B) Phosphorylated alpha-synuclein

Figure 3.7: Accumulation of total and phosphorylated a-syn deposits in BAC SNCA 9-month-old rats.

Figure 3.7: A. Sagittal sections of BAC SNCA rats were stained to assess total a-synuclein expression, particularly in the striatum, and to examine the difference in phospho-serine 129 accumulation with treatment. Notably, the total a-syn signal in treated animals spreads throughout the striatum, covering the entire region like a net. However, the effect of treatments on total a-syn pathology was not explicitly determined. Negative controls ruled out false positives. Magnification = 40X, Scale bar =20 µm, red channel = total a-syn, blue channel = DAPI.
B. Additionally, staining for phospho-serine 129 (EP1536Y) was performed with six animals from each treatment group, and cortex, striatum, and cortex-striatum junction regions were selected to check for phosphorylated a-syn deposits. An increased deposition of phosphorylated a-syn in the striatum was observed as compared to the cortex and cortex-striatum junction, particularly in the HFD and 1xLPS TG groups, marked with arrowheads. There have been increased perinuclear and cytoplasmic accumulations of phospho-serine 129 in the striatum and in the cortex, respectively. Minimal deposition was observed in the WT group, further confirmed by negative controls, indicating the specificity of the staining. Magnification = 40X, Scale bar =20 µm, red channel = phospho-serine 129, blue channel = DAPI.

3.4.3 Striatal accumulation of large pS129 aggregates is selectively enhanced in 4xLPS BAC SNCA rats

The description of the quantitative analysis has been described above in Section 2.3.12. The phospho-serine 129 counts were usually small and round in shape. Phosphorylated a-syn granules were observed in the cytoplasmic and perinuclear regions within the size range mentioned above in Section 2.3.12. The observed trends suggest that TG rats exhibit increased pS129 aggregate area, with statistically significant differences detected in the 10–30 pixel^2 and 30–70 pixel^2 size ranges. Unfortunately, no treatment-based effects could be observed, suggesting the role of genotype in pS129 accumulation even in the absence of external inflammatory stimuli (Fig. 3.8 A, B). While significant differences were observed in the aggregate area across genotype groups, no corresponding differences in pS129 counts were detected. This suggests that the number of aggregates remains relatively stable, but their size increases in TG animals.

To assess structural differences in pS129 aggregates, a morphology-based analysis was performed by classifying aggregate area into three size bins: 2–10, 10–30, and 30–70 pixel^2. Overall aggregate counts were excluded from the data since the significant changes were only reflected in the aggregate area. Across all TG groups, the aggregate area increased significantly with size, confirming the appropriate classification into small, intermediate, and large bins. Importantly, no significant treatment-dependent differences were observed, suggesting that the morphological characteristics of aggregates are predominantly driven by the genetic background, not by inflammatory or dietary interventions.

To explore whether aggregate deposition of pS129 continued at larger sizes, the range of the bin was extended to include aggregates up to 110 pixel^2. This increased the possibility of capturing any pS129 aggregate that may have been missed with the previous size threshold of 70 pixel^2. This analysis revealed a significant increase in both the count and area of large aggregates in the 4xLPS-treated TG group compared to SD TG, while genotype-based differences were not visible at this threshold range (Fig. 3.8 C, D).

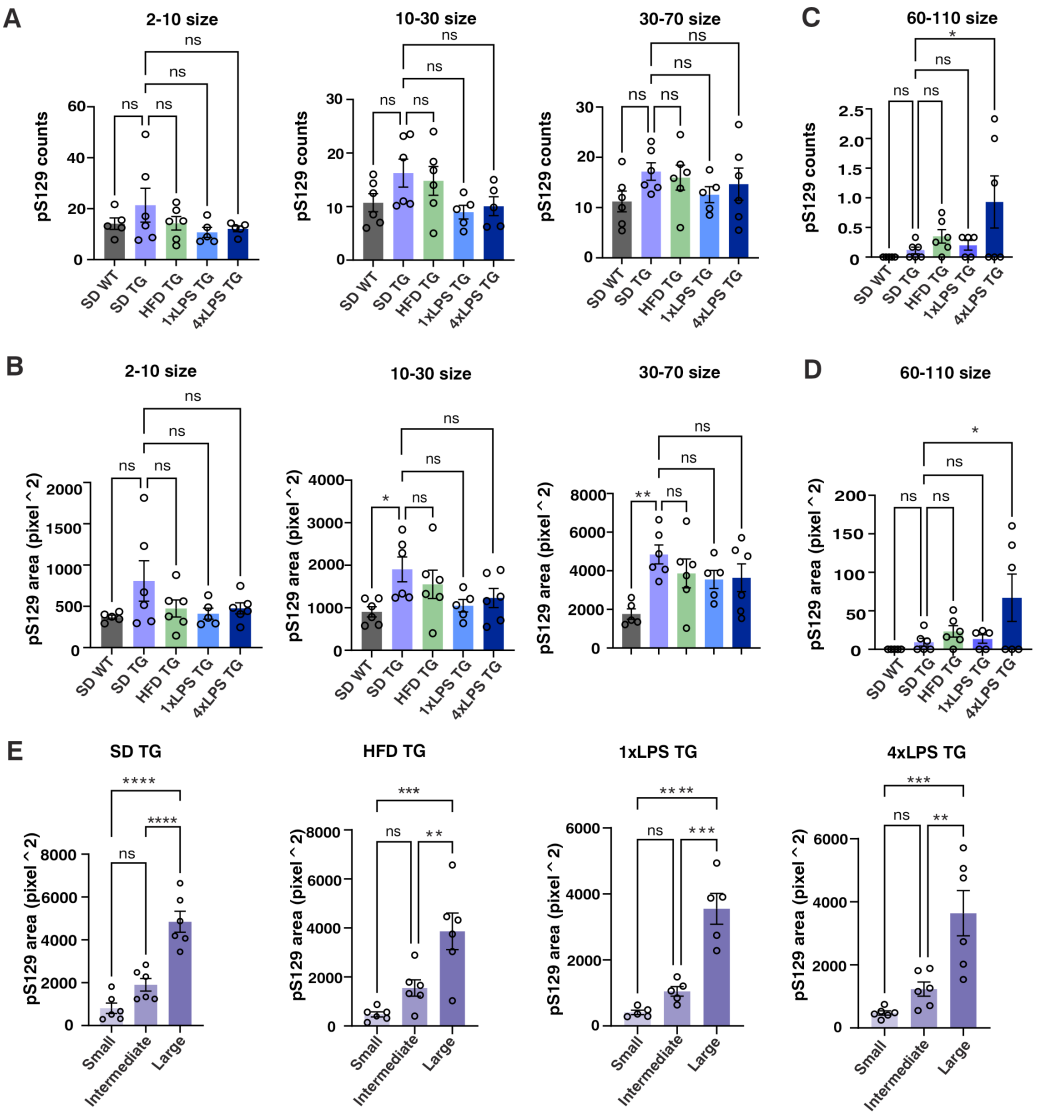

Figure 3.8: Quantified phosphorylated alpha-synuclein in BAC SNCA 9-month-old rats. **A.** Comparison of pS129 counts across different size bins (small pS129 - 2-10 pixel^2, intermediate pS129 - 10 -30 pixel^2 and large pS129 - 30-70 pixel^2, with circularity of 0.30-1.00. No difference was observed in ps129 counts across genotypes and treatments. **B.** Comparison of pS129 area across different size bins (small pS129 - 2-10 pixel^2, intermediate pS129 - 10 -30 pixel^2 and large pS129 - 30-70 pixel^2. Genotype-based differences could be observed for the intermediate and large pS129 particles. **C.** On a parallel analysis, for the large bins, the size was extended further to 60-110 pixel^2, with a circularity of 0.20-1.00, and an increase in pS129 counts with 4xLPS has been observed. **D.** Quantification of the pS129 area has been performed here with a bin size of 60-110 pixel^2, and an increase of pS129 area could be observed with 4xLPS. This suggests that repeated injections of inflammatory stimuli may drive an excessive accumulation of pS129 in the forebrain of BAC SNCA rats. **E.** This panel specifically focuses on the distribution of pS129 area across 'Small', 'Intermediate', and 'Large' aggregate sizes within each TG group. Here, small pS129 is 2-10 pixel^2, intermediate pS129 is 10 -30 pixel^2 and large pS129 is 30-70 pixel^2. It suggests that a substantial portion of the pS129 pathology exists as larger, more complex aggregates. Data are mean ± SEM, n = 6, one-way ANOVA with Dunnett multiple comparison test and *p<0.05.

This suggests that while genotype contributes to aggregate accumulation, the formation of large phospho-serine aggregates may be driven by repeated inflammatory stimuli. These findings imply that genotype primarily influences the accumulation of small to intermediate phosphorylated alpha-synuclein aggregates, while chronic inflammation may promote the formation of larger deposits.

3.5 HFD treatment shows increased pathological aggregation of a-syn at the age of 9 months in BAC SNCA rats

Accumulation of protein aggregates is a pathological hallmark of many neurodegenerative diseases, and thus, their detection might be an important step in understanding these diseases. For running the filter retardation assay, an antibody specific for total a-syn (BD Biosciences) was used. Phosphorylated a-syn (EP1536Y) and human a-syn (15G7) were not detected in this case. 4 samples from each treatment group from the 3-month-old cohort and 12 samples from each treatment group from the 9-month-old cohort were considered. Some HFD rats were eliminated from the study after they fell sick to the treatment, so there were nine samples present from the HFD group in the long-term cohort. After 20 µg of protein were loaded on a nitrocellulose membrane and a Filter retardation assay was performed, an age-dependent increase in the insoluble aggregates of a-syn was observed at the age of 9 months.

By comparing the WT and TG in both cohorts, TG showed a significantly higher aggregate load. In the 3-month-old cohort, a reduction in insoluble a-syn aggregates was seen in all treatment groups compared to the SD group (Fig. 3.9). With the HFD group, there was a significant decrease of insoluble aggregates of a-syn at the age of 3 months and might indicate towards immune tolerance. On the contrary, HFD significantly increased pathological aggregates of a-syn at the age of 9 months. There were no significant differences amongst the LPS treatment groups. This could confirm that HFD treatment in BAC SNCA rats activates immune memory and after 6 months, it leads to an increased deposition of a-syn in the forebrain of these rats (Fig. 3.9). Statistical significance was tested using one-way ANOVA as stated above in Section 2.3.13.

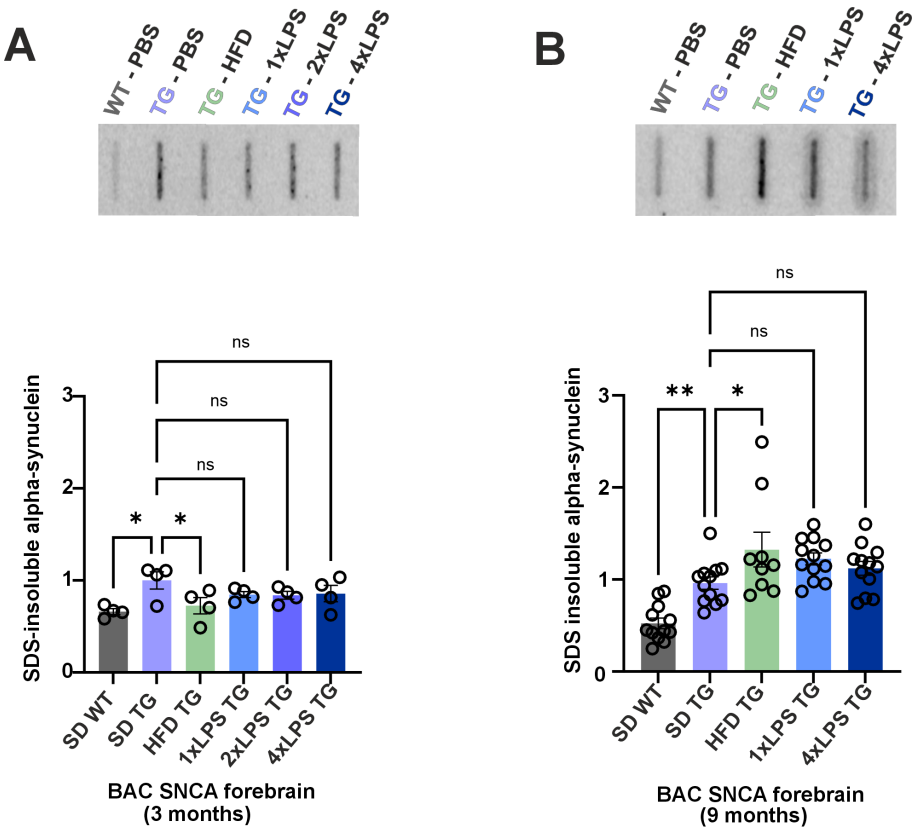

Figure 3.9: Filter retardation assay revealed an increased a-syn aggregation with HFD at the age of 9 months.

The respective blots illustrate the filter retardation assay of BAC SNCA 3 months and 9 months cohort using total a-syn antibody (BD Biosciences). There are significant differences between the WT and TG groups in both age groups. As described earlier, the HFD group showed opposite effects in the acute and long-term groups. By looking at the long-time cohort, HFD increased the level of SDS-insoluble a-syn in the forebrain, pointing towards immune training, whereas, for the acute group, it led to a decrease in the a-syn in the forebrain, indicating an immune tolerance effect. Statistical analysis was performed with one-way ANOVA, where *$p<0.05$ and multiple comparisons were performed using the Dunnett statistical test. Data are presented as mean ± SEM with n = 4 for the 3-month cohort and n = 12 for the 9-month cohort, except for n = 9 for the HFD TG group. A 27% decrease in insoluble a-synuclein was observed in the HFD group within the acute cohort, while a 37% increase in insoluble a-synuclein was noted in the HFD group compared to the SD group in the long-term cohort.

3.6 Acute cohort does not reveal any treatment based effects in BAC SNCA rats

After understanding the aggregation pattern of the SDS-insoluble aggregates of a-syn, a Western blot from the brain homogenates was further performed to check the effects of treatments on a-syn monomeric and oligomeric forms. Since a phosphatase inhibitor-containing buffer was not utilized for our blots, the possibility of detecting phosphorylated a-synuclein was ruled out, and only total a-synuclein was detected (human and rodent a-syn, BD Biosciences). The antibody specific for total a-syn binds to an epitope present

in the NAC domain (amino acid 91-96, BD Biosciences) and for the human a-syn (amino acid 116-131). The human a-syn was also included to check if the WT samples were getting any additional signals from this antibody. 20-25 µg of protein was used for western blotting. On each blot, two samples of SD WT, SD TG, HFD TG, 1xLPS TG, and 4xLPS TG were loaded, and all the groups were quantified relative to the SD TG samples present in the same blot. In total, 4 samples from each treatment group were analysed for the acute cohort.

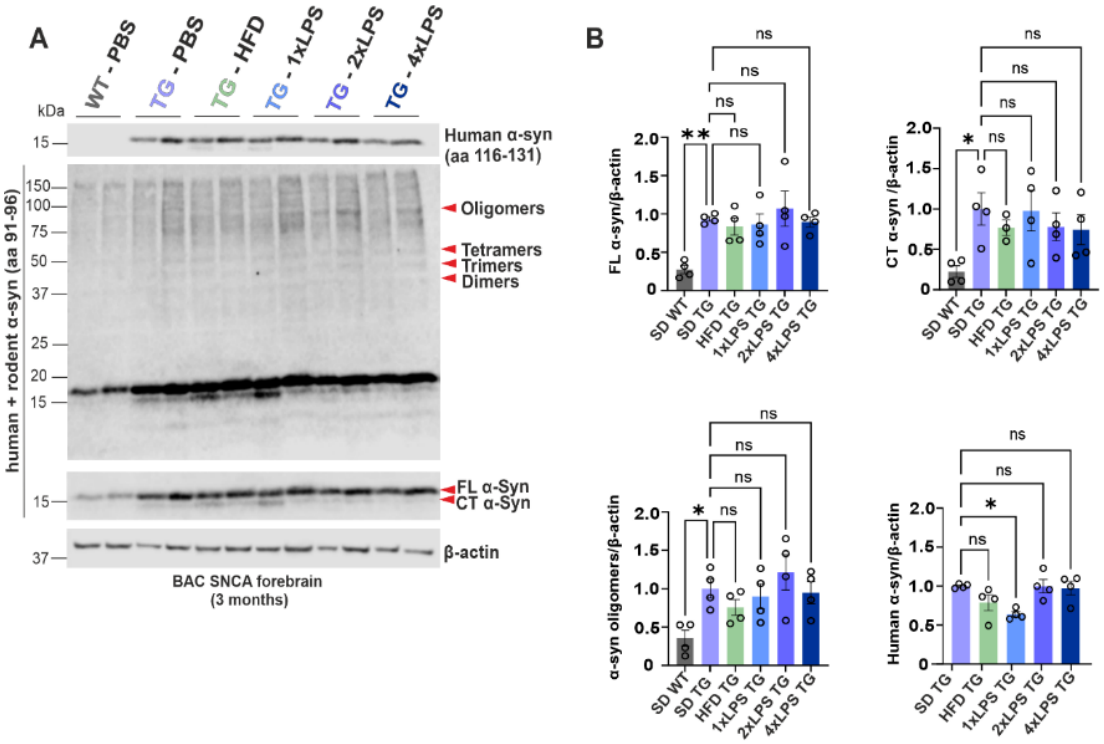

Figure 3.10: Western blot detection of BAC SNCA 3 months cohort did not show any treatment-based effects.

A. Western blot detection for 3-month and 9-month cohorts was done using the antibody specific for total a-syn from BD Biosciences. Two samples from each treatment group and SD WT group were analyzed. Detection with total a-syn resulted in full-length, C-terminal, dimer, trimer, tetramer and oligomeric levels of a-syn. The higher molecular weight of a-syn was less visible for the WT group. Further, human a-syn was also detected for the TG group. **B.** After quantification of the total a-syn normalized to β-actin, no significant differences were observed in between the treatment groups, apart from genotype differences. With the human a-syn, quantification revealed a significant decrease in the 1xLPS TG group with the SD TG group (36% reduction), which could point towards less soluble levels of human a-syn in the forebrain with the 1xLPS group, but an increase in the human a-syn levels with 2xLPS and 4xLPS TG groups does no point towards aggregation pattern of human a-syn. Data are mean ± SEM, n = 4, one-way ANOVA with Dunnett multiple comparison test, and *p<0.05.

While detecting the total a-syn, in addition to the monomeric form of a-syn, dimeric, trimeric, tetrameric and oligomeric forms of a-syn were also detected. In the monomeric form, both the full-length a-syn and C-terminal truncated a-syn were found. The C-terminal truncated form of a-syn was expressed very lightly in the WT group (negligible), and was more prominent within the different treatment groups in the TG section. Fragmentation (C-terminal a-syn) was stronger in the HFD and 1xLPS TG groups, relating to a more breakdown of a-syn with these treatments (Fig. 3.10). These truncated forms

of a-syn was slightly detected with the human a-syn too. As expected, the WT samples were not detected with the human a-syn and thus were excluded from the statistical analysis.

Significant differences between the two genotypes could be observed in the 3-month-old cohort. Since it is an early time-point, we did not see any major differences between the treatment groups. Upon quantifying the protein levels of a-syn with the control β-actin, there was a decrease in the HFD group in the full-length a-syn (FL a-syn), C-terminal a-syn (CT a-syn), oligomeric a-syn and human a-syn in comparison with the SD TG group, without any statistical significance. Amongst the LPS groups, the 2xLPS showed an increase in the FL a-syn and oligomeric a-syn with respect to the SD TG, whereas the fragmentation was decreased. The only statistically significant decrease was observed with the 1xLPS group in regard to the SD TG in the human a-syn group, that could relate to less production of human a-syn with the 1xLPS treatment (Fig. 3.10). Studies had earlier confirmed the presence of FL a-syn and CT a-syn in the forebrain of BAC SNCA rats, and an increase of FL a-syn was also observed with aging (Nuber et al. 2013).

3.7 HFD treatment leads to increased soluble levels of a-syn in BAC SNCA rats

Similar to the 3-month-old cohort, Western blots with two samples from each treatment group were performed to check soluble levels of a-syn in the long-term cohort, and 8 samples from each treatment group were considered. The antibody specific for total a-syn and human a-syn was used to detect the total a-syn and human a-syn protein levels and relate them to the acute cohort. When compared with the acute group, the long-term cohort displayed higher soluble forms of a-syn, and differences could be observed between the treatment groups. Stronger expression of the oligomeric forms of a-syn was observed in the 9-month-old cohort and the expression of CT a-syn was strongest in the HFD group in BAC SNCA rats.

Consistent analysis with the total a-syn revealed an increase of FL a-syn with the HFD group without any statistical significance. There was a decreasing trend in the fragmentation of a-syn with the 4xLPS group, indicating the presence of intact a-syn form with the 4xLPS group. Although the levels of SD TG and 1xLPS TG are not distinguishable in all the forms of a-syn and does not reveal clearly the effects of LPS on a-syn, there was a significant increase in the HFD group in the oligomeric form (Fig. 3.11). As stated earlier in Section 3.5, HFD treatment increased the levels of a-syn insoluble aggregates in the forebrain and the same effect in the soluble levels were also detected with western blotting (Fig. 3.11). Thus, HFD treatment leads to pathological aggregation in the BAC SNCA rats, relating to the role of environmental toxins in this disease.

When the two outlier samples from the 4xLPS group were removed by a statistical outlier test, there was a statistically significant decrease observed in the 4xLPS group in the CT a-syn. Since the number of samples (n = 12) is kept consistent in all the experiments, the outlier test was not included in the western blot further.

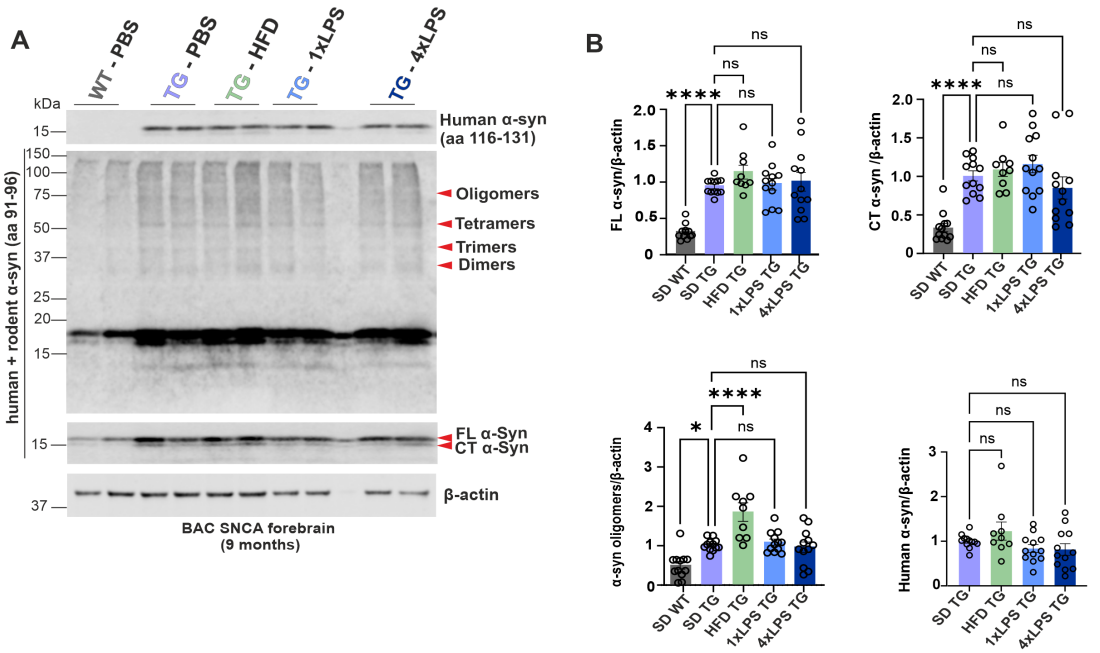

Figure 3.11: Western blot data of the BAC SNCA 9 months cohort revealed an increase in the oligomeric a-syn with HFD.
A. Representation of the blot with two samples from each treatment group, including SD WT. Similar expression of the total a-syn was observed in the 9-month-old in the BAC SNCA cohort, comparable to what was observed for the 3-month-old. Full-length, C-terminal, dimer, trimer, tetramer, and oligomeric forms of a-syn could be observed, and the expression of oligomeric forms was stronger for this cohort. Once more, the oligomeric form and C-terminal form of a-syn was less visible for the WT group. **B.** Upon quantification of the total a-syn normalized to β-actin, quite significant differences were observed between the WT and TG group. For the total a-syn, full-length, C-terminal and oligomeric forms of a-syn were detected. Although there were trends observed in full-length and C-terminal a-syn, there were no significant differences observed in between the treatment groups, with a mild decrease in the FL a-syn and a strong decrease with the fragmented a-syn. Since the data is variable, it did not reach a significance level. With HFD group, an increase in the oligomeric soluble levels of a-syn was witnessed (82% increase in HFD with the SD group). Dectection of human a-syn did not reveal any differences between the treatment groups. Data are represented as mean ± SEM, *p<0.05 with Dunnett multiple comparison statistical hypothesis and Grubbs's outlier test with alpha = 0.2 used to exclude statistical outlier.

3.8 Oligomeric-level changes were observed in the HFD group between acute and long-term cohort in the BAC SNCA cohort

We then wanted to investigate how the levels of FL a-syn, CT a-syn, oligomeric a-syn, and human a-syn differ between the two time points in the BAC SNCA cohort, and thus we conducted a comparison between the 3-month-old and 9-month-old cohorts. The analysis was followed with 4 samples from each treatment group of the acute cohort and 8 samples from each treatment group of the long-term cohort. Although the differences between the SD TG group was negligible, other treatment groups revealed some modifications

in the 9-month-old cohort. There was a significant increase in the oligomeric level of a-syn with the HFD group, with a 2-3 fold increase in the oligomerization in the 9-month cohort (Fig. 3.12, a-syn oligomers). Additionally, the HFD group showed a tendency towards an increase in FL a-syn and CT a-syn in the long-term cohort (Fig. 3.12, FL a-syn, CT a-syn). Looking at the LPS groups, there was no comparison for the 2xLPS group since it was only injected in the 3-month-old cohort to induce acute immune training. Amongst the 1xLPS and 4xLPS, no contrasting differences were seen between the acute and long-term cohort in the BAC SNCA rats (Fig. 3.12).

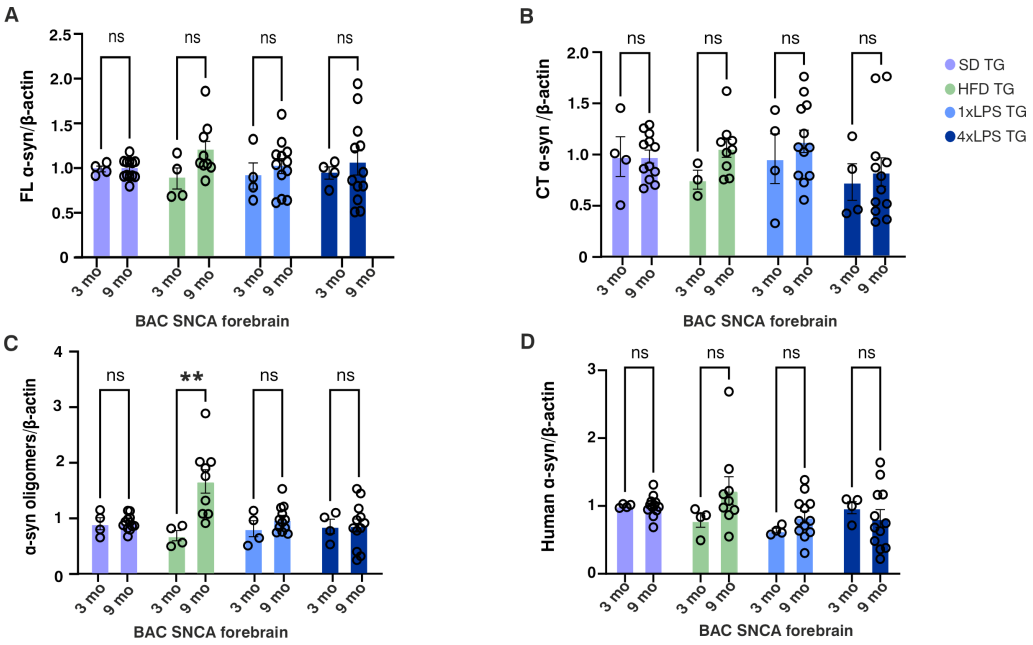

Figure 3.12: Western blot comparison of all the treatment groups between the acute and long-term group in the BAC SNCA cohort.
A. FL a-syn, **B.** CT a-syn, **C.** a-syn oligomers and **D.** Human a-syn. With older age, BAC SNCA rats display a higher amount of a-syn in the forebrain, as could be visible in the graphs. A higher amount of oligomeric a-syn was seen with the HFD group in the 9 months cohort (an increase of 45% when compared with the 3 months group). Data are mean ± SEM, n = 4 for 3 months cohort and n = 12 for 9 months cohort, with n = 9 for HFD for 9 months cohort. Statistical analysis was performed with a two-way ANOVA with *p<0.05.

3.9 Reduction of Lactate Dehydrogenase B expression in BAC SNCA rats

Lactate Dehydrogenase B (LDHB) is a key enzyme which takes part in glycolysis. LDHB in glycolysis converts lactate to pyruvate. Dysregulation of LDHB has been associated with mitochondrial impairment since studies have shown that its expression pattern changes with aging, and its change in pattern has been investigated in many neurodegenerative diseases like Parkinson's (Park et al. 2022). The microglia isolated from FACS were used for single-cell studies to check if microglial subtypes exist in BAC SNCA and BAC HD

disease models. 8 rats of 6 months of age were sacrificed for single-cell study. LDHB was one of the main genes differentially expressed in single-cell analysis. While comparing it with WT and BAC HD models, the expression of LDHB was found to be different and was less expressed for our BAC SNCA model (Fig. 3.13). Thus, to confirm the single-cell analysis, western blotting of LDHB was performed to check if the expression differs also in the protein level for the long-term cohort. Two samples of each treatment group were subjected to western blot analysis with a set of WT and TG samples on different blots and a strong expression of LDHB was observed in all samples. After normalization to β-actin, the SD TG signal was significantly downregulated in comparison with SD WT. Even though there were no treatment-based effects of LDHB, it was confirmed from the single-cell and western blot study that LDHB expression is reduced in BAC SNCA rats, which could be linked to the mitochondrial biogenesis in our study (Fig. 3.13).

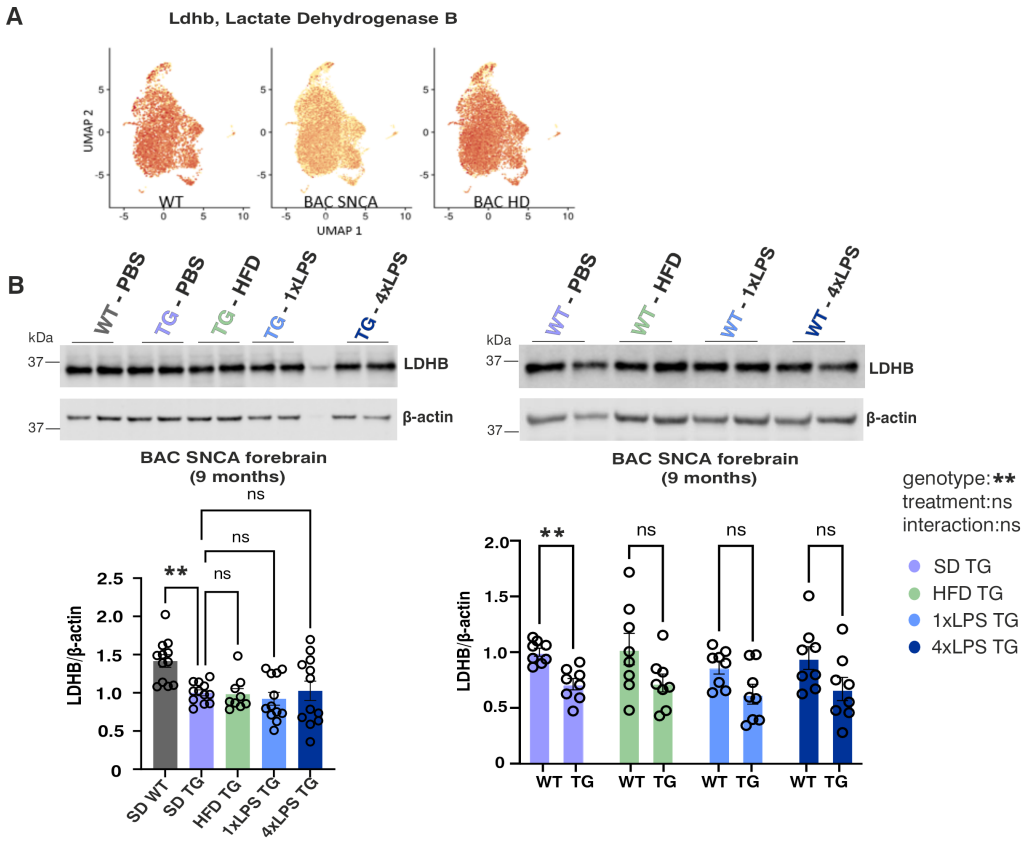

Figure 3.13: Western blot analysis showed a reduction in the expression of LDHB in the BAC SNCA TG rats at the age of 9 months.
A. Single-cell study confirming the lower expression of LDHB for BAC SNCA rats (n = 8, 33.282 cells age = 6 months). **B.** Western blot data of BAC SNCA 9 months cohort for LDHB. Two separate blots were used for western blotting, one containing two sets of each treatment group along with the SD WT and the other two sets of WT from each treatment group, keeping the same set for SD WT. After normalization of LDHB, genotype-based differences could be observed, with a significant reduction of SD TG as compared to the SD WT, confirming the lower expression of the TG group as seen in the single-cell analysis. Further, no treatment-based effects could be seen with LDHB. Data are mean ± SEM, n = 12 for the first graph, n = 8 for the second graph. Statistical analysis was performed using one-way and two-way ANOVA (for the grouped data) and multiple comparisons between the groups were analysed using the Dunnett test.

3.10 Reduction of HFD and LPS in complex V could point towards mitochondrial dysfunction in BAC SNCA cohort

As described in Section 1.3.1.6, mitochondrial dysfunction is one of the essential hallmarks of PD, and complex I deficiency is very common in damaged mitochondria (Moon and Paek 2015). Apart from complex I, a decrease in the function of complex III, IV and V has also been reported in PD patients [reviewed in (Keane et al. 2011)]. The SNCA gene has also been linked to mitochondrial toxicity (Mullin and Schapira 2013). SNCA plays an important role in regulating mitochondrial fusion and fission processes, along with mitophagy (Mullin and Schapira 2013). The Weighted gene co-expression network analysis (WGCNA) and Kyoto Encylopedia of Genes and Genomes (KEGG) for bulk-RNA sequencing of BAC SNCA 9-month-old rats was performed by our collaborators at DZNE, Tübingen. It revealed the various pathways involved in the BAC SNCA PD model, and one of the major ones was oxidative phosphorylation (Fig. 3.14A) (P. Liu 2022). Parallely, western blotting was done for mitochondrial oxidative phosphorylation proteins to check the effects of treatments on mitochondrial dysfunction in the BAC SNCA rat model, and to compare it with the bulk-RNA sequencing data.

For this, the BAC SNCA 9-month-old cohort was used. Two samples from each group of SD WT, SD TG, HFD TG, 1xLPS TG, and 4xLPS TG were taken on a blot, and from each treatment group, 12 samples were considered. The proteins were detected using the Total OXPHOS antibody, which detects all the five complexes of the mitochondria, namely, Complex I – NADH: ubiquinone oxidoreductase, Complex II – succinate dehydrogenase, Complex III – ubiquinol-cytochrome c oxidoreductase or cytochrome bc1 complex, Complex IV – cytochrome c oxidase and Complex V – ATP synthase. For our brain homogenate samples, there was no detection of complex II. A thick band of complex V was present, followed by bands of complex III and IV, and a less expressive band of complex I. Along with that, some high molecular weight oligomers were also present (Fig. 3.14B). All the complex proteins were detected exactly at the same height as other studies have reported.

After normalization to β-actin and doing a one-way ANOVA analysis, no changes between SD WT and SD TG were observed. Although the role of SNCA gene in regulating mitochondrial toxicity has been studied, it is not conclusive whether any mitochondrial deficiency is associated with the rat model of BAC SNCA used in our study. Thus, there was no proof to support why there is no dysregulation in the presence of the SNCA gene in the TG rats. Additionally, we do not see any major significant changes happening in the complex I of mitochondria. Despite of some minor trends in complex I, III and IV, it is not significant. HFD TG and 1xLPS TG in complex V show a significant decline with the SD TG (Fig. 3.14B). As stated earlier, complex V is important in carrying out oxidative phosphorylation, and its deficiency causes trouble in the ATP synthesis pathway. Oxidative phosphorylation was also one of the important pathways predicted in the WGCNA analysis. The presence of a-syn oligomers is known to induce dysfunction in the NADH and ATP synthesis pathway (Ludtmann et al. 2018). Since HFD treatment displayed a higher amount of oligomeric aggregates in the forebrain (Fig. 3.9), a dysregulation in complex V could be seen in our results (Fig. 3.14B). Dysregulation of the OXPHOS

chain leads to elevated production of reactive oxygen species (ROS), thereby fostering inflammation triggered by 1xLPS in our research findings. This confirms the fact that in addition to a-syn, HFD and LPS might play a role in impairing mitochondrial function (Fig. 3.14B). Additionally, a minor elevation is observed in the 4xLPS group compared to the 1xLPS group, suggesting that 4xLPS may not inherently induce mitochondrial dysfunction.

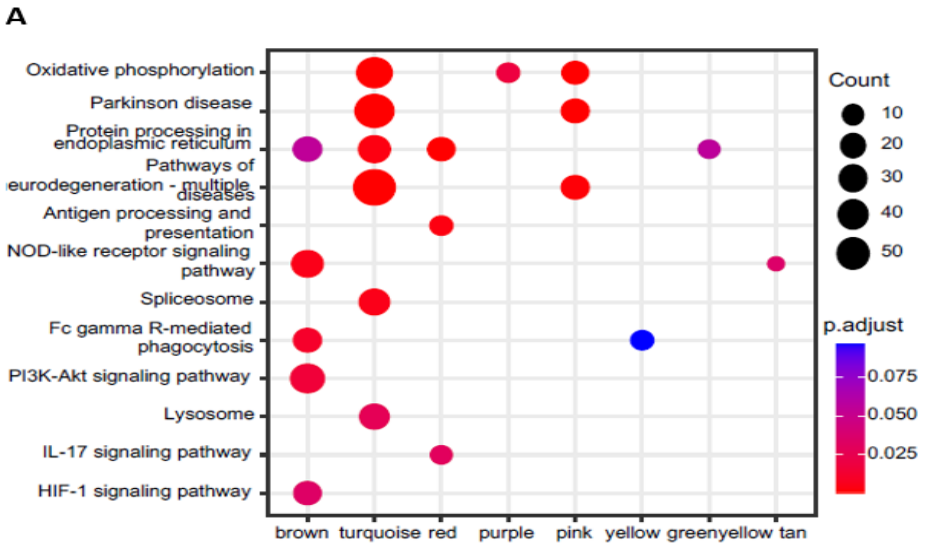

(A) KEGG module pathway of Parkinson's disease

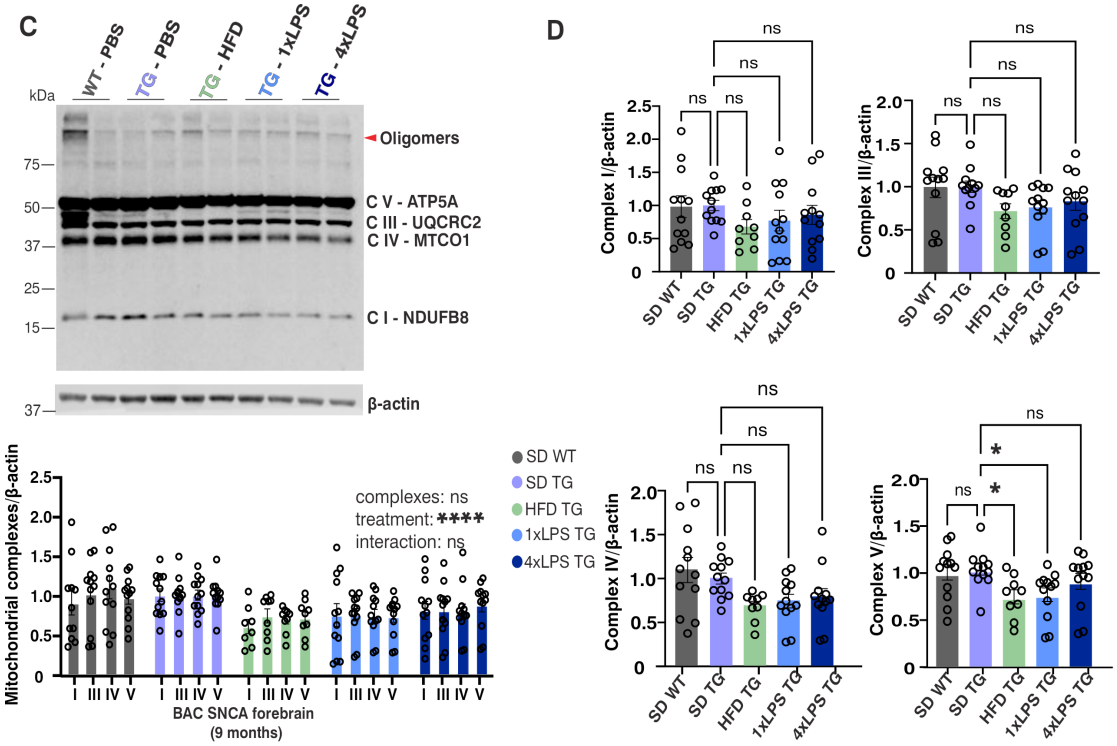

(B) Western blot analysis of the OXPHOS chain of BAC SNCA 9 months cohort

Figure 3.14: Mitochondrial dysfunction in BAC SNCA rat model.

Figure 3.14: A. The KEGG module pathway shows the various pathways present in Parkinson's disease and one of the highlighted pathways was oxidative phosphorylation. **B.(C.)** Western blot analysis of brain homogenates has revealed the presence of Complexes I, III, IV, V, and oligomeric configurations of mitochondrial OXPHOS proteins, using the antibody specific for OXPHOS (Abcam, ab 110413). Two sets of samples from each of the treatment groups including SD WT were detected on a blot and further quantified with β-actin. Complex I expression was very low and complex V expression was the strongest. **(D.)** Upon quantification of all the complexes, no genotype-based differences was observed. The HFD TG was always reduced when compared to SD TG – 32% in complex I, 28% in complex III, 31% in complex IV and significantly 29% in complex V. Although there are minor trends observed in each of the complexes, the significant decrease in complex V with HFD (29%) and 1xLPS (26%) point towards dysregulation in the ATP synthesis pathways. Also noticeably, there was an increase in the 4xLPS TG group in comparison with 1xLPS TG (19%) in complex V, indicating mitochondrial repair with 4xLPS. For the grouped data of mitochondrial complexes, there are no differences in between the complexes, although there are treatment-specific effects. Statistical analysis was done with one-way ANOVA using Dunnett multiple hypothesis testing and two-way ANOVA for the grouped data, where n = 12 (9 for HFD TG), data are represented as mean ± SEM and *p<0.05.

3.11 a-syn-VDAC 1 relationship points towards mitophagy in BAC SNCA cohort

To check how the mitochondrial dysfunction is happening, some of the key markers important for mitochondrial biogenesis were checked. These markers were detected on the same blot as the OXPHOS protein. The marker VDAC 1 is one of the key markers since it regulates the passage of metabolites and ions, and plays a role in apoptosis (Camara et al. 2017). Several research articles have pointed towards VDAC 1 ubiquitination, which is a critical stage involved in the regulation of mitophagy and apoptosis, and thus is important for understanding the pathogeneis of PD (Ham et al. 2020). a-syn is known potentially for blocking VDACs and does not allow the ions to pass through the channel (Rosencrans et al. 2021). Other than VDACs, a citrate synthase marker was used, which is a marker for detecting the presence of intact mitochondria. Changes in the levels of this marker usually point towards a problem with the mitochondrial mass (Foti et al. 2019). Shifts in mitochondrial fission and mitochondrial fusion were monitored using Opa 1 and Drp 1 markers. For PD, mitochondrial fragmentation has been studied extensively and occurs because of the problems happening with either mitochondrial fusion or fission (D. Santos et al. 2015).

After the detection of the OXPHOS protein, these markers were detected subsequently on the same blot as that of the OXPHOS chain, and all the markers were normalized to β-actin. There were no differences obtained in all the mitochondrial markers between the WT and TG group, similar to what was seen for the OXPHOS protein. This excludes the possibility of suggesting that a-syn aggregation contributes to the misregulation of VDACs in our BAC SNCA rats. Although there were no baseline changes in the TG group, there were significant reductions of VDAC 1 with HFD TG, 1xLPS TG and 4xLPS TG groups, with a more significant decrease with the 1xLPS TG group. The decline in VDAC 1 expression in these treatment groups could indicate the impairment of normal mitochondrial function and ATP synthesis with HFD and LPS treatments. The function of

HFD and LPS treatment is to induce inflammation, and that could disrupt mitochondrial biogenesis (Jill K. Morris and Geiger 2010; Batista et al. 2019). Also, for HFD, there was increased production in the oligomeric a-syn (Fig. 3.11), and it might have led to the dysregulation in the neuronal activity in BAC SNCA rats, which have also been demostrated in PD (Lu et al. 2013). A minimal variation was found between 1xLPS and 4xLPS groups (Fig. 3.15). There was no sign of 4xLPS acting as immune-protective in the case of mitochondrial activity.

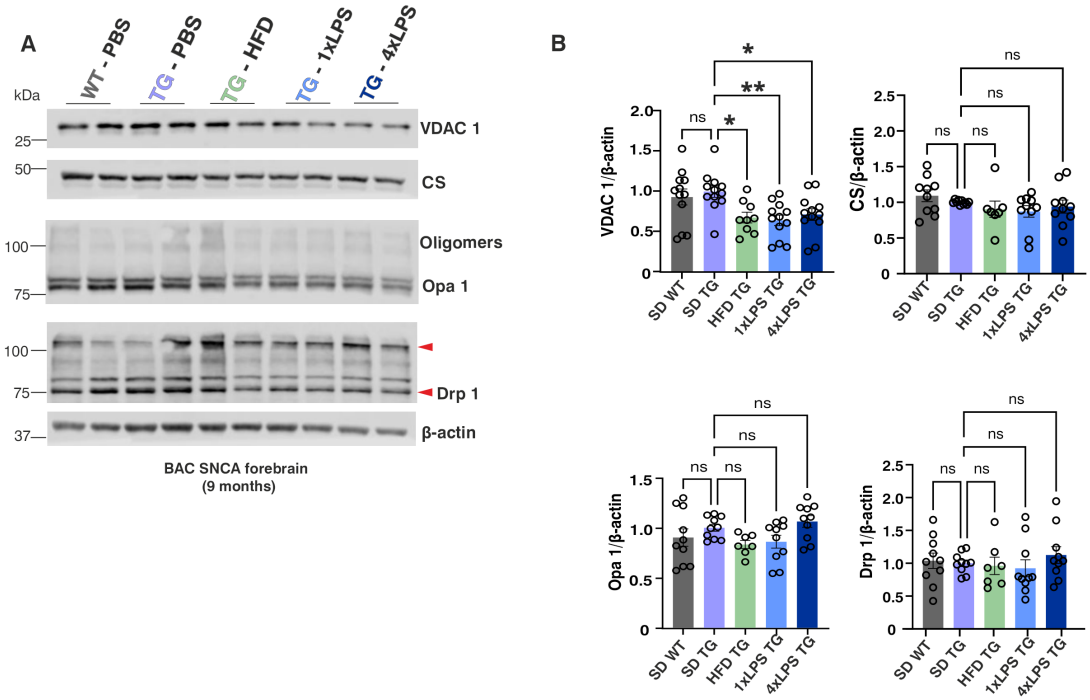

Figure 3.15: Analysis of mitochondrial membrane proteins and their association with mitophagy in the BAC SNCA cohort.
A. Western blot analysis of mitochondrial membrane proteins VDAC 1, CS, Opa 1 and Drp 1 with the antibodies specific for each of the proteins, normalized to β-actin. **B.** No genotype alterations could be seen between the WT and the TG group. With VDAC 1, there were significant changes observed in comparison to the control SD TG group, a reduction in the HFD TG group (32%), a reduction in the 1xLPS TG group (35%) and a reduction in the 4xLPS TG group (28%). An increase in 4xLPS TG could be seen with respect to 1xLPS TG (11%). The decline in VDAC 1 expression in HFD and LPS groups confirm the possibility of mitochondrial impairment and misregulation with the production of ATP. The CS marker analysis does not point towards loss of mitochondrial mass. Further, with Opa 1 and Drp 1, no substantial findings were noted regarding mitochondrial fusion and fission in our rat model. An increase in the 4xLPS TG group with 1xLPS TG has been seen for both Opa 1 and Drp 1, without any statistical significance (23% for Opa 1 and 21% for Drp 1). Data are mean ± SEM with one-way ANOVA and Dunnett multiple comparison with *p<0.05 was performed, where n = 12 for VDAC 1 and n = 10 for CS, Opa 1 and Drp 1, including n = 9 for all HFD TG samples.

Upon detection with citrate sythase (CS) marker, there were no changes observed between the treatment groups, revealing nothing about the mitochondrial mass in our BAC SNCA samples. Further, detections were done using Opa 1 and Drp 1 for checking mitochondrial fusion and fission, respectively. Despite the fact that there was no statistical significance, some trends were observed. The increasing trend in 4xLPS TG with respect to SD TG in Opa 1 could indicate increased mitochondrial fusion happening in our samples. On one

hand, where mitochondrial fission lead to mitochondrial fragmentation, fusion can lead to an elongation of the length of mitochondria (Westermann 2010). Thus, increased fusion may lead to an increase in oxidative phosphorylation, also preventing loss of metabolites and ions from the mitochondria (Yao et al. 2019), which might indicate a mitochondrial-specific repair with 4xLPS. Other trends in Opa 1 were not pointing to any direction. For Drp 1, our samples do not provide clear insight into the role of mitochondrial fission with LPS and HFD. In general, the data suggest mitochondrial dysregulation in the presence of HFD and a single dose of lipopolysaccharide (1xLPS) (Fig. 3.15), and further the negligible baseline differences obtained between WT and TG could also direct towards the reduced amount of mitochondria present in the brain homogenates.

3.12 Role of cyclooxygenase-2 and beta-arrestin 1 as regulators of inflammation in BAC SNCA rat model

LPS injections have been linked to the activation of various cascade pathways, leading to the release of inflammatory mediators in both the bloodstream and the brain. Cyclooxygenase isoforms COX-1 and COX-2 are known to be the key mediators of inflammation and are produced upon LPS stimulations. Mostly, the COX-2 isoform is present in abundance with inflammation (Saba Aid 2008). While doing the KEGG pathway analysis for the BAC SNCA rat model, one of the genes that was enriched with 4xLPS treatment was COX-2, and thus, a corresponding Western blot to detect protein levels of COX-2 was performed, which could help to understand the inflammation effect on different treatments (P. Liu 2022).

β-Arrestins are a small group of proteins that interact with G-protein coupled receptors and are associated with membrane trafficking (Dwivedi-Agnihotri and Hemlata 2020). Also, β-Arrestins are critical regulators of inflammation, and their roles are altered with LPS triggers (Fan 2014). Earlier studies have pointed towards the decrease in the expression of β-Arrestin 1 in the transcriptional levels of macrophages once stimulated by LPS (Fan 2014). For PD, both β-Arrestin 1 and β-Arrestin 2 are involved in the pathogenesis of PD and usually, the β-Arrestin 1 stimulates microglial immune response and β-Arrestin 2 inhibits the inflammatory response (Fang et al. 2021). Thus, both COX-2 and β-Arrestin 1 were investigated to check the inflammatory effects with HFD and LPS.

BAC SNCA 9 months cohort was considered for this detection and two samples per treatment group including SD WT were taken for the detection of these two markers. For COX-2, double bands and oligomeric forms of COX-2 were detected around 75 kDa and was normalized to β-actin (Fig. 3.16). For COX-2, no genotype-level differences were observed. There were no significant differences between the treatment groups, but a rapid increase in COX-2 protein levels could be observed with 4xLPS TG, as was also detected from KEGG pathway analysis (P. Liu 2022), which might point towards an increased inflammatory response. Although it is far from being significant, it challenges our study of the decrease in aggregate size and the amount of FL a-syn present with 4xLPS TG. Further, detections were performed with β-Arrestin 1 (ARRB1), and all the treatment groups showed a reduced trend with SD TG, most significantly the LPS treatment groups 1xLPS TG and 4xLPS TG. A notable reduction was noted in both LPS treatment groups,

validating the induction of microglial immune responses with LPS in BAC SNCA rats. LPS treatments significantly inhibited the expression of β-Arrestin 1 (Fig. 3.16).

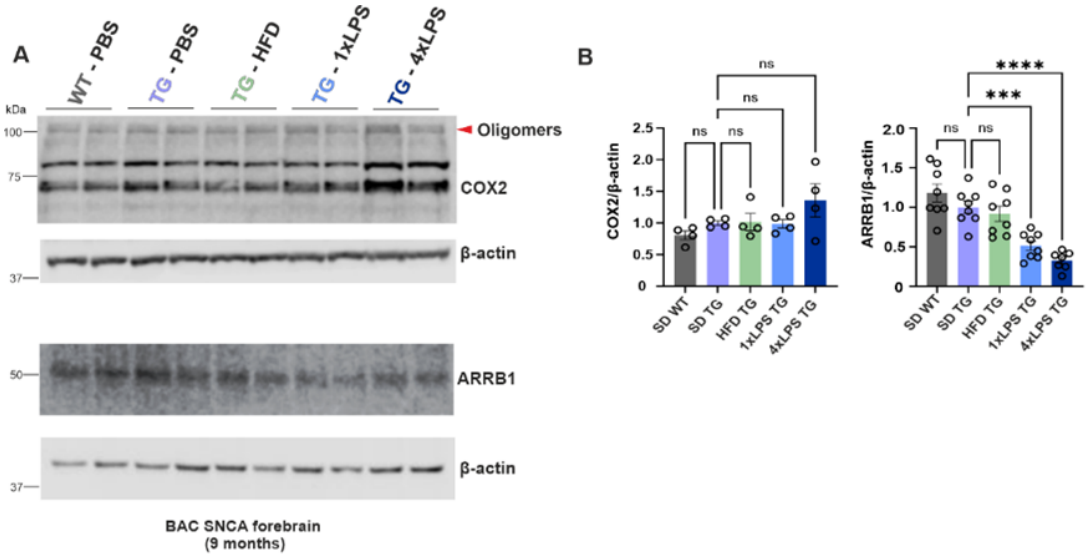

Figure 3.16: Inflammatory markers in the BAC SNCA rat model.

A. Western blot detection of COX-2 and ARRB1 with β-actin. Double bands of COX-2 expression could be seen, along with higher oligomeric detection. The expression of ARRB1 is faded and not that conclusive. **B.** After normalization with β-actin, no genotype and treatment-based alterations could be seen with COX-2, and the only difference visible is the upregulation of the COX-2 protein levels with 4xLPS TG (35% increase to SD TG). Further, on quantifying ARRB1, significant reductions with 1xLPS TG and 4xLPS TG could be observed in comparison to SD TG. A 67% decrease in 4xLPS and a 48% decrease in 1xLPS TG groups could be interpreted. Thus, both COX-2 and β-Arrestin 1 could point towards the inflammatory response of LPS caused in the forebrain of BAC SNCA rats. Data are mean ± SEM with a one-way ANOVA and Dunnett multiple comparison test including $^{*}p<0.05$, and n = 4 for COX-2, n = 8 for ARRB1.

3.13 Nuclear localization of mutant huntingtin has been observed with LPS treatment in BAC HD rats

To generate BAC HD transgenic rats, a human BAC construct was used containing the full-length huntingtin gene and the upstream and downstream regions with all the regulatory elements and the exons (Yu-Taeger et al. 2012). To investigate how pathological aggregation of huntingtin happens in BAC HD rats, brain sections of 9-month-old rats were exposed to immunohistochemistry stainings as previously described. Detection of huntingtin was done with the monoclonal mouse antibody EM48, which detects both human and mouse-specific huntingtin aggregates. DAB immunostaining was performed, and the accumulation of htt aggregates in nuclei was shown by Thionine staining.

The regions imaged were the cortex and striatum. Compared with WT, the TG animals

showed a dense population of granular forms of htt aggregates scattered throughout the cortex and in the striatum. The htt aggregates were round in shape and brown in color. The aggregates exhibited varying sizes and formed chain-like structures. They were observed in both the nuclei and the perinuclear region, appearing as either round or triangle-shaped structures (Fig. 3.17A). As quantification was not carried out for htt aggregates, unlike phospho-serine 129 for BAC SNCA, there is insufficient evidence to determine which treatment group is generating a higher quantity of aggregates. Nevertheless, the shared characteristics of nuclear localization and perinuclear accumulation of htt aggregates were observed in the LPS treatment groups 1xLPS and 4xLPS (Fig. 3.17B). An enlarged image has been provided to facilitate a more in-depth understanding of the aggregated form of mhtt (Fig. 3.17C).

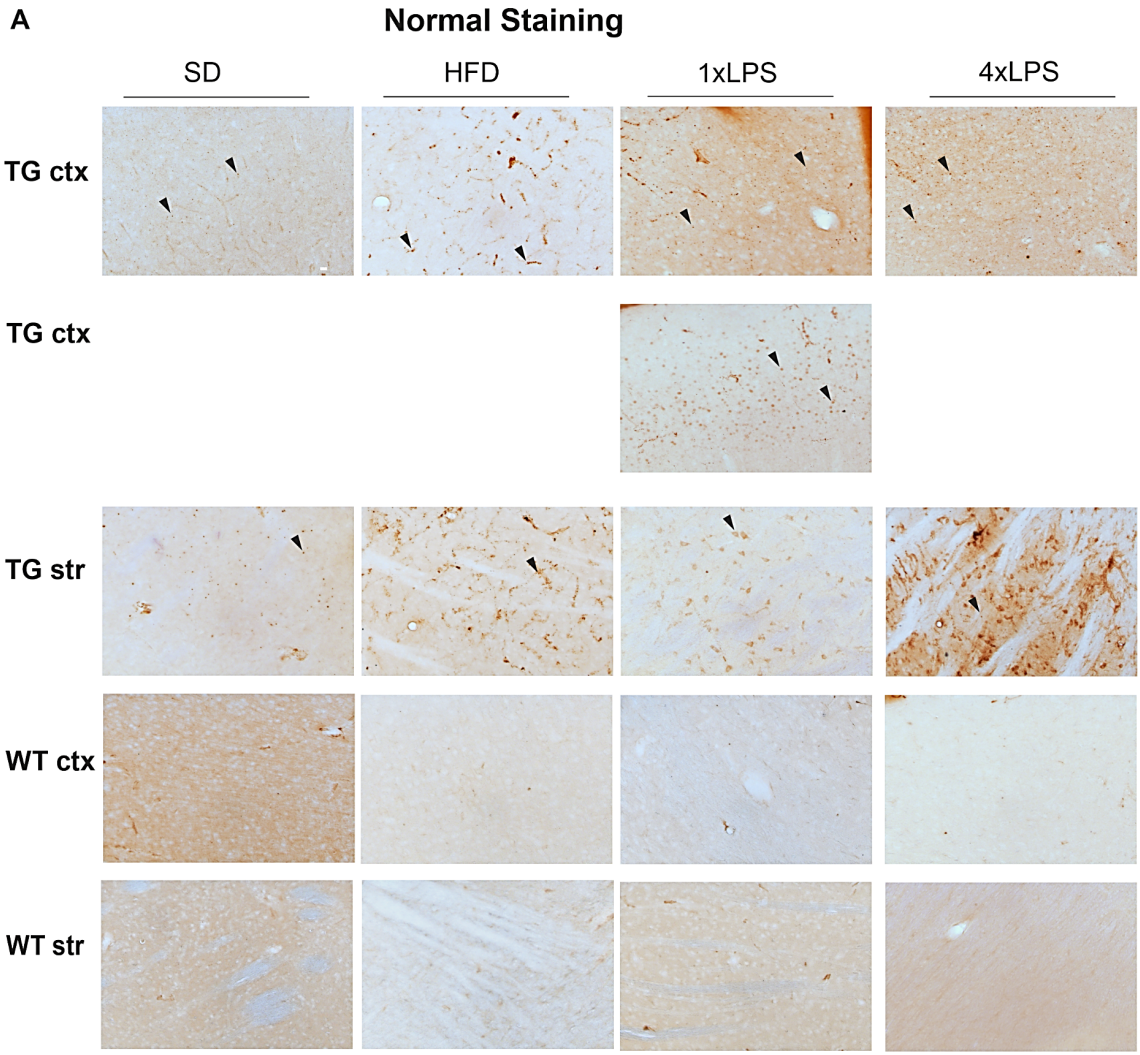

(A) Normal Staining showing the nuclear accumulation of mhtt in BAC HD TG rats at the age of 9 months.

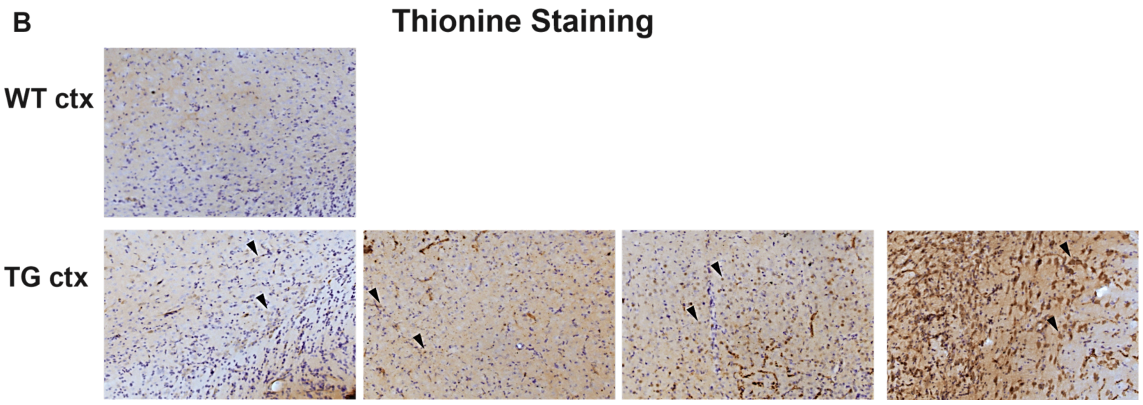

(B) Thionine Staining showing the nuclear accumulation of mhtt in BAC HD TG rats at the age of 9 months.

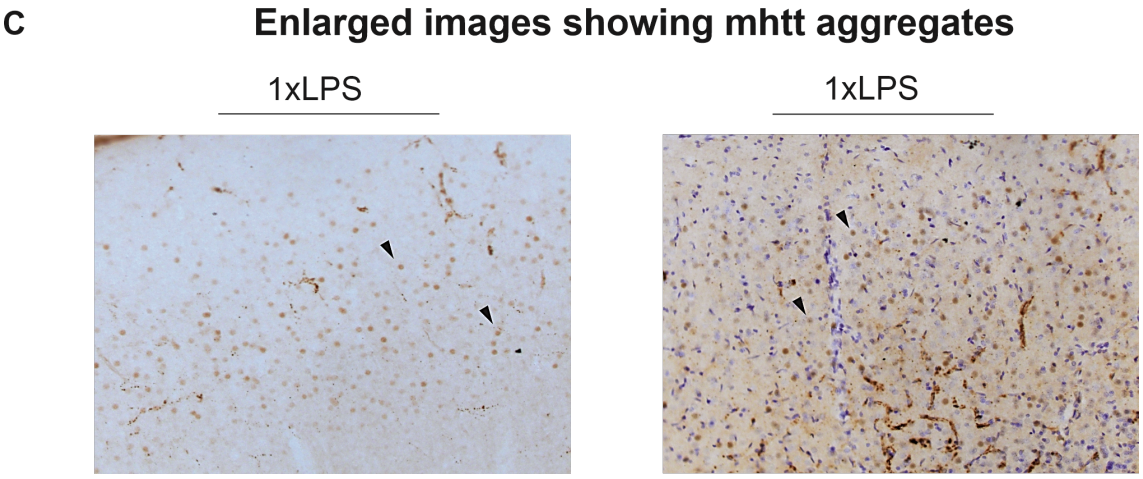

(C) Enlarged image of 1xLPS with normal and thionine staining.

Figure 3.17: Nuclear accumulation of N-terminal mhtt in BAC HD TG rats at the age of 9 months.

A. Htt aggregates were investigated using EM48 antibody which showed the spread of granular aggregates of mutant htt throughout cortex and striatum. The TG groups exhibit distinct aggregation patterns of mhtt with DAB, notably stronger expressions observed in the HFD TG, 1xLPS TG, and 4xLPS TG treatment groups compared to the SD TG. The aggregates are either round or chain-like, and the presence of perinuclear aggregates are abundant in 1xLPS and 4xLPS. The WT does not show any nuclear accumulation of mhtt.

B. Thionine staining of the samples were done to detect nuclear accumulation of mhtt aggregates. The WT does not show anything, while a greater incidence of nuclear and perinuclear accumulation, resembling round or triangle-shaped formations around the nucleus, has been noted in the LPS treatment groups. Additionally, there was an increase in the nuclear aggregation with HFD.

C. Enlarged examples of the 1xLPS images have been displayed here to show the aggregates with or without Thionine staining. Magnification = 40X, Scale bar =20 μm.

3.14 TR-FRET analysis shows no differences in soluble polyQ-expanded HTT among BAC HD rat treatment groups

TR-FRET analysis is a widely used approach to detect soluble and aggregated huntingtin levels (Baldo et al. 2012; Clemens et al. 2015; Singer et al. 2021). The amount of soluble huntingtin present in our samples was determined by a combination of antibody pair BKP1-Tb/ MW1-d2. Supernatants from BAC HD 3 months and 9 months cohort were considered for this analysis. After subtracting the sample signal from the background, substantial differences between WT and TG were observed, but no statistically significant changes were noted among the treatment groups in the 3-month and 9-month BAC HD rat cohorts. Only a minor reduction in the HFD group was observed, when compared with the SD group, without any significance. Thus, the TR-FRET data did not provide sufficient information to elucidate the aggregate-level changes of htt occurring with HFD and LPS in BAC HD rats (Fig. 3.18).

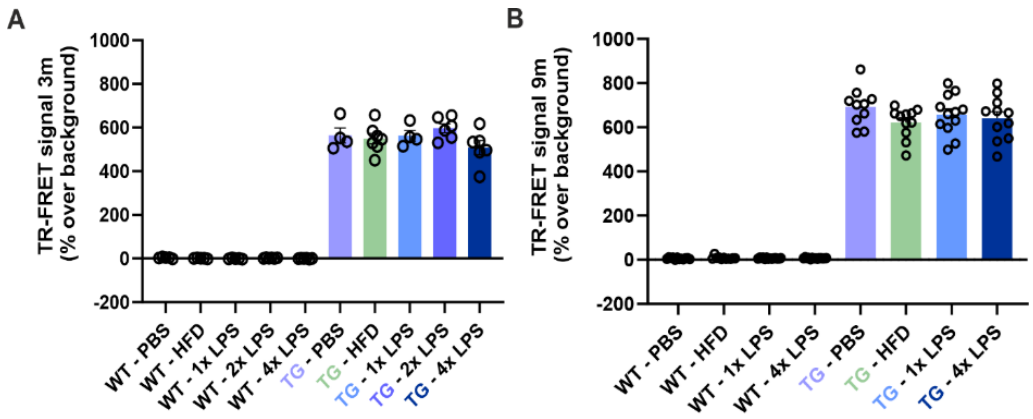

Figure 3.18: TR-FRET signal does not reveal significant changes in between the treatment groups in BAC HD cohort.
A.BAC HD 3 months cohort, **B.** BAC HD 9-month cohort. This detection was done using the antibody pair BKP1-Tb/ MW1-d2. Genotype-specific effects were evident, but there were no observable changes attributable to the treatment. Statistical analysis was performed with one-way ANOVA with Dunnett multiple comparison test and *p<0.05. The samples numbers vary with different treatment groups.

3.15 HFD and 4xLPS show a reduction in insoluble HTT levels at the age of 9 months in BAC HD rats

Since TR-FRET offered restricted insights into the impacts of treatment on soluble proteins, we subsequently conducted the Filter Retardation Assay to assess the presence of SDS-insoluble huntingtin in our samples. Oligomeric-level htt aggregates could be detected by this method. For the detection of SDS-insoluble polyQ-expanded htt levels, brain supernatants of the 3-month and 9-month cohorts were considered, and detection was

done using HTT-specific antibody 1HU-4C8. Supernatants from 3-month-old and 9-month-old BAC HD rats were considered for this assay. A total of 4-6 samples were taken from each treatment group in the 3-month-old cohort, while 12 samples were collected from each treatment group in the 9-month-old cohort. 10 µg of protein was loaded onto a nitrocellulose membrane and was detected. In both the acute and long-term cohorts, a genotype-based difference was observed, with TG exhibiting a higher aggregate count than WT. In the acute cohort, no alterations were observed among the treatment groups, although there is a declining trend observed in the 4xLPS group. In the long-term cohort, notable significant decreases were observed in both the HFD and 4xLPS groups when compared to the SD group. This suggests that in the context of Huntington's disease, immune tolerance may have been established in both the 4xLPS and HFD groups. This was opposite to that of the HFD group in Parkinson's, where there was an increased number of aggregates with HFD, indicating immune training. This may conclude that HFD and 4xLPS are acting as the 'good markers' in the case of HD and lead to a decrease in the pathological htt aggregation in the forebrain (Fig. 3.19).

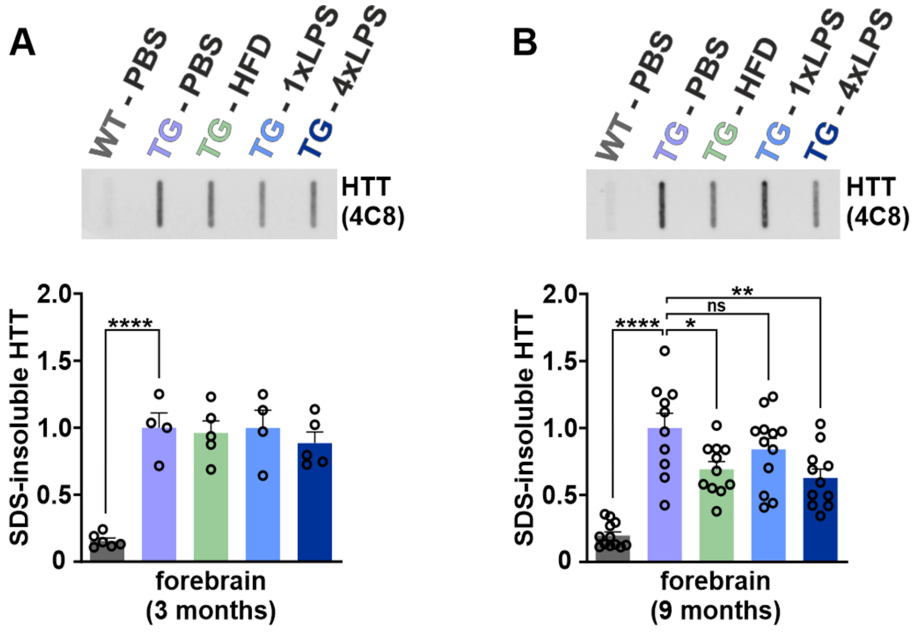

Figure 3.19: Filter retardation assay reveals a reduction in the htt accumulation with HFD and 4xLPS at the age of 9 months in BAC HD cohort.

The corresponding blots with the analysed results are displayed here. The analysis has been performed here with an antibody specific to Anti-Huntingtin (MAB2166, clone: 1HU-4C8). There were significant differences between the WT and TG groups in both cohorts. No treatment-based changes were observed in the acute group. Observing the long-term cohort, both the HFD (30%) and 4xLPS (37%) groups demonstrated a decrease in the level of SDS-insoluble huntingtin in the forebrain. For BAC SNCA, HFD elevated the pathological aggregation of alpha-synuclein, while conversely, HFD and 4xLPS diminished the number of huntingtin aggregates in the forebrain of BAC HD rats. Data are mean ± SEM. Statistical analysis was performed with one-way ANOVA, where *$p<0.05$ and multiple comparisons were performed using the Dunnett statistical test. For 3 months cohort, n = 6 (SD WT), 4 (SD TG & 1xLPS TG) and 5 (HFD TG & 4xLPS TG). For 9 months cohort, n = 12 (SD WT & 1xLPS TG), 11 (HFD TG & 4xLPS TG) and 10 (SD TG).

3.16 No treatment-based effects could be detected with Western blot in BAC HD

As the HFD and 4xLPS groups indicated a tendency towards decreased aggregation in Huntington's disease models, Western blotting was employed to examine soluble-level htt aggregates. This was done to gain insights into the impact of LPS and HFD treatments on the overall aggregation of huntingtin. 20-25 µg of the brain supernatants were used and for Western blotting, BAC HD 9-month-old cohort was considered, as there was no difference observed in the treatments at the age of 3 months. For the detection, 8 samples from each treatment group were considered, and two samples of SD WT, SD TG, HFD TG, 1xLPS TG, and 4xLPS TG were loaded on the same blot and were quantified with respect to the SD TG group. Western blotting was performed using 10% Bis-Tris gels and HTT-specific antibody 1F10, and high molecular weight and fragmented htt were visualized together.

Quantification with *β*III-tubulin revealed substantial differences between the WT and TG groups, with no observed treatment-related effects at this point. Intra-group variation was noted among samples, along with a significant degree of fragmentation (Fig. 3.20). Moreover, there was an elevation in the full-length htt HFD and 4xLPS TG, along with a reduction in fragmented htt with 4xLPS TG when compared to SD TG, although the differences did not reach statistical significance. Hence, the alterations noted in the HFD and 4xLPS TG group through the Filter Retardation Assay were not corroborated by the Western blot results. (Fig. 3.20).

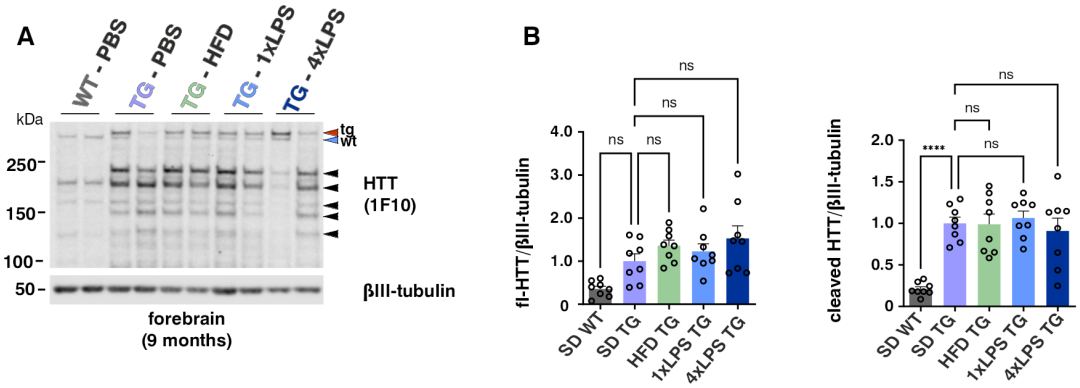

Figure 3.20: Western blot detection of BAC HD 9 months cohort does not show any treatment-based effects contrary to the Filter retardation assay.
A. The blot has been displayed above and the detection for mutant htt at the age of 9 months has been done using the antibody specific for anti-huntingtin 1F10 (BSM-54305R). Two samples from each treatment group and SD WT group have been loaded here and further normalized to *β*III-tubulin. Since differences were significant with the SDS-insoluble htt at the age of 9 months, a Western blot was further performed for this cohort. Here, the presence of both full-length (FL) htt and its fragmentation can be observed. **B.** No significant differences were observed between WT and TG for FL htt, whereas the cleaved htt shows significant upregulation with SD TG. No changes in treatment could be detected with FL htt and cleaved htt. An increasing trend in HFD and 4xLPS groups could be observed here with FL htt in comparison to the SD TG, opposite to the filter retardation story. Data are mean ± SEM, and one-way ANOVA analysis performed with Tukey multiple comparison test with *p<0.05 and n = 8.

3.17 No improvement in autophagy in HFD and LPS was observed for BAC SNCA and BAC HD rats

Autophagy is a bodily mechanism of repairing old and damaged cells with new and healthy cells. The disruption of autophagy has been implicated in the development of neurodegenerative diseases. (Fang Guo and Le 2018). The autophagosomes are formed, which engulf the cargoes with the help of p62 and lead to degradation. LC3 exists in two forms, LC3-I and LC3-II. LC3-II acts as a marker for autophagosomes, whereas activation of LC3-I occurs when autophagy is impaired (Runwal et al. 2019). Thus, to see how the a-syn and htt effects are justified, autophagy markers p62 and LC3B were detected for both PD and HD. Two sets of samples of each treatment group SD WT, SD TG, HFD TG, 1xLPS TG and 4xLPS TG were put on a blot and detected and 30 µg of the protein sample was considered. The first effect was observed with BAC SNCA and 8 samples were considered for this analysis, whereas for BAC HD, later only 4 samples were considered to see the statistics and the variability between the samples.

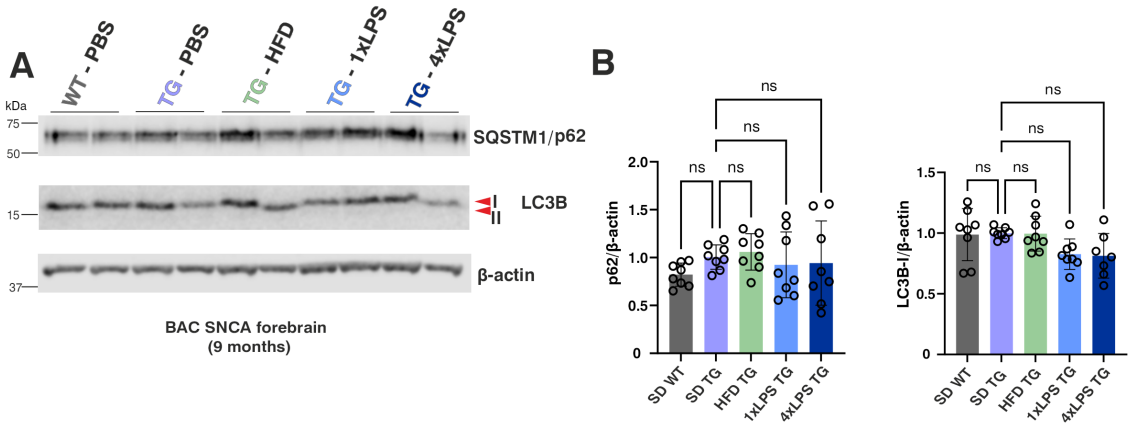

Figure 3.21: BAC SNCA rats with treatment does not show any advancement in autophagy.
A. Western blot analysis of LC3B and p62 in BAC SNCA rat models. This detection was performed with antibodies specific for LC3B and p62 (Cell Signaling and Abcam respectively). Only LC3B-I band is detectable and there is no band for LC3B-II. All the qunatifications were further performed with β-actin. **B.** Western blot data displays the trends observed in p62 and LC3B-I for BAC SNCA. A decrease (p = 0.0788, 18%) in the LC3B-I marker level with 4xLPS TG could be interpretated with respect to SD TG. The values might not be significant, but the trend promotes autophagy activation. Data are mean ± SEM, and one-way ANOVA analysis performed with Dunnett multiple comparison test with *p<0.05 and n = 8, outlier test performed with Grubbs' test with alpha = 0.1.

Usually, two forms of LC3B are detected, and LC3-II is usually quantified to understand autophagy. For BAC HD, both forms of LC3B were detected (Fig. 3.22), but for BAC SNCA, there was no detection of LC3-II (Fig. 3.21). The presence of LC3-I and not LC3-II also occurs when autophagy has been impaired. No baseline differences between WT and TG groups were observed in both cohorts when normalized to β-actin. For BAC SNCA, the trends show a decrease in the 4xLPS TG in comparison to the SD TG group with LC3B-I, which could indicate an active autophagy process, although it is not significant.

A mild decrease in the 4xLPS TG group could also be observed with p62 level. Both the markers point to an activation of autophagic processes with 4xLPS group in our BAC SNCA rat model (Fig. 3.21). Thus, the induction of autophagy could possibly lead to the decrease of FL and CT a-syn with 4xLPS TG observed earlier (Fig. 3.21). When compared to the control SD TG, opposing trends for LC3-II and p62 were observed in the case of BAC HD (Fig. 3.22), and the decreasing trend in LC3-II protein levels for HFD TG and 4xLPS TG indicates treatment-induced impairment of autophagy. The LC3B-II/I ratio is a determinant of autophagic flux. A marked significant reduction in the LC3-II/I ratio was observed with both HFD and 4xLPS TG models compared to SD TG in the BAC HD model (Fig. 3.22). This observation may reflect impaired autophagy associated with these treatments, however, without statistical difference, no connection between htt accumulation and autophagy could be established.

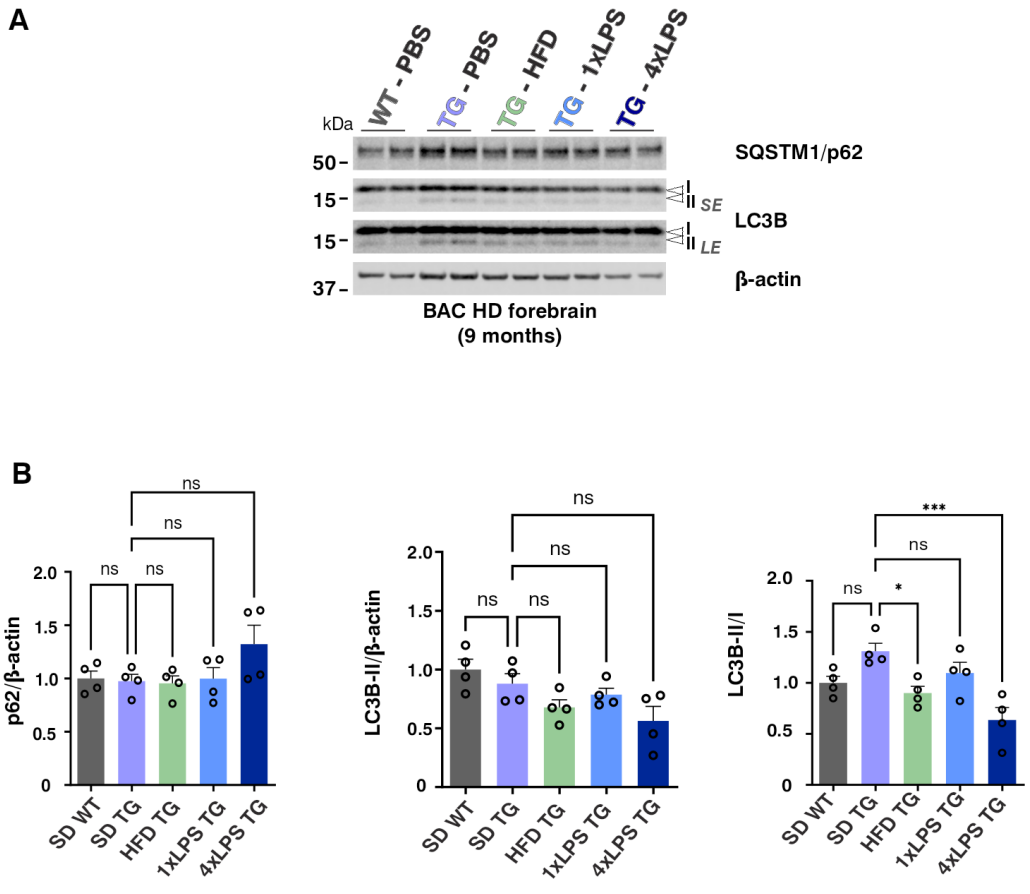

Figure 3.22: No effects in treatment could be observed with autophagy markers in BAC HD.

A. Western blot analysis of LC3B and p62 in BAC HD rat models. A strong expression of LC3B-I and a mild expression of LC3B-II could be seen here and further the p62 and LC3B levels were quantified with β-actin. **B.** A non-significant increase of p62 levels with 4XLPS TG point towards autophagic blockage, and it have been associated with the decrease in the LC3B-II levels with 4xLPS TG ($p = 0.0650$, 35%). The ratio of LCB-II/I shows significant reductions with HFD TG and 4XLPS TG treatment groups. A 51% reduction with the 4xLPS group and a 31% reduction with HFD TG was noted here, and might lead to the hypothesis of autophagic inhibition with these treatments. Data are mean ± SEM, and one-way ANOVA analysis performed with Dunnett multiple comparison test with $^*p<0.05$ and $n = 4$, outlier test performed with Grubbs' test with alpha = 0.1.

Chapter 4

Discussion

Neurodegenerative diseases, such as Alzheimer's, Parkinson's, and Huntington's diseases, which are usually characterized by the degeneration of neurons in the CNS, play an important role in regulating neuroinflammation. The interplay of immune responses and neuroinflammation has been extensively studied now. Apart from adaptive memory, evidence suggests that macrophages exhibit immune memory in the form of innate immune memory (Netea, Joosten et al. 2016). Recently, questions have emerged regarding the role of innate immune memory in neurodegenerative diseases and how it plays an important role in triggering neuroinflammation. Depending on their previous stimuli, macrophages alter their responses between neurotoxic and neuroprotective states, which are 'trained' and 'tolerant' respectively (Quintin et al. 2014; Dominguez-Andres and Netea 2019). The importance of the innate immune system in disease development has been extensively studied. Innate immune memory is a change in the reactivity of the innate immune cells and generally occurs in response to environmental stimuli (Boraschi and Italiani 2018). The training and tolerance are enhanced and suppressed immune responses respectively, and the training is associated with various epigenetic modifications (Netea, Dominguez-Andres et al. 2020). These immune responses are also associated with the production of pro-inflammatory and anti-inflammatory cytokines. Microglia, the brain-resident macrophages, are responsible for mediating the innate immune response in the central nervous system and studies have established that peripheral inflammation could lead to epigenetic reprogramming of microglia (Wendeln et al. 2018). In response to various stimulations, microglia can adapt to either the M1 state (classically activated state) or the M2 state (alternatively activated state). While inflammatory cytokines like IL-1β, TNF-α, and IL-6 are released in the M1 state, the M2 state produces more neuro-protective factors (Zhou et al. 2017). Studies have been conducted on the effects of trained immunity and tolerance in the formation of plaques in Alzheimer's mice models, which persisted in the brain for at least 6 months. It was observed that training leads to an increase in the deposition of amyloid beta plaques while tolerance suppresses it. The mice were given intraperitoneal doses of LPS: a single dose of LPS caused immune training, whereas four consecutive doses caused immune tolerance. (Wendeln et al. 2018). Little has been explored for the role of immune memory in BAC SNCA and BAC HD rat models, which are the representative rat models of PD and HD consecutively. In PD and HD disease models, the connection between microglia and inflammation has already been established and have been the cause for neuronal death for these diseases (M. Liu and Bing 2011; Ellrichmann et al. 2013; Kannarkat, Boss and Tansey 2013; Palpagama et al.

2019). Thus, the purpose of this thesis is to investigate how LPS and HFD (also known to cause inflammation and has been described earlier in this thesis) trigger immune memory in our disease models of PD and HD.

4.1 LPS and HFD-induced changes in BAC SNCA and BAC HD rats

The administration of LPS and HFD treatments has been observed to elicit distinct alterations in animal models. Upon receiving LPS doses, their social and exploratory behaviors get reduced, and locomotory activities are decreased with reduced food intake (Biesmans et al. 2013). A dose-dependent sickness-like behavior was observed in male Wistar rats when injected with an LPS dose of 200 µg/kg body weight (Bassi et al. 2012). The inflammatory response of LPS is accompanied by loss of body weight, apart from the sickness behavior (Lasselin et al. 2020; Kisipan et al. 2022). Research has been conducted on HFD-fed rats that displayed higher levels of anxiety than the control group, resulting in the production of inflammatory cytokines in the brain (Noronha et al. 2019). C57BL/6J mice have been shown to display depression and anxiety-like behavioral patterns with HFD (Aslani et al. 2015). For the experimental setup, male rats were grouped in sets of four within each cage (2 TG and 2 WT) and randomly assigned to LPS, HFD, and PBS groups. Various doses of LPS were administered intraperitoneally (i.p.) to the rats, and their weight was monitored for both acute and long-term cohorts. Simultaneously, another group of rats was fed HFD starting at the age of 2 months, with continuous monitoring, while a control group received PBS (i.p.) injections. The behavior and weight of all rats were consistently monitored until the time of FACS isolation.

As illustrated in Figure 3.5, the weight graphs for both the 3-month and 9-month cohorts were presented. With LPS injections, rats were losing their body weight, and the most significant weight decrease was visible with 4xLPS. The rats became ill and had difficulty walking or interacting socially with the other group of rats. Subsequently, when examining cytokine responses after LPS injections, a single LPS injection increased cytokine levels. However, after 2xLPS and 4xLPS injections, a reduction in both blood and brain cytokines was noted, suggesting brain-specific training and tolerance effects of LPS in our rat models. Thus, a link could be established between the sickness behavior caused by LPS treatment and the elevation/drop in the cytokine levels (P. Liu 2022).

Along with LPS, HFD and PBS rats were also monitored regularly. While the PBS rats maintained a certain body weight, the HFD rats gained weight within the 4 weeks of time-frame. Earlier evidence has concluded that Western diet feeding is involved with the activation of cytokines after 4 weeks of feeding (Christ et al. 2018). However, there were no significant alterations observed in the cytokine level in blood and brain (P. Liu 2022). Examining the impact of LPS and HFD and its associated changes is essential for understanding the influence of these treatment groups on the development of a-syn and mhtt pathogenesis in our BAC SNCA and BAC HD rat models.

4.2 Neuropathology of phosphorylated a-syn and mhtt promoted the presence of aggregates with LPS and HFD in BAC SNCA and BAC HD rats

In gaining insights into neurodegenerative diseases, conducting neuropathological studies is crucial to assess the pathogenesis of the disease within the forebrain. Usually, rats display a higher amount of aggregates than mice models, and thus, for our project, BAC SNCA and BAC HD rat models have been used. The pathology was more pronounced in the aged rats, and thus 9 months was suitable for studying the pathological responses. BAC SNCA rats containing full-length human SNCA encoding alpha-synuclein have been used (Nuber et al. 2013), and BAC HD with full-length human mutant HTT including 97 CAG/CAA repeats (Yu-Taeger et al. 2012). According to an earlier study, expression of alpha-synuclein was observed at different ages. It was concluded that with increasing age, the presence of alpha-synuclein in the dopaminergic region of BAC SNCA also increases (Nuber et al. 2013), and thus neuropathology of total a-syn, human a-syn and phosphorylated a-syn was checked for our BAC SNCA rats.

Sagittal brain sections from TG and WT rats, when subjected to staining with total and human a-syn, revealed the existence of a-syn in all forebrain regions. Additionally, endogenous expression was evident in the WT groups, as observed in previous studies. (Nuber et al. 2013). a-syn undergoes various post-translational modifications like acetylation, nitration, ubiquitination, and phosphorylation at serine 129, and this phosphorylated state of a-syn has been accumulated in Lewy body PD pathology, making it extremely important to study and understand the pathogenesis of PD (Ghanem et al. 2022; Yaribash, Mohammadi and Alizadeh Sani 2025). For the misfolding of a-syn, phosphorylated forms of a-syn are mostly visible (Sevgi et al. 2021). Several studies have reported the presence of phosphorylated a-syn in the brains of PD rodent models. However, there is limited evidence regarding the BAC SNCA rats used in our study. Our stainings showed a lot of variability in between the samples but also drew a conclusive difference in between the treatment groups (Fig. 3.7B). Genotype and treatment-based differences could be observed for pS129 across different size ranges in our study. In PD animal models, induction of LPS leads to the death of dopamine neurons in the substantia nigra, which further lead to the increase of cytokine level (M. Liu and Bing 2011). A higher number of phosphorylated a-syn counts was observed with the 4xLPS TG group, accompanied by an increase in the area of the counts too (Fig. 3.8 C, D). The immune profile activated in the microglia leads to an increase in the presence of a-syn in the brain and has been demonstrated earlier (Kasen et al. 2022). Wendeln et al. concluded the increase in the deposition of amyloid plaques in the brain with immune training (1xLPS) and a decrease in the plaques in the brain with immune tolerance (4xLPS) (Wendeln et al. 2018), however an increase in pS129 with 4xLPS might suggest that a-syn pathology follow a different immune modulation. Apart from LPS, HFD treatment has a role in inducing inflammation (Christ et al. 2018). While there is a lack of conclusive evidence on the role of HFD in BAC SNCA models, it has been studied earlier in other PD animal models, and it has been observed that HFD-induced obesity activates neuroinflammation, triggering the premature onset of a-synuclein deposits in the brainstem (Rotermund et al. 2014). Dietary restrictions can

also cause an activation of pro- and anti-inflammatory processes in the brain, leading to a change in the gut microbiome. Studies have also established a link between the activation of microglia and HFD, triggering neuroinflammation (Elabi et al. 2021). In our BAC SNCA model, there were no significant differences observed for the HFD group in comparison to the SD in terms of pathology with phosphorylated a-syn (Fig 3.8). Also, the presence of inclusion formation has been linked to the loss of dopamine neurons in the brain, influencing PD disease progression (Froula et al. 2019), and a positive spread of total a-syn with inclusion formation could be seen in all the treatment groups (Fig. 3.7A). Hence, neuropathological investigations could validate the ability of LPS to modify alpha-synuclein pathology in our BAC SNCA rat model, with no further role of HFD on phosphorylated alpha-synuclein pathology.

Sagittal sections of WT and TG brains were checked for the neuropathology of BAC HD, and all forms of mhtt aggregates was observed, from a round-shaped aggregate to a linear shaped aggregate (Fig. 3.17A). The different expression patterns of mhtt aggregates were previously described (Yu-Taeger et al. 2012), and the distribution is widespread in the cortex region. Moreover, with our stainings, nuclear localization has been apparent with the LPS treatment groups 1xLPS and 4xLPS. In the case of HD, microglia activation occurs at an early stage (Palpagama et al. 2019). The protein mutant huntingtin is also expressed in microglia and thus may be the reason for causing inflammation in the CNS (Ellrichmann et al. 2013). Earlier studies have pointed towards the decline in motor activity and activation of inflammation with HFD across neurodegenrative mice models (Hong et al. 2021). Polyunsaturated fatty acid accumulation has been linked to the progression of HD (Block et al. 2010). Although there are no published reports on our BAC HD model and HFD, our rat model demonstrated the presence of mhtt aggregates in the forebrain of 9-month-old rats and the aggregates are more concentrated than the control rats (Fig. 3.17A). Peripheral injections with LPS have been reported in HD disease models, confirming the alterations in inflammatory cytokines (Batista et al. 2019). It has been observed that with LPS, a significant amount of nuclear and perinuclear localization of mhtt aggregates is present, which is denser than in the HFD and PBS groups. The nuclear accumulation has been strongly linked to the onset of disease pathogenesis in HD (Desmond 2012; Yu-Taeger et al. 2012). On the one hand, there is a lot of evidence providing the association of nuclear localization of those aggregates and neuronal death; there are some reports which indicate this as a protective mechanism from polyglutamine neurotoxicity (Kuemmerle et al. 1999). Thus, the staining results should be compared with Filter retardation assay and Western blot data to find a conclusion about the disease pathogenesis.

4.3 HFD treatment shows distinct effects in two disease models

The neuropathological stainings were a basic idea to see how the a-syn and mhtt aggregates are displayed in the forebrain for 9 months, and confirmation with the protein detection methods was necessary to correlate with the pathological data. The scope of filter retardation studies for detecting alpha-synuclein aggregates has been quite restricted. The majority of studies have focused on diseases characterized by polyglutamine stretches, and currently, efforts have been made to explore techniques for detecting SDS-insoluble

alpha-synuclein aggregates (Oullier et al. 2020). An optimization involving buffers and various antibody forms was conducted, followed by the detection of both total and phosphorylated insoluble alpha-synuclein. Due to the absence of a phosphatase inhibitor in the buffer used for preparing our brain homogenates, the detection of phosphorylated alpha-synuclein was not possible through Filter Retardation Assay and Western blot. Consequently, we were able to detect insoluble and soluble total-synuclein, along with soluble human alpha-synuclein. The high molecular weight proteins are usually thought to be involved in many aspects of cellular processes and thus getting an insight into this would provide us the information how the treatments are affecting the formation of insoluble a-syn and htt aggregates (Emin et al. 2022).

The study of insoluble a-syn aggregates in vivo is still controversial. Thus, for our BAC SNCA study, the amount of insoluble total a-syn was detected in both acute and long term groups. HFD treatment showed completely different effects in both cohorts. On the one hand, there was a reduction observed in the level of insoluble a-syn in the acute group, and there was an increase in the a-syn level at the age of 9 months (Fig. 3.9). In other PD disease models, it has been observed that HFD accelerates the progression of PD at an increased rate. Additionally, HFD-induced obesity has been linked to dopamine depletion in the brain and the induction of neuroinflammation (Bittencourt et al. 2020; Kilzheimer et al. 2023). For our study, HFD induces immune tolerance in the forebrain of the acute group, and immune training in the forebrain of the long-term cohort, suggesting that pathology responses were altered within a timespan of 6 months (Fig. 3.9). The LPS groups showed slight upregulation compared to the control group. However, no significant changes could be observed. Also, upon comparing the acute and long-term groups, the Western blot data revealed an elevation in the oligomeric form of a-syn with the HFD in the long-term group (Fig. 3.12). It is very well-known that environmental factors like high dairy products and pesticides contribute to the progression of Parkinson's (Agim and J. R. Cannon 2015), and our study represented the fact that giving HFD at the age of 3 months has a long-term effect in developing a-syn plaques in the brain, and this long-term effect has been induced by a 'memory' form in the microglia.

Apart from a-syn, mhtt aggregates have also been studied reportedly both for acute and long-term groups and a lot of filter retardation studies have been focused on this (Ast et al. 2018). Although there were no apparent changes observed in between the treatment group in the acute cohort, there were significant reductions with HFD and 4xLPS groups at the age of 9 months, contrary to the BAC SNCA cohort. This indicates that HFD and 4xLPS groups induce immune tolerance in the forebrain of BAC HD rats (Fig. 3.19). The pathology responses act as a secondary stimulus for a-syn and htt. While the presence of a-syn worsens the impact of HFD treatment, the presence of htt pathology improves the effectiveness of treatments involving both HFD and 4xLPS. This has been studied on R6/2 mice, where repeated LPS injections alleviated HD pathology (S. W. Lee et al. 2018). While numerous reports highlight the detrimental effects of a ketogenic diet on the body, research has also explored its potential benefits for certain diseases. It has been seen that these diets delay disease progression and improve mitochondrial function in a mouse model of HD (Ruskin et al. 2011). Thus, in the case of HD, higher body weight slows the progresssion of the disease (E. Dickson et al. 2022), and this was apparent with our BAC HD rat model.

In summary, it can be suggested that there is a noticeable increase in SDS-insoluble alpha-synuclein and huntingtin aggregates in the TG animals in both cohorts (Fig. 3.9,

3.19). Parallely, reduced mhtt accumulation in BAC HD rat model speaks for a protective effect of HFD and 4xLPS, and the increased a-syn accumulation in BAC SNCA rat model indicate a toxic effect of HFD group.

4.4 Soluble levels of high molecular weight proteins were detectable following treatments for alpha-synuclein and huntingtin

The insoluble aggregates are an indication of accumulation of higher molecular weight proteins, and thus soluble-level accumulations of a-syn and mhtt were investigated to check the soluble-level difference of the proteins with treatments. Total a-syn and human a-syn were investigated for soluble-level detection. Detailed analysis of the a-syn expression pattern revealed an accumulation of soluble full-length and fragmented a-syn. Along with the monomeric form of a-syn, our model also showed dimeric, trimeric, tetrameric, and oligomeric forms of a-syn (Fig. 3.10, 3.11), and these forms of a-syn have been previously reported (Nuber et al. 2013). Recent studies have focused on the presence of oligomeric forms of a-syn, which contribute to the pathogenesis of PD and are also known to induce mitochondrial dysfunction and neuroinflammation (Du, Xie and R. T. Liu 2020). The a-syn oligomers are even present in the brains of PD patients and are known to be toxic (Bengoa-Vergniory et al. 2017; Froula et al. 2019). Our blots show stronger expression of oligomeric a-syn more with HFD and LPS treatments and very little with the WT animals (Fig. 3.11). While comparing both the acute and long-term cohort, an increased expression in the monomeric and oligomeric forms was observed at the age of 9 months, similar to the way it has been observed in 16 months of age (Fig. 3.12) (Nuber et al. 2013).

It has been observed that inflammatory stimuli such as LPS can induce a conformational change in alpha-synuclein, shifting it from monomers to oligomers. Additionally, mice treated with LPS have shown elevated levels of alpha-synuclein compared to untreated mice (Kasen et al. 2022). Also, the activation of microglia can lead to the generation of ROS in mitochondria and subsequently activating NLRP3 inflammasome, with the excess production of a-syn aggregates (Panicker et al. 2019). The change in a-syn formation into different forms depends on the disease stage, and also depends if microglia would take up the monomeric or oligomeric a-syn. Microglia produces the inflammatory response depending on the uptake of a-syn form (Ferreira and Romero-Ramos 2018). It has been concluded that the monomeric a-syn produces an anti-inflammatory effect on microglia, whereas the oligomeric form of a-syn produces a pro-inflammatory effect inducing neuroinflammation (N. Li et al. 2020). Apart from LPS, diet-induced triggers could also affect the a-syn formation, leading to neurodegeneration. Research studies have confirmed a decrease in dopamine levels in the brain with a high-fat diet (J. K. Morris et al. 2010).

Our Western blot depicted the effects of treatments on a-syn. No significant differences were observed in the acute group. A slight reduction in human a-syn was observed in the 1xLPS group, suggesting an immune tolerance effect occurring with 1xLPS at the age of 3 months (Fig. 3.10). In the long-term cohort, a downward trend in CT a-syn was noted with 4xLPS, indicating a potential reduction in the degradation of a-syn with repeated

LPS doses, although without statistical significance (Fig. 3.11). Studies have shown that the CT a-syn is capable of forming fibrillar structures and leading to the pathological condition (Mishizen-Eberz et al. 2005), indicating that 4xLPS may decrease the amount of fragmented a-syn in the forebrain. On checking the soluble levels, HFD confirmed the presence of oligomeric a-syn in the forebrain, in a similar way that was also seen with our SDS-insoluble a-syn aggregates (Fig. 3.11). These studies suggest that 4xLPS could be beneficial in reducing the amount of a-syn in the brain, and supporting that HFD has a strong immune training effect, leading to the over-production of a-syn aggregates in the brain in the case of our BAC SNCA model.

Detection of huntingtin protein revealed the presence of FL htt protein along with fragmented htt (Fig. 3.20), as earlier detected in (Yu-Taeger et al. 2012; Clemens et al. 2015; Singer et al. 2021), although the level of fragmented htt is more in our blots. The cleavage of huntingtin protein and formation of N-terminal fragments is an important step for the pathogenesis of HD (El-Daher et al. 2015). The BAC HD rats showed different results in the insoluble and soluble levels. While the TR-FRET analysis revealed no differences between treatment groups (Fig. 3.18), the Filter retardation assay showed the reduction of SDS-insoluble mhtt with HFD and 4xLPS in the forebrain (Fig. 3.19). Our Western blot data showed a high degree of htt fragmentation present in our samples (Fig. 3.20). As most fragments are known to promote aggregate formation, this could indicate the accumulation of more fragments in our samples (Cooper et al. 1998). The untreated WT rats show less fragmentation compared to the treated ones. However, the presence of a higher degree of intra-group variation in the samples may also suggest poor sample quality. Utilizing suboptimal buffer solutions during sample preparation and the need for mechanical homogenization pose a risk of deteriorating higher molecular weight proteins in the samples. The only significant difference observed was the increase in the amount of cleaved htt with SD TG in comparison to the SD WT group (Fig. 3.20).

A rising trend in the soluble levels of mhtt is observed with HFD and 4xLPS, while a decreasing trend is noted with the cleaved mhtt in the presence of 4xLPS, without statistical significance. As stated earlier, repeated doses of LPS have been shown to lessen disease progression in an HD disease mouse model (S. W. Lee et al. 2018). Thus, the non-significant reduction in cleaved mhtt with 4xLPS may indicate a direction towards alleviating mhtt aggregates. Research studies have concluded that an increase in body weight corresponds to an increase in HD disease models (Pouladi et al. 2010), and thus, the increase in FL-htt level with HFD could support this hypothesis. This contrasts with the levels of SDS-insoluble htt, where the decrease in htt protein levels contributes to the neuroprotective effect of HFD. The rise in FL mhtt levels within the 4xLPS group, coupled with the decline in fragmented mhtt within the same group, could not be correlated. Thus, our BAC HD Western blot data failed to establish a connection between the insoluble and soluble-level detections and could not confirm the additional treatment-based effects observed with HFD and 4xLPS in Filter retardation assay.

4.5 Mitochondrial dysfunction in BAC SNCA model

As previously mentioned, one of the primary characteristics of Parkinson's disease is mitochondrial dysfunction, resulting in an excessive generation of reactive oxygen

species (ROS) proteins (Moon and Paek 2015). The alterations caused by HFD and LPS prompted us to adopt the theory of mitochondrial dysfunction for our BAC SNCA PD study. Furthermore, we aimed to correlate these changes with microglial dysfunction in our disease models. There have been limited studies with our BAC SNCA model and mitochondrial dysfunction associated with this rat model.

The KEGG pathway analysis showed that genes in our BAC SNCA rat model are enriched in oxidative phosphorylation, and a downregulation with the 1xLPS group could be observed (P. Liu 2022). The total OXPHOS protein chain complexes were detected, and additionally, some mitochondrial markers were identified to detect disruptions in the mitochondrial pathway. Complex II was not detected in our samples, and the visibility of complex I was notably faint as well. Since complex I deficiency is the main aspect of PD pathogenesis (Moon and Paek 2015), this was a drawback for our study since the detection for complex I was not good due to which we saw negligible changes in between genotypes and treatment (Fig. 3.14B). a-syn aggregates is known to bind to mitochondria disrupting the mitochondrial ATP function and also affect the mitophagy process (Thorne and Tumbarello 2022). Mitochondrial damage from a-syn also impair normal dopaminergic function and cause mitochondrial fragmentation (Nakamura 2013).

Although there were reductions in the treatment groups in all complexes, complex V was the most prominent. Complex V is responsible for ATP synthesis and is the major energy source produced in the cellular mitochondria. The reduction in complex V is more observed with HFD and 1xLPS, and an upregulation is observed with the 4xLPS group, which could indicate that the dysregulation associated with HFD and 1xLPS is repaired by 4xLPS treatment (Fig. 3.14B). LPS releases more ROS into the mitochondria and with the activation of micoglia with 1xLPS, impairment of complexes I and V could be seen subsequently (M. Liu and Bing 2011). It has also been indicated that LPS-induced inflammation might be associated with respiratory chain dysfunction, and the combined effects of inflammation, oxidative stress, and mitochondrial dysfunction drive dopaminergic neuronal death and activation of microglia in PD (Hunter et al. 2007; Valenzuela-Arzeta et al. 2023). Hence, the dysregulation noted with 1xLPS might be less prominent with 4xLPS, indicating that a repeated LPS dosage could potentially enhance immune function and promote mitochondria biogenesis in our disease model. From the filter retardation assay and Western blot detection, HFD contributed towards the progression of a-syn by the production of oligomeric and insoluble aggregated a-syn in our BAC SNCA 9 months cohort. a-syn oligomers tend to disrupt the ATP synthesis pathway and lead to ROS production (Risiglione et al. 2021). The HFD increases inflammatory responses in the brain leading to impairment of mitochondrial biogenesis (Jill K. Morris and Geiger 2010). HFD-led dysfunction has been studied in other models of PD and has been linked with increased lipid metabolism in the brain affecting the normal microglial function (Chou et al. 2022), thus the increase in the aggregated form of a-syn could justify the downregulation of HFD with complex V, indicating a disruption in our BAC SNCA disease model (Fig. 3.14B).

VDACs act as a regulator controlling the entry and exit of ions and metabolites into mitochondria, functioning as a gateway, and additionally, VDAC mediates apoptosis in the mitochondria (Shoshan-Barmatz et al. 2010). The interaction of VDAC and mitochondria is related to identify PD pathogenesis (Varughese, Buchanan and Pitt 2021). Additionally, a-syn interferes with VDACs and does not allow the ions to pass through the mitochondrial channel (Rosencrans et al. 2021). A decrease in the expression of

VDAC 1 has been noted in the treatment groups HFD, 1xLPS, and 4xLPS. Consequently, the diminished expression of VDAC 1 lends support to the narrative of dysregulated mitochondrial biogenesis in our BAC SNCA model (Fig. 3.15). This suggests that under HFD and LPS treatments, there is a disruption in metabolic flux, leading to a reduction in the flow of ATP and ADP across the mitochondrial membrane (Varda Shoshan-Barmatz and Krelin 2010). Citrate synthase activity serves as an indicator of alterations in mitochondrial mass, and deficiencies in citrate synthase activity have consistently been linked to PD (Ferretta et al. 2014). For our BAC SNCA model, no changes were observed between genotypes and treatments, indicating that no changes in mitochondrial mass are associated with our model and the treatments. Opa 1 and Drp 1 induce mitochondrial fusion and mitochondrial fission, respectively. Mitochondrial fission can lead to mitochondrial fragmentation, and mitochondrial fusion can lead to an elongation of the length of mitochondria (Westermann 2010). While no notable alterations were detected in our BAC SNCA model concerning Opa 1 and Drp 1, an increasing trend in Opa 1 was observed in the 4xLPS TG compared to the SD TG. This heightened fusion could potentially enhance oxidative phosphorylation, concurrently averting the loss of metabolites and ions from the mitochondria (Fig. 3.15) (Yao et al. 2019). Therefore, the pathology response of alpha-synuclein with 4xLPS may prove advantageous in addressing the immune and mitochondrial imbalance induced by 1xLPS.

Thus, we could confirm from our disease model that HFD and LPS treatments are dysregulating the ATP Synthesis pathway, and 4xLPS is balancing the mitochondrial biogenesis in a way that the metabolites are not reduced and a healthy exhange of metabolites and ions are carried out through the mitochondrial membrane. While this examination of the BAC SNCA model offers some understanding of how HFD and LPS affect mitochondrial dysfunction, there were no discernible differences between the WT and TG groups. Consequently, no definitive conclusions can be drawn regarding a-syn and mitochondrial biogenesis in our BAC SNCA model. This is why no further study for BAC HD model and mitochondrial dysfunction was performed thereafter.

4.6 LPS injections crucial for triggering inflammation

Microglia activation by LPS triggers a lot of inflammatory stimuli, both pro-inflammatory and anti-inflammatory effects, depending on the dosage of LPS (Wendeln et al. 2018). This activation is followed by the production of cytokines in the brain. Pro-inflammatory cytokines like IL-1β and along with that production of prostaglandins (PG) also occur. PG synthesis is catalyzed by an enzyme named cyclooxygenase (COX), and COX isoforms could exist in COX-1 and COX-2, and COX-2 is induced by LPS and is expressed with the production of pro-inflammatory stimuli (Eliopoulos et al. 2002). The KEGG pathway information from the BAC SNCA 9-month cohort also highlights certain crucial genes associated with oxidative phosphorylation, showing upregulation in response to 4xLPS and notably, one of these genes is COX-2 (P. Liu 2022). The expression of COX-2 in LPS-stimulated cells and tissues could provide a detailed idea on LPS-induced pathology. Increased microglial COX-2 expression has been seen in PD patient brains, indicating that the isoform play a role in a-syn accumulation (Bartels and Leenders 2010). Although the Western blot results are far from being significant, the upregulation with 4xLPS in BAC

SNCA 9 months cohort is indicating in the same direction as the KEGG pathway analysis (Fig. 3.16), and increased expression of COX-2 has been associated with the inflammation and development of age-related diseases (J. Kim et al. 2016). Thus, the overexpression of COX-2 with 4xLPS does not support our previous data regarding inflammatory responses. Although studies have related COX-2 to inflammatory processes, transcriptional study in our project revealed the upregulation of COX-2 in oxidative phosphorylation (P. Liu 2022), and the presence of COX-2 in OXPHOS chain is directly related to the improvement of mitochondrial function (Fuertes-Agudo et al. 2022). Thus, the upregulation observed with 4xLPS might indicate the restoration of mitochondrial ATP synthesis which has been dysregulated by 1xLPS (Fig. 3.16).
Other than COX-2-induced inflammation, β-arrestins also play a major role in LPS-mediated inflammation (Porter et al. 2010). Previous findings suggest that β-arrestin 1 and 2 play contrasting roles in PD, where β-Arrestin 1 stimulates microglial immune response and β-Arrestin 2 inhibits the inflammatory response (Fang et al. 2021). LPS leads to a decrease in β-arrestin 1 level, indicating an alteration of inflammatory response on stimulation, and the expression is also decreased at transcriptional levels (Fan 2014). Western blot analysis of our data brought into light the dysregulation of the TG concerning the WT group, and a further significant reduction in the treatment groups (Fig. 3.16). A significant decrease has been observed with 1xLPS and 4xLPS groups. Since the Western blot data for β-arrestin 1 is not visually clear, there is little evidence to provide if the reduction is supported with the inflammatory response. Collectively, COX-2 and β-arrestin 1 support LPS-mediated inflammation in our BAC SNCA disease model.

4.7 Autophagy regulation observed in BAC SNCA and BAC HD rats

Autophagy is the process of removing degraded cellular components and replacing them with newer ones. Dysregulation of autophagy has been involved in the pathogenesis of neurodegenerative diseases like Parkinson's and Huntington's (Fang Guo and Le 2018). The autophagy-lysosomal pathway has not only been involved in the removal of aggregated a-syn but also participates in the intracellular aggregation process of a-syn (Poehler et al. 2014). Microglial autophagy is common in PD where aggregated a-syn triggers neuroinflammation and accelerates the loss of dopaminergic neurons in the brain (R. Zhu et al. 2022). So, a long-standing connection exists between a-syn aggregation and autophagy-lysosomal pathway (Sepulveda et al. 2022). Parallel to PD, mutant htt aggregation also impairs autophagy and causes disruption in the autophagy-lysosomal pathway (Pircs et al. 2018). HD is a disease with the expansion of the polyQ tract, and this expanded tract slows the degradation of mhtt, impairing the uptake of mhtt by autophagic process (Jarosinska and Rudiger 2021). Thus, impairment in the autophagic process could highlight the responses of the associated misfolded proteins like a-syn and mhtt.

LPS induces ROS overproduction, leading to a decrease in autophagic flux (Sul et al. 2017). Studies have been conducted on PD disease models and peripheral LPS injections have caused impairment of autophagy, causing neuroinflammation (Zheng et al. 2013). In transcriptional levels, for BAC SNCA, the 2xLPS group at the age of 3 months showed some alterations in autophagy, but the other treatment groups did not show any alterations at the age of 9 months. For BACHD, autophagic upregulation could be seen with 4xLPS

in the acute term but no further long-term effects could be monitored (P. Liu 2022). Reductions in LC3B-II levels in LPS-treated mice have been observed at the age of 7 months, indicating towards a long-term impairment of autophagy (Zheng et al. 2013), however, such effects were not observed for our disease models (fig. 3.21, 3.22). In the BAC HD disease model, a declining pattern in the levels of LC3-II protein was evident in HFD TG and 4xLPS TG, suggesting a potential impairment of autophagy induced by the treatments. Additionally, the LC3B-II/I levels show a significant decrease with both HFD and 4xLPS, supporting the earlier theory of autophagy impairment with these treatments. However, this data does not align with the Filter retardation assay, where HFD and 4xLPS significantly reduced mhtt aggregates in the forebrain of the BAC HD 9-month cohort. It could also imply that even though HFD and 4xLPS are showing a trend toward immune tolerance, it does not selectively repair the autophagic process in our BAC HD disease model. For BAC SNCA, a non-significant decrease in the protein levels of p62 and LC3B-I could be observed with the 4xLPS group, pointing to activation of autophagic processes with the 4xLPS group in PD (Fig. 3.21). Thus, the induction of autophagy could possibly lead to the decrease of FL and CT a-syn with 4xLPS TG observed earlier. Despite the detection of a-syn oligomer accumulation and mitochondrial dysfunction in the HFD group of the BAC SNCA model, the minimal alterations in the HFD groups exclude the possibility of autophagy involvement in our BAC SNCA model. However, evidence of mitophagy suppression in the HFD group can be derived from the Oxphos Western blot data (Fig. 3.15), and the inhibition of mitophagy leading to cognitive impairment with HFD has been established earlier (Wen et al. 2023).

Thus, a strong correlation could not be drawn between the a-syn and mhtt protein levels and autophagy regulation for both the disease models at the age of 9 months.

4.8 Acute microglial immune responses to peripheral stimuli and the associated transcriptional changes in BAC SNCA and BAC HD (extended results)

In addition to identifying alpha-synuclein and huntingtin aggregates in the forebrain, we conducted cytokine analysis using Enzyme-linked immunosorbent assay (ELISA) to examine acute and long-term cytokine profiles in BAC SNCA and BAC HD. This analysis served as a means to establish a connection between peripheral stimulation and the associated microglial immune responses. The brain homogenates and blood serum collected during microglia isolation were used for the cytokine analysis study. In the 3-month cohort, following the administration of 1xLPS injections, elevated levels of pro-inflammatory cytokines (IL-1β, IFN-γ, KC/GRO, and TNF-α) were observed in both the blood and brain compared to the PBS injections in both disease models, confirming an acute immune response in the periphery and brain. After the 2xLPS and 4xLPS injections, a decrease in the pro-inflammatory cytokine level was observed in both cohorts, demonstrating the effect of immune tolerance with 2xLPS and 4xLPS in the periphery and brain. The long-term effects of cytokine responses were still apparent for some of the cytokines, indicating that immune memory induced by peripheral stimuli may persist for a long time. For BAC HD, the brain levels of the anti-inflammatory cytokines

TNF-α and IL-13 were increased after 4xLPS, indicating long-term immune responses in HD. Apart from LPS injections, brain homogenates and blood serum cytokines were further compared with HFD and PBS groups and a decrease in IFN-γ cytokine level was observed in the HFD group (P. Liu 2022).

Microglial gene expression changes in response to LPS and HFD were studied (P. Liu 2022). Microglia were isolated using CD11b and CD45 markers through FACS isolation. Subsequently, RNA was extracted from the microglia, which was then employed for Bulk-RNA sequencing, single-cell RNA sequencing, and single-cell ATAC sequencing. Bulk RNA sequencing was done to check how the epigenetic alterations are happening with different treatments. From the bulk RNA sequencing data, it was found out that microglia activation was activating a lot of inflammatory pathways in the forebrain and LPS inflammation is inducing long-term differential expression in the older rats. However, our rat models exhibited slight alterations in microglial expression in response to pathology. To detect if microglia subtypes exist in PD and HD models, single-cell RNA sequencing was performed which did not reveal any pathology-specific microglial sub-population in our BAC SNCA and BAC HD rats at the age of 9 months. This could be attributed to the fact that the time-point represents an initial phase of pathological development with minimal impact on the microglial transcriptome. Intracellular protein aggregates of PD and HD might correspond to the minimal changes observed at the single-cell level. Additionally, there was a significant reduction in LDHB levels observed in BAC SNCA rats. Considering the previous assertion that LDHB deficiency may lead to mitochondrial dysfunction, these findings suggest the potential involvement of LDHB and associated mitochondrial dysfunction in the pathogenesis of our BAC SNCA rat model (P. Liu 2022).

Chapter 5

Conclusion, limitations and future perspectives

Wendeln et al. supported the concept of innate immune memory in microglia, illustrating how microglia can adopt either an immunoprotective or immunosuppressive state. Furthermore, they observed variations in the pathological aggregation of amyloid beta plaques in the brain of an Alzheimer's mouse model, with alterations corresponding to the dosage of LPS (Wendeln et al. 2018). Our study established the presence of innate immune memory in BAC SNCA and BAC HD rat models neuropathologically and with specific gene-protein expression levels. The results of my thesis underscore the role of LPS and HFD in triggering immune responses, suggesting a substantial link between the stimulus and the initiation of immune memory. Nevertheless, the effects of the stimulus differ across various disease models, exhibiting potential benefits in some and harm in others. This variability also relies on the pathological response observed in disease models, where pathology serves as a secondary stimulus exacerbating the condition.

Overall, this study showed the pathological accumulation of phosphorylated a-syn and mhtt in the forebrain and how much the pathology changes with different treatment groups. Furthermore, it was confirmed that the HFD group is causing different effects in both BAC SNCA and BAC HD rat models. In PD, HFD leads to an increased accumulation of a-syn oligomers in the brain, whereas it decreases the mhtt accumulation in the forebrain. This could indicate that HFD may be inducing immune training in BAC SNCA and immune tolerance in BAC HD. The pathological response of a-syn and mhtt may be the reason for the different effects of HFD in both disease models. In the BAC SNCA group, the occurrence of mitochondrial dysfunction, along with dysregulation in the ATP synthesis pathway, was apparent in cohorts subjected to the treatments of HFD, 1xLPS, and 4xLPS. This observation solidifies the notion that both the HFD and LPS groups contribute to the heightened accumulation of a-syn and mitochondrial dysfunction in our PD model. An increased inflammatory response has also been observed with the LPS groups in the PD rat model, with an increase in the amount of phosphorylated a-syn with 4xLPS. Although the treatment groups are indicating alterations in the accumulation of a-syn and htt, no disruption in the autophagy process could be observed, apart from some trends that could be seen towards disruption of autophagy in both disease models.

Even though significant results could be obtained by many, there were some limitations to our study. The primary limitation lies in the in vitro comparison of immune memory

triggered by LPS and HFD, utilizing human cell models of neurodegeneration. It is essential to conduct an integrated study to elucidate the disparities observed between rat models and human systems. Further, we examined the effects of immune memory in 3-month-old and 9-month-old rats, whereas, studies have shown that with higher age, rats display a higher amount of pathological aggregation. Hence, owing to time limitations, 12-month-old BAC SNCA and BAC HD rat models were omitted. However, incorporating an older time cohort rat would have been advantageous to observe effects that might not have been as apparent in the younger rats. The brain homogenates utilized in TR-FRET, Filter Retardation Assay, and Western blot were not prepared optimally. Employing commercially available buffers and kits under optimal conditions would eliminate the chance of fragmented proteins, as noted in the Western blot for BAC HD. Consequently, we were unable to validate the Western blot results of BAC HD using our Filter Retardation Assay. Furthermore, the brain homogenates generated during microglia isolation underwent mechanical homogenization, impacting the stability of proteins and leading to suboptimal detection in Western blot analysis. In conclusion, there was considerable variability observed among the samples in our phosphorylated alpha-synuclein stainings. This could have been prevented by utilizing a well-established and reliable antibody for our BAC SNCA rats. In particular, this study demonstrates a comprehensive analysis of the different responses of LPS and HFD in BAC SNCA and BAC HD disease models and establishes a neuropathological connection with these environmental stimuli.

Future work should rely on exploring the impact of LPS and HFD in other disease models and finding a common ground on how these stimuli can impact neuropathology. Research work should also focus on using the concept of long-term reprogramming of immune cells and developing treatments that target the epigenetic profiles of immune cells. This study of epigenetic reprogramming has been established in cancer already (Netea, Dominguez-Andres et al. 2020), and it would be interesting to explore that further in neurodegenerative diseases. Our parallel study has identified distinct epigenomic profiles associated with LPS and HFD in our disease models (P. Liu 2022) and would be fascinating to investigate in human patients with PD and HD. Our study has confirmed the fundamental connection between the applied stimuli, the activation of microglia, and the correlated pathological response. This revelation could potentially pave the way for the development of immunomodulatory therapies for these diseases. Since both genetic and environmental factors cause neurodegeneration, such research studies may unravel the involvement of environmental stimuli activating the inflammatory processes involved with neurodegenerative diseases.

Contributions

This work was a collaborative Ph.D. project performed with DZNE, Tübingen and I was assisted by Dr. Ping Liu in this project. I was mainly involved with the neuropathological staining in both disease models and protein-level changes in Parkinson's disease, along with animal experimentation, genotyping and microglia isolation. An outline of the different contributions has been listed below:

Experimental design: Dr. Julia Schulze-Hentrich and Dr. Jonas Neher

Animal breeding: Reema Chowdhury (under supervision) and Celina Tomczak

Animal experimentation: Reema Chowdhury (under supervision) and Dr. Ping Liu

Dr. Ping Liu performed the handling of the animals and I did the injections.

Weight measurement: Reema Chowdhury and Dr. Ping Liu

DNA isolation/genotyping: BAC SNCA 3 mo/9 mo – Reema Chowdhury, BAC HD 3 mo - Reema Chowdhury, BAC HD 9 mo – Dr. Ping Liu

Tissue collection: Animal anaesthesia performed by Reema Chowdhury and Dr. Ping Liu with assistance from Katleen Wild

FACS sorting: Animal surgery by Dr. Ping Liu

Brain homogenization by Reema Chowdhury

Assisted Dr. Ping Liu in the FACS sorting

Tissue sectioning: Anna Hendlinger and Katleen Wild

Stainings: PD - 15G7/anti a-syn/phospho-serine 129 – Reema Chowdhury, HD - EM48 – Reema Chowdhury with the assistance of Dr. Libo Yu-Taeger

Image J analysis: Reema Chowdhury

Filter retardation assay: PD – Reema Chowdhury, HD – Dr. Jonasz J. Weber and Priscila P. Sena

Western blot: PD 3 mo a-syn/9 mo a-syn, LDHB, COX 2, β-arrestin 1, mitochondrial protein detection, autophagy – Reema Chowdhury, HD – 9 mo htt, autophagy - Dr. Jonasz

J. Weber

Data statistics: PD – Reema Chowdhury, HD – Dr. Jonasz J. Weber

Finally, I did the data integration, and the figures were generated using CorelDRAW software.

Library preparation and sequencing: NGS Competence Centre Tübingen (NCCT).

Data processing: Dr. Thomas Hentrich and Dr. Julia Schulze-Hentrich

Bibliography

Agim, Z. S. and J. R. Cannon (2015):
'Dietary factors in the etiology of Parkinson's disease',
in: *Biomed Res Int* 2015, p. 672838. ISSN: 2314-6141 (Electronic) 2314-6133 (Print). DOI: 10.1155/2015/672838. URL: https://www.ncbi.nlm.nih.gov/pubmed/25688361.

Alam, M., A. Mayerhofer and W. J. Schmidt (2004):
'The neurobehavioral changes induced by bilateral rotenone lesion in medial forebrain bundle of rats are reversed by L-DOPA',
in: *Behav Brain Res* 151.1-2, pp. 117–24. ISSN: 0166-4328 (Print) 0166-4328 (Linking). DOI: 10.1016/j.bbr.2003.08.014. URL: https://www.ncbi.nlm.nih.gov/pubmed/15084427.

Anderson, John P. et al. (2006):
'Phosphorylation of Ser-129 Is the Dominant Pathological Modification of α-Synuclein in Familial and Sporadic Lewy Body Disease',
in: *Journal of Biological Chemistry* 281.40, pp. 29739–52.

Arawaka, S. et al. (2017):
'Mechanisms of Ser129-phosphorylation in alpha-synuclein aggregates',
in: *Acta Neuropathol Commun* 5.1, p. 48. ISSN: 2051-5960 (Electronic). DOI: 10.1186/s40478-017-0452-6. URL: https://www.ncbi.nlm.nih.gov/pubmed/28619113.

Aslani, S. et al. (2015):
'The effect of high-fat diet on rat's mood, feeding behavior and response to stress',
in: *Transl Psychiatry* 5.11, e684. ISSN: 2158-3188 (Electronic) 2158-3188 (Linking). DOI: 10.1038/tp.2015.178. URL: https://www.ncbi.nlm.nih.gov/pubmed/26795748.

Ast, A. et al. (2018):
'A Filter Retardation Assay Facilitates the Detection and Quantification of Heat-Stable, Amyloidogenic Mutant Huntingtin Aggregates in Complex Biosamples',
in: *Methods Mol Biol* 1780, pp. 31–40. ISSN: 1940-6029 (Electronic) 1064-3745 (Linking). DOI: 10.1007/978-1-4939-7825-0_3. URL: https://www.ncbi.nlm.nih.gov/pubmed/29856013.

Atwal, Randy Singh et al. (2007):
'Huntingtin has a membrane association signal that can modulate huntingtin aggregation, nuclear entry and toxicity',
in: *Human Molecular Genetics* 16.

B L Goodwin, G C Kite (1998):
'Environmental MPTP as a factor in the aetiology of Parkinson's disease?',
in: *Journal of Neural Transmission* 105(10-12):1265-9.

Baldo, B. et al. (2012):
'TR-FRET-based duplex immunoassay reveals an inverse correlation of soluble and aggregated mutant huntingtin in huntington's disease',
in: *Chem Biol* 19.2, pp. 264–75. ISSN: 1879-1301 (Electronic) 1074-5521 (Linking). DOI: 10.1016/j.chembiol.2011.12.020. URL: https://www.ncbi.nlm.nih.gov/pubmed/22365609.

BALL, N. ET AL. (2019):
'Parkinson's Disease and the Environment',
in: *Front Neurol* 10, p. 218. ISSN: 1664-2295 (Print) 1664-2295 (Electronic) 1664-2295 (Linking). DOI: 10.3389/fneur.2019.00218. URL: https://www.ncbi.nlm.nih.gov/pubmed/30941085.

BARTELS, A. L. and K. L. LEENDERS (2010):
'Cyclooxygenase and neuroinflammation in Parkinson's disease neurodegeneration',
in: *Curr Neuropharmacol* 8.1, pp. 62–8. ISSN: 1875-6190 (Electronic) 1570-159X (Print) 1570-159X (Linking). DOI: 10.2174/157015910790909485. URL: https://www.ncbi.nlm.nih.gov/pubmed/20808546.

BASSI, GABRIEL S. ET AL. (2012):
'Lipopolysaccharide-Induced Sickness Behaviour Evaluated in Different Models of Anxiety and Innate Fear in Rats',
in: *Basic amp; Clinical Pharmacology amp; Toxicology* 110.4, pp. 359–369. ISSN: 1742-7835. DOI: 10.1111/j.1742-7843.2011.00824.x. URL: https://dx.doi.org/10.1111/j.1742-7843.2011.00824.x.

BATES, G. P. ET AL. (2015):
'Huntington disease',
in: *Nat Rev Dis Primers* 1, p. 15005. ISSN: 2056-676X (Electronic) 2056-676X (Linking). DOI: 10.1038/nrdp.2015.5. URL: https://www.ncbi.nlm.nih.gov/pubmed/27188817.

BATISTA, C. R. A. ET AL. (2019):
'Lipopolysaccharide-Induced Neuroinflammation as a Bridge to Understand Neurodegeneration',
in: *Int J Mol Sci* 20.9. ISSN: 1422-0067 (Electronic) 1422-0067 (Linking). DOI: 10.3390/ijms20092293. URL: https://www.ncbi.nlm.nih.gov/pubmed/31075861.

BEITZ, J. M. (2014):
'Parkinson's disease: a review',
in: *Front Biosci (Schol Ed)* 6.1, pp. 65–74. ISSN: 1945-0524 (Electronic) 1945-0516 (Linking). DOI: 10.2741/s415. URL: https://www.ncbi.nlm.nih.gov/pubmed/24389262.

BENGOA-VERGNIORY, N. ET AL. (2017):
'Alpha-synuclein oligomers: a new hope',
in: *Acta Neuropathol* 134.6, pp. 819–838. ISSN: 1432-0533 (Electronic) 0001-6322 (Print) 0001-6322 (Linking). DOI: 10.1007/s00401-017-1755-1. URL: https://www.ncbi.nlm.nih.gov/pubmed/28803412.

BEZARD, E. and S. PRZEDBORSKI (2011):
'A tale on animal models of Parkinson's disease',
in: *Mov Disord* 26.6, pp. 993–1002. ISSN: 1531-8257 (Electronic) 0885-3185 (Linking). DOI: 10.1002/mds.23696. URL: https://www.ncbi.nlm.nih.gov/pubmed/21626544.

BIESMANS, S. ET AL. (2013):
'Systemic immune activation leads to neuroinflammation and sickness behavior in mice',
in: *Mediators Inflamm* 2013, p. 271359. ISSN: 1466-1861 (Electronic) 0962-9351 (Print) 0962-9351 (Linking). DOI: 10.1155/2013/271359. URL: https://www.ncbi.nlm.nih.gov/pubmed/23935246.

BITTENCOURT, ALINE ET AL. (2020):
'High fat diet-induced obesity causes a reduction in brain tyrosine hydroxylase levels and non-motor features in rats through metabolic dysfunction, neuroinflammation and oxidative stress',
in: *Nutritional Neuroscience*.

BJÖRKQVIST, M. ET AL. (2008):
'A novel pathogenic pathway of immune activation detectable before clinical onset in Huntington's disease',
in: *The Journal of Neuropathology & Experimental Neurology* 68.

BLANDINI, F., M. T. ARMENTERO and E. MARTIGNONI (2008):
'The 6-hydroxydopamine model: news from the past',
in: *Parkinsonism Relat Disord* 14 Suppl 2, S124–9. ISSN: 1353-8020 (Print) 1353-8020 (Linking). DOI: 10.1016/j.parkreldis.2008.04.015. URL: https://www.ncbi.nlm.nih.gov/pubmed/18595767.

BLESA, J. and S. PRZEDBORSKI (2014):
'Parkinson's disease: animal models and dopaminergic cell vulnerability',
in: *Front Neuroanat* 8, p. 155. ISSN: 1662-5129 (Print) 1662-5129 (Electronic) 1662-5129 (Linking). DOI: 10.3389/fnana.2014.00155. URL: https://www.ncbi.nlm.nih.gov/pubmed/25565980.

BLOCK, R. C. ET AL. (2010):
'Altered cholesterol and fatty acid metabolism in Huntington disease',
in: *J Clin Lipidol* 4.1, pp. 17–23. ISSN: 1933-2874 (Print) 1876-4789 (Linking). DOI: 10.1016/j.jacl.2009.11.003. URL: https://www.ncbi.nlm.nih.gov/pubmed/20802793.

BONIFATI, V. ET AL. (2003):
'DJ-1(PARK7), a novel gene for autosomal recessive, early onset parkinsonism',
in: *Neurological Sciences* 24.3, pp. 159–160. ISSN: 1590-1874. DOI: 10.1007/s10072-003-0108-0. URL: https://dx.doi.org/10.1007/s10072-003-0108-0.

BORASCHI, D. and P. ITALIANI (2018):
'Innate Immune Memory: Time for Adopting a Correct Terminology',
in: *Front Immunol* 9, p. 799. ISSN: 1664-3224 (Print) 1664-3224 (Linking). DOI: 10.3389/fimmu.2018.00799. URL: https://www.ncbi.nlm.nih.gov/pubmed/29725331.

BOSE, A. and M. F. BEAL (2019):
'Mitochondrial dysfunction and oxidative stress in induced pluripotent stem cell models of Parkinson's disease',
in: *Eur J Neurosci* 49.4, pp. 525–532. ISSN: 1460-9568 (Electronic) 0953-816X (Linking). DOI: 10.1111/ejn.14264. URL: https://www.ncbi.nlm.nih.gov/pubmed/30408242.

BOUSQUET, M. ET AL. (2012):
'High-fat diet exacerbates MPTP-induced dopaminergic degeneration in mice',
in: *Neurobiol Dis* 45.1, pp. 529–538. ISSN: 0969-9961. DOI: 10.1016/j.nbd.2011.09.009. URL: https://www.ncbi.nlm.nih.gov/pubmed/21971528.

BRAAK, H. ET AL. (2003):
'Staging of brain pathology related to sporadic Parkinson's disease',
in: *Neurobiol Aging* 24.2, pp. 197–211. ISSN: 0197-4580 (Print) 0197-4580 (Linking). DOI: 10.1016/s0197-4580(02)00065-9. URL: https://www.ncbi.nlm.nih.gov/pubmed/12498954.

BROWN, G. C., M. CAMACHO and C. H. WILLIAMS-GRAY (2023):
'The Endotoxin Hypothesis of Parkinson's Disease',
in: *Mov Disord.* ISSN: 1531-8257 (Electronic), 0885-3185 (Linking). DOI: 10.1002/mds.29432. URL: https://www.ncbi.nlm.nih.gov/pubmed/37157885.

BROWN, GUY C. (2019):
'The endotoxin hypothesis of neurodegeneration',
in: *Journal of Neuroinflammation* 16.1. ISSN: 1742-2094. DOI: 10.1186/s12974-019-1564-7. URL: https://dx.doi.org/10.1186/s12974-019-1564-7.

BURRE, J., M. SHARMA and T. C. SUDHOF (2018):
'Cell Biology and Pathophysiology of alpha-Synuclein',
in: *Cold Spring Harb Perspect Med* 8.3. ISSN: 2157-1422 (Electronic) 2157-1422 (Linking). DOI: 10.1101/cshperspect.a024091. URL: https://www.ncbi.nlm.nih.gov/pubmed/28108534.

BURRE, J., M. SHARMA, T. TSETSENIS ET AL. (2010):
'Alpha-synuclein promotes SNARE-complex assembly in vivo and in vitro',
in: *Science* 329.5999, pp. 1663–7. ISSN: 1095-9203 (Electronic) 0036-8075 (Print) 0036-8075 (Linking). DOI: 10.1126/science.1195227. URL: https://www.ncbi.nlm.nih.gov/pubmed/20798282.

BUTLER, M. J. (2021):
'The role of Western diets and obesity in peripheral immune cell recruitment and inflammation in the central nervous system',

in: *Brain Behav Immun Health* 16, p. 100298. ISSN: 2666-3546 (Electronic) 2666-3546 (Linking). DOI: 10.1016/j.bbih.2021.100298. URL: https://www.ncbi.nlm.nih.gov/pubmed/34589790.

CALABRESI, P. ET AL. (2023):
'Alpha-synuclein in Parkinson's disease and other synucleinopathies: from overt neurodegeneration back to early synaptic dysfunction',
in: *Cell Death Dis* 14.3, p. 176. ISSN: 2041-4889 (Electronic). DOI: 10.1038/s41419-023-05672-9. URL: https://www.ncbi.nlm.nih.gov/pubmed/36859484.

CAMARA, AMADOU K. S. ET AL. (2017):
'Mitochondrial VDAC1: A Key Gatekeeper as Potential Therapeutic Target',
in: *Frontiers* 8.

CANNON, JASON R. and J. TIMOTHY GREENAMYRE (2013):
'Gene–environment interactions in Parkinson's disease: Specific evidence in humans and mammalian models',
in: *Neurobiology of Disease* 57, pp. 38–46. ISSN: 0969-9961. DOI: 10.1016/j.nbd.2012.06.025. URL: https://dx.doi.org/10.1016/j.nbd.2012.06.025.

CARR, J. ET AL. (2003):
'Familial and sporadic Parkinson's disease usually display the same clinical features',
in: *Parkinsonism Relat Disord* 9.4, pp. 201–4. ISSN: 1353-8020 (Print) 1353-8020 (Linking). DOI: 10.1016/s1353-8020(02)00048-2. URL: https://www.ncbi.nlm.nih.gov/pubmed/12618054.

CATTANEO, E. ET AL. (2001):
'Loss of normal huntingtin function: new developments in Huntington's disease research',
in: *Trends Neurosci* 24.3, pp. 182–8. ISSN: 0166-2236 (Print) 0166-2236 (Linking). DOI: 10.1016/s0166-2236(00)01721-5. URL: https://www.ncbi.nlm.nih.gov/pubmed/11182459.

CEPEDA, C. ET AL. (2010):
'Rescuing the Corticostriatal Synaptic Disconnection in the R6/2 Mouse Model of Huntington's Disease: Exercise, Adenosine Receptors and Ampakines',
in: *PLoS Curr* 2. ISSN: 2157-3999 (Electronic) 2157-3999 (Linking). DOI: 10.1371/currents.RRN1182. URL: https://www.ncbi.nlm.nih.gov/pubmed/20877458.

CHERAY, M. and B. JOSEPH (2018):
'Epigenetics Control Microglia Plasticity',
in: *Front Cell Neurosci* 12, p. 243. ISSN: 1662-5102 (Print) 1662-5102 (Linking). DOI: 10.3389/fncel.2018.00243. URL: https://www.ncbi.nlm.nih.gov/pubmed/30123114.

CHOU, M. C. ET AL. (2022):
'Long-Term High-Fat Diet Consumption Depletes Glial Cells and Tyrosine Hydroxylase-Containing Neurons in the Brain of Middle-Aged Rats',
in: *Cells* 11.2, p. 295. ISSN: 2073-4409. DOI: 10.3390/cells11020295. URL: https://www.ncbi.nlm.nih.gov/pubmed/35053411.

CHRIST, ANETTE ET AL. (2018):
'Western Diet Triggers NLRP3-Dependent Innate Immune Reprogramming',
in: *Cell* 172.1-2, 162–175.e14. ISSN: 0092-8674. DOI: 10.1016/j.cell.2017.12.013. URL: https://dx.doi.org/10.1016/j.cell.2017.12.013.

CICCOCIOPPO, FAUSTA (2020):
'Neurodegenerative diseases as proteinopathies-driven immune disorders',
in: *Neural Regeneration Research*.

CLEMENS, L. E. ET AL. (2015):
'Olesoxime suppresses calpain activation and mutant huntingtin fragmentation in the BACHD rat',
in: *Brain* 138.Pt 12, pp. 3632–53. ISSN: 1460-2156 (Electronic) 0006-8950 (Linking). DOI: 10.1093/brain/awv290. URL: https://www.ncbi.nlm.nih.gov/pubmed/26490331.

CLIFFORD, J. J. ET AL. (2002):
'Essential fatty acids given from conception prevent topographies of motor deficit in a transgenic model of Huntington's disease',
in: *Neuroscience* 109.1, pp. 81–8. ISSN: 0306-4522 (Print) 0306-4522 (Linking). DOI: 10.1016/s0306-4522(01)00409-2. URL: https://www.ncbi.nlm.nih.gov/pubmed/11784701.

COOPER, J. K. ET AL. (1998):
'Truncated N-terminal fragments of huntingtin with expanded glutamine repeats form nuclear and cytoplasmic aggregates in cell culture',
in: *Hum Mol Genet* 7.5, pp. 783–90. ISSN: 0964-6906 (Print) 0964-6906 (Linking). DOI: 10.1093/hmg/7.5.783. URL: https://www.ncbi.nlm.nih.gov/pubmed/9536081.

CROTTI, A. and C. K. GLASS (2015):
'The choreography of neuroinflammation in Huntington's disease',
in: *Trends Immunol* 36.6, pp. 364–73. ISSN: 1471-4981 (Electronic) 1471-4906 (Print) 1471-4906 (Linking). DOI: 10.1016/j.it.2015.04.007. URL: https://www.ncbi.nlm.nih.gov/pubmed/26001312.

EL-DAHER, M. T. ET AL. (2015):
'Huntingtin proteolysis releases non-polyQ fragments that cause toxicity through dynamin 1 dysregulation',
in: *EMBO J* 34.17, pp. 2255–71. ISSN: 1460-2075 (Electronic) 0261-4189 (Print) 0261-4189 (Linking). DOI: 10.15252/embj.201490808. URL: https://www.ncbi.nlm.nih.gov/pubmed/26165689.

DAVIES, S. W. ET AL. (1997):
'Formation of neuronal intranuclear inclusions underlies the neurological dysfunction in mice transgenic for the HD mutation',
in: *Cell* 90.3, pp. 537–48. ISSN: 0092-8674 (Print) 0092-8674 (Linking). DOI: 10.1016/s0092-8674(00)80513-9. URL: https://www.ncbi.nlm.nih.gov/pubmed/9267033.

DAWES, H. ET AL. (2015):
'Exercise testing and training in people with Huntington's disease',
in: *Clin Rehabil* 29.2, pp. 196–206. ISSN: 1477-0873 (Electronic) 0269-2155 (Linking). DOI: 10.1177/0269215514540921. URL: https://www.ncbi.nlm.nih.gov/pubmed/25142278.

DAWSON, T. M., H. S. KO and V. L. DAWSON (2010):
'Genetic animal models of Parkinson's disease',
in: *Neuron* 66.5, pp. 646–61. ISSN: 1097-4199 (Electronic) 0896-6273 (Print) 0896-6273 (Linking). DOI: 10.1016/j.neuron.2010.04.034. URL: https://www.ncbi.nlm.nih.gov/pubmed/20547124.

DAY, J. O. and S. MULLIN (2021):
'The Genetics of Parkinson's Disease and Implications for Clinical Practice',
in: *Genes (Basel)* 12.7. ISSN: 2073-4425 (Electronic) 2073-4425 (Linking). DOI: 10.3390/genes12071006. URL: https://www.ncbi.nlm.nih.gov/pubmed/34208795.

DE MIRANDA, B. R. ET AL. (2022):
'Preventing Parkinson's Disease: An Environmental Agenda',
in: *J Parkinsons Dis* 12.1, pp. 45–68. ISSN: 1877-718X (Electronic) 1877-7171 (Print) 1877-7171 (Linking). DOI: 10.3233/JPD-212922. URL: https://www.ncbi.nlm.nih.gov/pubmed/34719434.

DEAS, E., N. W. WOOD and H. PLUN-FAVREAU (2011):
'Mitophagy and Parkinson's disease: the PINK1-parkin link',
in: *Biochim Biophys Acta* 1813.4, pp. 623–33. ISSN: 0006-3002 (Print), 0006-3002 (Linking). DOI: 10.1016/j.bbamcr.2010.08.007. URL: https://www.ncbi.nlm.nih.gov/pubmed/20736035.

DEMAIO, A. ET AL. (2022):
'The role of the adaptive immune system and T cell dysfunction in neurodegenerative diseases',
in: *J Neuroinflammation* 19.1, p. 251. ISSN: 1742-2094 (Electronic) 1742-2094 (Linking). DOI: 10.1186/s12974-022-02605-9. URL: https://www.ncbi.nlm.nih.gov/pubmed/36209107.

DESMOND, C.R. (2012):
'Nuclear Localization of the Huntingtin Protein',
Thesis.

DHAVALE, DHRUVA D. ET AL. (2024):
'Structure of alpha-synuclein fibrils derived from human Lewy body dementia tissue',
in: *Nat Commun* 15, p. 2750. ISSN: 2041-1723. DOI: 10.1038/s41467-024-46832-5. URL: https://www.nature.com/articles/s41467-024-46832-5.

DI MAIO, R. ET AL. (2018):
'LRRK2 activation in idiopathic Parkinson's disease',
in: *Sci Transl Med* 10.451. ISSN: 1946-6242 (Electronic) 1946-6234 (Print) 1946-6234 (Linking). DOI: 10.1126/scitranslmed.aar5429. URL: https://www.ncbi.nlm.nih.gov/pubmed/30045977.

DIAS, V., E. JUNN and M. M. MOURADIAN (2013):
'The role of oxidative stress in Parkinson's disease',
in: *J Parkinsons Dis* 3.4, pp. 461–91. ISSN: 1877-718X (Electronic) 1877-7171 (Print) 1877-7171 (Linking). DOI: 10.3233/JPD-130230. URL: https://www.ncbi.nlm.nih.gov/pubmed/24252804.

DICKEY, A. S. and A. R. LA SPADA (2018):
'Therapy development in Huntington disease: From current strategies to emerging opportunities',
in: *Am J Med Genet A* 176.4, pp. 842–861. ISSN: 1552-4833 (Electronic) 1552-4825 (Linking). DOI: 10.1002/ajmg.a.38494. URL: https://www.ncbi.nlm.nih.gov/pubmed/29218782.

DICKSON, DENNIS W. (2018):
'Neuropathology of Parkinson disease',
in: *Parkinsonism amp; Related Disorders* 46, S30–S33. ISSN: 1353-8020. DOI: 10.1016/j.parkreldis.2017.07.033. URL: https://dx.doi.org/10.1016/j.parkreldis.2017.07.033.

DICKSON, E. ET AL. (2022):
'Hypothalamic expression of huntingtin causes distinct metabolic changes in Huntington's disease mice',
in: *Mol Metab* 57, p. 101439. ISSN: 2212-8778 (Electronic) 2212-8778 (Linking). DOI: 10.1016/j.molmet.2022.101439. URL: https://www.ncbi.nlm.nih.gov/pubmed/35007790.

DIFIGLIA, M. ET AL. (1997):
'Aggregation of huntingtin in neuronal intranuclear inclusions and dystrophic neurites in brain',
in: *Science* 277.5334, pp. 1990–1993. ISSN: 0036-8075. DOI: 10.1126/science.277.5334.1990. URL: https://www.ncbi.nlm.nih.gov/pubmed/9302293.

DOMINGUEZ-ANDRES, J. and M. G. NETEA (2019):
'Long-term reprogramming of the innate immune system',
in: *J Leukoc Biol* 105.2, pp. 329–338. ISSN: 1938-3673 (Electronic) 0741-5400 (Linking). DOI: 10.1002/JLB.MR0318-104R. URL: https://www.ncbi.nlm.nih.gov/pubmed/29999546.

DONG, X. and S. CONG (2021):
'MicroRNAs in Huntington's Disease: Diagnostic Biomarkers or Therapeutic Agents?',
in: *Front Cell Neurosci* 15, p. 705348. ISSN: 1662-5102 (Print) 1662-5102 (Linking). DOI: 10.3389/fncel.2021.705348. URL: https://www.ncbi.nlm.nih.gov/pubmed/34421543.

DOTY, K. R., M. V. GUILLOT-SESTIER and T. TOWN (2015):
'The role of the immune system in neurodegenerative disorders: Adaptive or maladaptive?',
in: *Brain Res* 1617, pp. 155–73. ISSN: 1872-6240 (Electronic) 0006-8993 (Print) 0006-8993 (Linking). DOI: 10.1016/j.brainres.2014.09.008. URL: https://www.ncbi.nlm.nih.gov/pubmed/25218556.

DU, X. Y., X. X. XIE and R. T. LIU (2020):
'The Role of alpha-Synuclein Oligomers in Parkinson's Disease',
in: *Int J Mol Sci* 21.22. ISSN: 1422-0067 (Electronic) 1422-0067 (Linking). DOI: 10.3390/ijms21228645. URL: https://www.ncbi.nlm.nih.gov/pubmed/33212758.

DUAN, W. ET AL. (2003):
'Dietary restriction normalizes glucose metabolism and BDNF levels, slows disease progression, and increases survival in huntingtin mutant mice',
in: *Proc Natl Acad Sci U S A* 100.5, pp. 2911–6. ISSN: 0027-8424 (Print) 0027-8424 (Linking). DOI: 10.1073/pnas.0536856100. URL: https://www.ncbi.nlm.nih.gov/pubmed/12589027.

DUDA, JOHN E. ET AL. (2002):
'Novel antibodies to synuclein show abundant striatal pathology in Lewy body diseases',
in: *Annals of Neurology*.

DUYAO, M. ET AL. (1993):
'Trinucleotide repeat length instability and age of onset in Huntington's disease',
in: *Nat Genet* 4.4, pp. 387–92. ISSN: 1061-4036 (Print) 1061-4036 (Linking). DOI: 10.1038/ng0893-387. URL: https://www.ncbi.nlm.nih.gov/pubmed/8401587.

DWIVEDI-AGNIHOTRI, ARUN K. SHUKLA AND HEMLATA (2020):
'Structure and function of β-arrestins, their emerging role in breast cancer, and potential opportunities for therapeutic manipulation',
in: *PubMed Central* 2020.

EHRNHOEFER, D. E., L. SUTTON AND M. R. HAYDEN (2011):
'Small changes, big impact: posttranslational modifications and function of huntingtin in Huntington disease',
in: *Neuroscientist* 17.5, pp. 475–92. ISSN: 1089-4098 (Electronic) 1073-8584 (Linking). DOI: 10.1177/1073858410390378. URL: https://www.ncbi.nlm.nih.gov/pubmed/21311053.

EJ, SLOW ET AL. (2003):
'Selective striatal neuronal loss in a YAC128 mouse model of Huntington disease',
in: *Human Molecular Genetics* 12.

ELABI, O. F. ET AL. (2021):
'High-fat diet-induced diabetes leads to vascular alterations, pericyte reduction, and perivascular depletion of microglia in a 6-OHDA toxin model of Parkinson disease',
in: *J Neuroinflammation* 18.1, p. 175. ISSN: 1742-2094 (Electronic) 1742-2094 (Linking). DOI: 10.1186/s12974-021-02218-8. URL: https://www.ncbi.nlm.nih.gov/pubmed/34376193.

ELENA-REAL, C. A. ET AL. (2023):
'The structure of pathogenic huntingtin exon 1 defines the bases of its aggregation propensity',
in: *Nat Struct Mol Biol* 30.3, pp. 309–320. ISSN: 1545-9985 (Electronic) 1545-9985 (Linking). DOI: 10.1038/s41594-023-00920-0. URL: https://www.ncbi.nlm.nih.gov/pubmed/36864173.

ELIOPOULOS, ARISTIDES G. ET AL. (2002):
'Induction of COX-2 by LPS in macrophages is regulated by Tpl2-dependent CREB activation signals',
in: *EMBO* 21, pp. 4831–4840.

ELLRICHMANN, G. ET AL. (2013):
'The role of the immune system in Huntington's disease',
in: *Clin Dev Immunol* 2013, p. 541259. ISSN: 1740-2530 (Electronic) 1740-2522 (Linking). DOI: 10.1155/2013/541259. URL: https://www.ncbi.nlm.nih.gov/pubmed/23956761.

EMIN, D. ET AL. (2022):
'Small soluble alpha-synuclein aggregates are the toxic species in Parkinson's disease',
in: *Nat Commun* 13.1, p. 5512. ISSN: 2041-1723 (Electronic) 2041-1723 (Linking). DOI: 10.1038/s41467-022-33252-6. URL: https://www.ncbi.nlm.nih.gov/pubmed/36127374.

FAN, H. (2014):
'beta-Arrestins 1 and 2 are critical regulators of inflammation',
in: *Innate Immun* 20.5, pp. 451–60. ISSN: 1753-4267 (Electronic) 1753-4259 (Print) 1753-4259 (Linking). DOI: 10.1177/1753425913501098. URL: https://www.ncbi.nlm.nih.gov/pubmed/24029143.

FANG, Y. ET AL. (2021):
'Opposing functions of beta-arrestin 1 and 2 in Parkinson's disease via microglia inflammation and Nprl3',
in: *Cell Death Differ* 28.6, pp. 1822–1836. ISSN: 1476-5403 (Electronic) 1350-9047 (Print) 1350-9047 (Linking). DOI: 10.1038/s41418-020-00704-9. URL: https://www.ncbi.nlm.nih.gov/pubmed/33686256.

FANG GUO XINYAO LIU, HUAIBIN CAI and WEIDONG LE (2018):
'Autophagy in neurodegenerative diseases: pathogenesis and therapy',
in: *Brain Pathology*.

FARSHIM, P. P. and G. P. BATES (2018):
'Mouse Models of Huntington's Disease',
in: *Methods Mol Biol* 1780, pp. 97–120. ISSN: 1940-6029 (Electronic) 1064-3745 (Linking). DOI: 10.1007/978-1-4939-7825-0_6. URL: https://www.ncbi.nlm.nih.gov/pubmed/29856016.

FAULL, R. L. and R. LAVERTY (1969):
'Changes in dopamine levels in the corpus striatum following lesions in the substantia nigra',
in: *Exp Neurol* 23.3, pp. 332–40. ISSN: 0014-4886 (Print) 0014-4886 (Linking). DOI: 10.1016/0014-4886(69)90081-8. URL: https://www.ncbi.nlm.nih.gov/pubmed/5767257.

FERREIRA, S. A. and M. ROMERO-RAMOS (2018):
'Microglia Response During Parkinson's Disease: Alpha-Synuclein Intervention',
in: *Front Cell Neurosci* 12, p. 247. ISSN: 1662-5102 (Print) 1662-5102 (Electronic) 1662-5102 (Linking). DOI: 10.3389/fncel.2018.00247. URL: https://www.ncbi.nlm.nih.gov/pubmed/30127724.

FERRETTA, A. ET AL. (2014):
'Effect of resveratrol on mitochondrial function: implications in parkin-associated familiar Parkinson's disease',
in: *Biochim Biophys Acta* 1842.7, pp. 902–15. ISSN: 0006-3002 (Print) 0006-3002 (Linking). DOI: 10.1016/j.bbadis.2014.02.010. URL: https://www.ncbi.nlm.nih.gov/pubmed/24582596.

FLOOR, E. and M. G. WETZEL (1998):
'Increased protein oxidation in human substantia nigra pars compacta in comparison with basal ganglia and prefrontal cortex measured with an improved dinitrophenylhydrazine assay',
in: *J Neurochem* 70.1, pp. 268–75. ISSN: 0022-3042 (Print) 0022-3042 (Linking). DOI: 10.1046/j.1471-4159.1998.70010268.x. URL: https://www.ncbi.nlm.nih.gov/pubmed/9422371.

FOTI, S. C. ET AL. (2019):
'Cerebral mitochondrial electron transport chain dysfunction in multiple system atrophy and Parkinson's disease',
in: *Sci Rep* 9.1, p. 6559. ISSN: 2045-2322 (Electronic) 2045-2322 (Linking). DOI: 10.1038/s41598-019-42902-7. URL: https://www.ncbi.nlm.nih.gov/pubmed/31024027.

FRANCELLE, L. ET AL. (2017):
'Contribution of Neuroepigenetics to Huntington's Disease',
in: *Front Hum Neurosci* 11, p. 17. ISSN: 1662-5161 (Print) 1662-5161 (Electronic) 1662-5161 (Linking). DOI: 10.3389/fnhum.2017.00017. URL: https://www.ncbi.nlm.nih.gov/pubmed/28194101.

FROULA, J. M. ET AL. (2019):
'Defining alpha-synuclein species responsible for Parkinson's disease phenotypes in mice',
in: *J Biol Chem* 294.27, pp. 10392–10406. ISSN: 1083-351X (Electronic) 0021-9258 (Print) 0021-9258 (Linking). DOI: 10.1074/jbc.RA119.007743. URL: https://www.ncbi.nlm.nih.gov/pubmed/31142553.

FUERTES-AGUDO, M. ET AL. (2022):
'COX-2 Expression in Hepatocytes Improves Mitochondrial Function after Hepatic Ischemia-Reperfusion Injury',
in: *Antioxidants (Basel)* 11.9. ISSN: 2076-3921 (Print) 2076-3921 (Electronic) 2076-3921 (Linking). DOI: 10.3390/antiox11091724. URL: https://www.ncbi.nlm.nih.gov/pubmed/36139798.

FUJIWARA, HIDEO ET AL. (2002):
'α-Synuclein is phosphorylated in synucleinopathy lesions',
in: *Nature Cell Biology* 4, pp. 160–164.

GAFNI, J. and L. M. ELLERBY (2002):
'Calpain activation in Huntington's disease',
in: *J Neurosci* 22.12, pp. 4842–9. ISSN: 1529-2401 (Electronic) 0270-6474 (Print) 0270-6474 (Linking). DOI: 10.1523/JNEUROSCI.22-12-04842.2002. URL: https://www.ncbi.nlm.nih.gov/pubmed/12077181.

GALIANO-LANDEIRA, J. ET AL. (2020):
'CD8 T cell nigral infiltration precedes synucleinopathy in early stages of Parkinson's disease',
in: *Brain* 143.12, pp. 3717–3733. ISSN: 1460-2156 (Electronic) 0006-8950 (Linking). DOI: 10.1093/brain/awaa269. URL: https://www.ncbi.nlm.nih.gov/pubmed/33118032.

GAO, HUI-MING ET AL. (2011):
'Neuroinflammation and *α*-Synuclein Dysfunction Potentiate Each Other, Driving Chronic Progression of Neurodegeneration in a Mouse Model of Parkinson's Disease',
in: *Environmental Health Perspectives (Open Access)* 119.

GHANEM, SIMONA S. ET AL. (2022):
'α-Synuclein phosphorylation at serine 129 occurs after initial protein deposition and inhibits seeded fibril formation and toxicity',
in: *PNAS* 119.15.

GOETZ, CHRISTOPHER G (2011):
'The history of Parkinson's disease: early clinical descriptions and neurological therapies',
in: *Cold Spring Harbor perspectives in medicine* 1.1, a008862. ISSN: 2157-1422.

GOMPERTS, S. N. (2016):
'Lewy Body Dementias: Dementia With Lewy Bodies and Parkinson Disease Dementia',
in: *Continuum (Minneap Minn)* 22.2 Dementia, pp. 435–63. ISSN: 1538-6899 (Electronic) 1080-2371 (Linking). DOI: 10.1212/CON.0000000000000309. URL: https://www.ncbi.nlm.nih.gov/pubmed/27042903.

GONCALVES, S. and T. F. OUTEIRO (2013):
'Assessing the subcellular dynamics of alpha-synuclein using photoactivation microscopy',
in: *Mol Neurobiol* 47.3, pp. 1081–92. ISSN: 1559-1182 (Electronic) 0893-7648 (Print) 0893-7648 (Linking). DOI: 10.1007/s12035-013-8406-x. URL: https://www.ncbi.nlm.nih.gov/pubmed/23389286.

GROTEMEYER, ALEXANDER ET AL. (2022):
'Neuroinflammation in Parkinson's Disease – Putative Pathomechanisms and Targets for Disease-Modification',
in: *Frontiers in Immunology* 13.

GUTEKUNST, C. A. ET AL. (1999):
'Nuclear and neuropil aggregates in Huntington's disease: relationship to neuropathology',
in: *J Neurosci* 19.7, pp. 2522–34. ISSN: 0270-6474 (Print) 1529-2401 (Electronic) 0270-6474 (Linking). DOI: 10.1523/JNEUROSCI.19-07-02522.1999. URL: https://www.ncbi.nlm.nih.gov/pubmed/10087066.

HALLIDAY, G. M. and C. H. STEVENS (2011):
'Glia: initiators and progressors of pathology in Parkinson's disease',
in: *Mov Disord* 26.1, pp. 6–17. ISSN: 1531-8257 (Electronic) 0885-3185 (Linking). DOI: 10.1002/mds.23455. URL: https://www.ncbi.nlm.nih.gov/pubmed/21322014.

HAM, SU JIN ET AL. (2020):
'Decision between Mitophagy and Apoptosis by Parkin via VDAC1 Ubiquitination',
in: *PNAS* 117.8, pp. 4281–4291.

HAMON, M. A. and J. QUINTIN (2016):
'Innate immune memory in mammals',

in: *Semin Immunol* 28.4, pp. 351–8. ISSN: 1096-3618 (Electronic) 1044-5323 (Linking). DOI: 10.1016/j.smim.2016.05.003. URL: https://www.ncbi.nlm.nih.gov/pubmed/27264334.

HAN, JIAN ET AL. (2020):
'High-Fat Diet-Induced Weight Gain, Behavioral Deficits, and Dopamine Changes in Young C57BL/6J Mice',
in: *Frontiers in Nutrition* 7, p. 591161. ISSN: 2296-861X. DOI: 10.3389/fnut.2020.591161. URL: https://www.ncbi.nlm.nih.gov/pubmed/33553228.

HANTIKAINEN, ESSI ET AL. (2022):
'Dietary fat intake and risk of Parkinson disease: results from the Swedish National March Cohort',
in: *European Journal of Epidemiology* 37.6, pp. 603–613. DOI: 10.1007/s10654-022-00863-8. URL: https://doi.org/10.1007/s10654-022-00863-8.

HAO, LING-YANG, BENOIT I. GIASSON AND NANCY M. BONINI (2010):
'DJ-1 is critical for mitochondrial function and rescues PINK1 loss of function',
in: *Proceedings of the National Academy of Sciences* 107.21, pp. 9747–9752. ISSN: 0027-8424. DOI: 10.1073/pnas.0911175107. URL: https://dx.doi.org/10.1073/pnas.0911175107.

HAUSER, DAVID N. AND TERESA G. HASTINGS (2013):
'Mitochondrial dysfunction and oxidative stress in Parkinson's disease and monogenic parkinsonism',
in: *Neurobiology of Disease* 51, pp. 35–42. ISSN: 0969-9961. DOI: 10.1016/j.nbd.2012.10.011. URL: https://dx.doi.org/10.1016/j.nbd.2012.10.011.

HODGSON, J. G. ET AL. (1999):
'A YAC mouse model for Huntington's disease with full-length mutant huntingtin, cytoplasmic toxicity, and selective striatal neurodegeneration',
in: *Neuron* 23.1, pp. 181–92. ISSN: 0896-6273 (Print) 0896-6273 (Linking). DOI: 10.1016/s0896-6273(00)80764-3. URL: https://www.ncbi.nlm.nih.gov/pubmed/10402204.

HONG, S. ET AL. (2021):
'A high fat, sugar, and salt Western diet induces motor-muscular and sensory dysfunctions and neurodegeneration in mice during aging: Ameliorative action of metformin',
in: *CNS Neurosci Ther* 27.12, pp. 1458–1471. ISSN: 1755-5949 (Electronic) 1755-5930 (Print) 1755-5930 (Linking). DOI: 10.1111/cns.13726. URL: https://www.ncbi.nlm.nih.gov/pubmed/34510763.

HOULDEN, H. AND A. B. SINGLETON (2012):
'The genetics and neuropathology of Parkinson's disease',
in: *Acta Neuropathol* 124.3, pp. 325–38. ISSN: 1432-0533 (Electronic) 0001-6322 (Print) 0001-6322 (Linking). DOI: 10.1007/s00401-012-1013-5. URL: https://www.ncbi.nlm.nih.gov/pubmed/22806825.

HUANG, MINHONG ET AL. (2023):
'Microglial immune regulation by epigenetic reprogramming through histone H3K27 acetylation in neuroinflammation',
in: *Frontiers in Immunology* 14.

HUANG, WEN-JUAN, WEI-WEI CHEN AND XIA ZHANG (2016):
'Huntington's disease: Molecular basis of pathology and status of current therapeutic approaches',
in: *Experimental and Therapeutic Medicine* 12.4, pp. 1951–1956. ISSN: 1792-0981. DOI: 10.3892/etm.2016.3566. URL: https://dx.doi.org/10.3892/etm.2016.3566.

HUGHES, A. J. ET AL. (1992):
'Accuracy of clinical diagnosis of idiopathic Parkinson's disease: a clinico-pathological study of 100 cases',
in: *Journal of Neurology, Neurosurgery & Psychiatry* 55.3, pp. 181–184. DOI: 10.1136/jnnp.55.3.181. URL: https://www.ncbi.nlm.nih.gov/pubmed/1564476.

HUNTER, R. L. ET AL. (2007):
'Inflammation induces mitochondrial dysfunction and dopaminergic neurodegeneration in the nigrostriatal system',

in: *J Neurochem* 100.5, pp. 1375–86. ISSN: 0022-3042 (Print) 0022-3042 (Linking). DOI: 10.1111/j.1471-4159.2006.04327.x. URL: https://www.ncbi.nlm.nih.gov/pubmed/17254027.

HYEON, J. W., A. H. KIM and H. YANO (2021):
'Epigenetic regulation in Huntington's disease',
in: *Neurochem Int* 148, p. 105074. ISSN: 1872-9754 (Electronic) 0197-0186 (Linking). DOI: 10.1016/j.neuint.2021.105074. URL: https://www.ncbi.nlm.nih.gov/pubmed/34038804.

IMARISIO, S. ET AL. (2008):
'Huntington's disease: from pathology and genetics to potential therapies',
in: *Biochem J* 412.2, pp. 191–209. ISSN: 1470-8728 (Electronic), 0264-6021 (Linking). DOI: 10.1042/BJ20071619. URL: https://www.ncbi.nlm.nih.gov/pubmed/18466116.

JANG, YUNSEON ET AL. (2017):
'A High-fat Diet Induces a Loss of Midbrain Dopaminergic Neuronal Function That Underlies Motor Abnormalities',
in: *Experimental Neurobiology* 26.2, pp. 104–112. ISSN: 1226-2560. DOI: 10.5607/en.2017.26.2.104. URL: https://dx.doi.org/10.5607/en.2017.26.2.104.

JANSEN, ANNE H. P. ET AL. (2017):
'Frequency of nuclear mutant huntingtin inclusion formation in neurons and glia is cell-type-specific',
in: *Glia* 65.1, pp. 50–61. ISSN: 0894-1491. DOI: 10.1002/glia.23050. URL: https://dx.doi.org/10.1002/glia.23050.

JAROSINSKA, O. D. and S. G. D. RUDIGER (2021):
'Molecular Strategies to Target Protein Aggregation in Huntington's Disease',
in: *Front Mol Biosci* 8, p. 769184. ISSN: 2296-889X (Print) 2296-889X (Electronic) 2296-889X (Linking). DOI: 10.3389/fmolb.2021.769184. URL: https://www.ncbi.nlm.nih.gov/pubmed/34869596.

JAVITCH, J. A. ET AL. (1985):
'Parkinsonism-inducing neurotoxin, N-methyl-4-phenyl-1,2,3,6 -tetrahydropyridine: uptake of the metabolite N-methyl-4-phenylpyridine by dopamine neurons explains selective toxicity',
in: *Proceedings of the National Academy of Sciences* 82.7, pp. 2173–2177. ISSN: 0027-8424. DOI: 10.1073/pnas.82.7.2173. URL: https://dx.doi.org/10.1073/pnas.82.7.2173.

JEON, B. S., V. JACKSON-LEWIS and R. E. BURKE (1995):
'6-Hydroxydopamine lesion of the rat substantia nigra: time course and morphology of cell death',
in: *Neurodegeneration* 4.2, pp. 131–7. ISSN: 1055-8330 (Print) 1055-8330 (Linking). DOI: 10.1006/neur.1995.0016. URL: https://www.ncbi.nlm.nih.gov/pubmed/7583676.

JHA, M. K., W. H. LEE and K. SUK (2016):
'Functional polarization of neuroglia: Implications in neuroinflammation and neurological disorders',
in: *Biochem Pharmacol* 103, pp. 1–16. ISSN: 1873-2968 (Electronic) 0006-2952 (Linking). DOI: 10.1016/j.bcp.2015.11.003. URL: https://www.ncbi.nlm.nih.gov/pubmed/26556658.

JILL K. MORRIS GREGORY L. BOMHOFF, JOHN A. STANFORD and PAIGE C. GEIGER (2010):
'Neurodegeneration in an animal model of Parkinson's disease is exacerbated by a high-fat diet',
in: *American Journal of Physiology*.

JOERS, V. ET AL. (2017):
'Microglial phenotypes in Parkinson's disease and animal models of the disease',
in: *Prog Neurobiol* 155, pp. 57–75. ISSN: 1873-5118 (Electronic) 0301-0082 (Print) 0301-0082 (Linking). DOI: 10.1016/j.pneurobio.2016.04.006. URL: https://www.ncbi.nlm.nih.gov/pubmed/27107797.

KAHLE, P. J. ET AL. (2001):
'Selective insolubility of alpha-synuclein in human Lewy body diseases is recapitulated in a transgenic mouse model',
in: *Am J Pathol* 159.6, pp. 2215–25. ISSN: 0002-9440 (Print) 1525-2191 (Electronic) 0002-9440 (Linking). DOI: 10.1016/s0002-9440(10)63072-6. URL: https://www.ncbi.nlm.nih.gov/pubmed/11733371.

KANNARKAT, G. T., J. M. BOSS and M. G. TANSEY (2013):
'The role of innate and adaptive immunity in Parkinson's disease',
in: *J Parkinsons Dis* 3.4, pp. 493–514. ISSN: 1877-718X (Electronic) 1877-7171 (Linking). DOI: 10.3233/JPD-130250. URL: https://www.ncbi.nlm.nih.gov/pubmed/24275605.

KASEN, A. ET AL. (2022):
'Upregulation of alpha-synuclein following immune activation: Possible trigger of Parkinson's disease',
in: *Neurobiol Dis* 166, p. 105654. ISSN: 1095-953X (Electronic) 0969-9961 (Linking). DOI: 10.1016/j.nbd.2022.105654. URL: https://www.ncbi.nlm.nih.gov/pubmed/35143968.

KATSUNO, M. ET AL. (2008):
'Molecular genetics and biomarkers of polyglutamine diseases',
in: *Curr Mol Med* 8.3, pp. 221–34. ISSN: 1566-5240 (Print) 1566-5240 (Linking). DOI: 10.2174/156652408784221298. URL: https://www.ncbi.nlm.nih.gov/pubmed/18473821.

KAUR, K. ET AL. (2017):
'Neuroinflammation - A major cause for striatal dopaminergic degeneration in Parkinson's disease',
in: *J Neurol Sci* 381, pp. 308–314. ISSN: 1878-5883 (Electronic) 0022-510X (Linking). DOI: 10.1016/j.jns.2017.08.3251. URL: https://www.ncbi.nlm.nih.gov/pubmed/28991704.

KAWAHATA, I., D. I. FINKELSTEIN and K. FUKUNAGA (2022):
'Pathogenic Impact of alpha-Synuclein Phosphorylation and Its Kinases in alpha-Synucleinopathies',
in: *Int J Mol Sci* 23.11. ISSN: 1422-0067 (Electronic) 1422-0067 (Linking). DOI: 10.3390/ijms23116216. URL: https://www.ncbi.nlm.nih.gov/pubmed/35682892.

KAYE, J., T. REISINE and S. FINKBEINER (2021):
'Huntington's disease mouse models: unraveling the pathology caused by CAG repeat expansion',
in: *Fac Rev* 10, p. 77. ISSN: 2732-432X (Electronic) 2732-432X (Linking). DOI: 10.12703/r/10-77. URL: https://www.ncbi.nlm.nih.gov/pubmed/34746930.

KEANE, P. C. ET AL. (2011):
'Mitochondrial Dysfunction in Parkinson's Disease',
in: *Parkinson's Disease* 2011, pp. 1–18. ISSN: 2042-0080. DOI: 10.4061/2011/716871. URL: https://dx.doi.org/10.4061/2011/716871.

KILZHEIMER, A. ET AL. (2023):
'Failure of diet-induced transcriptional adaptations in alpha-synuclein transgenic mice',
in: *Hum Mol Genet* 32.3, pp. 450–461. ISSN: 1460-2083 (Electronic) 0964-6906 (Print) 0964-6906 (Linking). DOI: 10.1093/hmg/ddac205. URL: https://www.ncbi.nlm.nih.gov/pubmed/36001352.

KIM, J. ET AL. (2016):
'Transgenic expression of cyclooxygenase-2 (COX2) causes premature aging phenotypes in mice',
in: *Aging (Albany NY)* 8.10, pp. 2392–2406. ISSN: 1945-4589 (Electronic) 1945-4589 (Linking). DOI: 10.18632/aging.101060. URL: https://www.ncbi.nlm.nih.gov/pubmed/27750221.

KIM, R. ET AL. (2018):
'Peripheral blood inflammatory markers in early Parkinson's disease',
in: *J Clin Neurosci* 58, pp. 30–33. ISSN: 1532-2653 (Electronic) 0967-5868 (Linking). DOI: 10.1016/j.jocn.2018.10.079. URL: https://www.ncbi.nlm.nih.gov/pubmed/30454693.

KIM, Y. J. ET AL. (2001):
'Caspase 3-cleaved N-terminal fragments of wild-type and mutant huntingtin are present in normal and Huntington's disease brains, associate with membranes, and undergo calpain-dependent proteolysis',
in: *Proc Natl Acad Sci U S A* 98.22, pp. 12784–9. ISSN: 0027-8424 (Print) 1091-6490 (Electronic) 0027-8424 (Linking). DOI: 10.1073/pnas.221451398. URL: https://www.ncbi.nlm.nih.gov/pubmed/11675509.

KIP, E. and L. C. PARR-BROWNLIE (2023):
'Healthy lifestyles and wellbeing reduce neuroinflammation and prevent neurodegenerative and psychiatric disorders',

in: *Front Neurosci* 17, p. 1092537. ISSN: 1662-4548 (Print) 1662-453X (Electronic) 1662-453X (Linking). DOI: 10.3389/fnins.2023.1092537. URL: https://www.ncbi.nlm.nih.gov/pubmed/36875655.

KIP, ELODIE and LOUISE C. PARR-BROWNLIE (2022):
'Reducing neuroinflammation via therapeutic compounds and lifestyle to prevent or delay progression of Parkinson's disease',
in: *Ageing Res Rev* 78, p. 101618. ISSN: 1872-9649 (Electronic) 1568-1637 (Linking). DOI: 10.1016/j.arr.2022.101618. URL: https://www.ncbi.nlm.nih.gov/pubmed/35395416.

KISIPAN, M. L. ET AL. (2022):
'Bodyweight, locomotion, and behavioral responses of the naked mole rat (Heterocephalus glaber) to lipopolysaccharide administration',
in: *J Comp Physiol A Neuroethol Sens Neural Behav Physiol* 208.4, pp. 493–504. ISSN: 1432-1351 (Electronic) 0340-7594 (Print) 0340-7594 (Linking). DOI: 10.1007/s00359-022-01557-y. URL: https://www.ncbi.nlm.nih.gov/pubmed/35731263.

KITADA, TOHRU ET AL. (1998):
'Mutations in the parkin gene cause autosomal recessive juvenile parkinsonism',
in: *Nature* 392.6676, pp. 605–608. ISSN: 0028-0836. DOI: 10.1038/33416. URL: https://dx.doi.org/10.1038/33416.

KO, J., S. OU and P. H. PATTERSON (2001):
'New anti-huntingtin monoclonal antibodies: implications for huntingtin conformation and its binding proteins',
in: *Brain Res Bull* 56.3-4, pp. 319–29. ISSN: 0361-9230 (Print) 0361-9230 (Linking). DOI: 10.1016/s0361-9230(01)00599-8. URL: https://www.ncbi.nlm.nih.gov/pubmed/11719267.

KOULI, A., K. M. TORSNEY and W. L. KUAN (2018):
'Parkinson's Disease: Etiology, Neuropathology, and Pathogenesis',
in: *Parkinson's Disease: Pathogenesis and Clinical Aspects*. Ed. by T. B. Stoker and J. C. Greenland. Brisbane (AU). ISBN: 978-0-9944381-6-4. DOI: 10.15586/codonpublications.parkinsonsdisease.2018.ch1. URL: https://www.ncbi.nlm.nih.gov/pubmed/30702842.

KRASHIA, P. ET AL. (2019):
'Blunting neuroinflammation with resolvin D1 prevents early pathology in a rat model of Parkinson's disease',
in: *Nat Commun* 10.1, p. 3945. ISSN: 2041-1723 (Electronic) 2041-1723 (Linking). DOI: 10.1038/s41467-019-11928-w. URL: https://www.ncbi.nlm.nih.gov/pubmed/31477726.

KREUTZBERG, G. W. (1996):
'Microglia: a sensor for pathological events in the CNS',
in: *Trends Neurosci* 19.8, pp. 312–8. ISSN: 0166-2236 (Print) 0166-2236 (Linking). DOI: 10.1016/0166-2236(96)10049-7. URL: https://www.ncbi.nlm.nih.gov/pubmed/8843599.

KSHIRSAGAR, PAYAL B. ET AL. (2021):
'Huntington's disease: Pathophysiology and therapeutic intervention',
in: *GSC Biological and Pharmaceutical Sciences* 13, pp. 171–184.

KUEMMERLE, S. ET AL. (1999):
'Huntington Aggregates May Not Predict Neuronal Death in Huntington's Disease',
in: *Annals of Neurology* 46.6, pp. 842–849. DOI: 10.1002/1531-8249(199912)46:6<842::AID-ANA1>3.0.CO;2-Q. URL: https://doi.org/10.1002/1531-8249(199912)46:6%3C842::AID-ANA1%3E3.0.CO;2-Q.

KWON, H. S. and S. H. KOH (2020):
'Neuroinflammation in neurodegenerative disorders: the roles of microglia and astrocytes',
in: *Transl Neurodegener* 9.1, p. 42. ISSN: 2047-9158 (Print) 2047-9158 (Electronic) 2047-9158 (Linking). DOI: 10.1186/s40035-020-00221-2. URL: https://www.ncbi.nlm.nih.gov/pubmed/33239064.

LABBÉ, CATHERINE, OSWALDO LORENZO-BETANCOR and OWEN A. ROSS (2016):
'Epigenetic regulation in Parkinson's disease',
in: *Acta Neuropathologica* 132.4, pp. 515–530. ISSN: 0001-6322. DOI: 10.1007/s00401-016-1590-9. URL: https://dx.doi.org/10.1007/s00401-016-1590-9.

LANGLEY, M. R. ET AL. (2022):
'Editorial: Environmental Effect on Neuroinflammation and Neurodegeneration',
in: *Front Cell Neurosci* 16, p. 935190. ISSN: 1662-5102 (Print) 1662-5102 (Electronic) 1662-5102 (Linking). DOI: 10.3389/fncel.2022.935190. URL: https://www.ncbi.nlm.nih.gov/pubmed/35800133.

LASSELIN, J. ET AL. (2020):
'Comparison of bacterial lipopolysaccharide-induced sickness behavior in rodents and humans: Relevance for symptoms of anxiety and depression',
in: *Neurosci Biobehav Rev* 115, pp. 15–24. ISSN: 1873-7528 (Electronic) 0149-7634 (Linking). DOI: 10.1016/j.neubiorev.2020.05.001. URL: https://www.ncbi.nlm.nih.gov/pubmed/32433924.

LEE, J. ET AL. (2013):
'Epigenetic mechanisms of neurodegeneration in Huntington's disease',
in: *Neurotherapeutics* 10.4, pp. 664–76. ISSN: 1878-7479 (Electronic) 1878-7479 (Linking). DOI: 10.1007/s13311-013-0206-5. URL: https://www.ncbi.nlm.nih.gov/pubmed/24006238.

LEE, SUNG WON ET AL. (2018):
'Repeated immune activation with low-dose lipopolysaccharide attenuates the severity of Huntington's disease in R6/2 transgenic mice',
in: *Animal Cells and Systems* 22.4, pp. 219–226. ISSN: 1976-8354. DOI: 10.1080/19768354.2018.1473291. URL: https://dx.doi.org/10.1080/19768354.2018.1473291.

LI, H. ET AL. (2001):
'Huntingtin aggregate-associated axonal degeneration is an early pathological event in Huntington's disease mice',
in: *The Journal of Neuroscience* 21.21, pp. 8473–8481. ISSN: 0270-6474. DOI: 10.1523/JNEUROSCI.21-21-08473.2001. URL: https://www.jneurosci.org/content/21/21/8473.

LI, JIE-QIONG, LAN TAN and JIN-TAI YU (2014):
'The role of the LRRK2 gene in Parkinsonism',
in: *Molecular Neurodegeneration* 9.1, p. 47. ISSN: 1750-1326. DOI: 10.1186/1750-1326-9-47. URL: https://dx.doi.org/10.1186/1750-1326-9-47.

LI, N. ET AL. (2020):
'Immunoregulation of microglial polarization: an unrecognized physiological function of alpha-synuclein',
in: *J Neuroinflammation* 17.1, p. 272. ISSN: 1742-2094 (Electronic) 1742-2094 (Linking). DOI: 10.1186/s12974-020-01940-z. URL: https://www.ncbi.nlm.nih.gov/pubmed/32943057.

LI, R. ET AL. (2022):
'Abnormal B-Cell and Tfh-Cell Profiles in Patients With Parkinson Disease: A Cross-sectional Study',
in: *Neurol Neuroimmunol Neuroinflamm* 9.2. ISSN: 2332-7812 (Electronic) 2332-7812 (Linking). DOI: 10.1212/NXI.0000000000001125. URL: https://www.ncbi.nlm.nih.gov/pubmed/34955458.

LI, SHENG ET AL. (2025):
'A Crazy Trio in Parkinson's Disease: Metabolism Alteration, α-Synuclein Aggregation, and Oxidative Stress'. English,
in: *Molecular and Cellular Biochemistry* 480.1, pp. 139–157. ISSN: 0300-8177. DOI: 10.1007/s11010-024-04985-3. URL: https://doi.org/10.1007/s11010-024-04985-3.

LI, W. ET AL. (2006):
'Expression and characterization of full-length human huntingtin, an elongated HEAT repeat protein',
in: *J Biol Chem* 281.23, pp. 15916–22. ISSN: 0021-9258 (Print) 0021-9258 (Linking). DOI: 10.1074/jbc.M511007200. URL: https://www.ncbi.nlm.nih.gov/pubmed/16595690.

LIN, B. ET AL. (1993):
'Differential 3' polyadenylation of the Huntington disease gene results in two mRNA species with variable tissue expression',
in: *Hum Mol Genet* 2.10, pp. 1541–5. ISSN: 0964-6906 (Print) 0964-6906 (Linking). DOI: 10.1093/hmg/2.10.1541. URL: https://www.ncbi.nlm.nih.gov/pubmed/7903579.

LIU, M. and G. BING (2011):
'Lipopolysaccharide animal models for Parkinson's disease',
in: *Parkinsons Dis* 2011, p. 327089. ISSN: 2042-0080 (Electronic) 2042-0080 (Linking). DOI: 10.4061/2011/327089. URL: https://www.ncbi.nlm.nih.gov/pubmed/21603177.

LIU, PING (2022):
'Transcriptional signatures of microglial innate immune memory in models of Parkinson's and Huntington's disease',
Thesis.

LIU, T. W., C. M. CHEN and K. H. CHANG (2022):
'Biomarker of Neuroinflammation in Parkinson's Disease',
in: *Int J Mol Sci* 23.8. ISSN: 1422-0067 (Electronic) 1422-0067 (Linking). DOI: 10.3390/ijms23084148. URL: https://www.ncbi.nlm.nih.gov/pubmed/35456966.

LONG-SMITH, C. M., A. M. SULLIVAN and Y. M. NOLAN (2009):
'The influence of microglia on the pathogenesis of Parkinson's disease',
in: *Prog Neurobiol* 89.3, pp. 277–87. ISSN: 1873-5118 (Electronic) 0301-0082 (Linking). DOI: 10.1016/j.pneurobio.2009.08.001. URL: https://www.ncbi.nlm.nih.gov/pubmed/19686799.

LU, L. ET AL. (2013):
'Voltage-dependent anion channel involved in the alpha-synuclein-induced dopaminergic neuron toxicity in rats',
in: *Acta Biochim Biophys Sin (Shanghai)* 45.3, pp. 170–8. ISSN: 1745-7270 (Electronic) 1672-9145 (Linking). DOI: 10.1093/abbs/gms114. URL: https://www.ncbi.nlm.nih.gov/pubmed/23291291.

LUDTMANN, M. H. R. ET AL. (2018):
'alpha-synuclein oligomers interact with ATP synthase and open the permeability transition pore in Parkinson's disease',
in: *Nat Commun* 9.1, p. 2293. ISSN: 2041-1723 (Electronic) 2041-1723 (Linking). DOI: 10.1038/s41467-018-04422-2. URL: https://www.ncbi.nlm.nih.gov/pubmed/29895861.

MACDONALD, M. (1993):
'A novel gene containing a trinucleotide repeat that is expanded and unstable on Huntington's disease chromosomes',
in: *Cell* 72.6, pp. 971–983. ISSN: 0092-8674. DOI: 10.1016/0092-8674(93)90585-e. URL: https://dx.doi.org/10.1016/0092-8674(93)90585-e.

MACHIYA ET AL. (2010):
'Phosphorylated alpha-synuclein at Ser-129 is targeted to the proteasome pathway in a ubiquitin-independent manner',
in: *Journal of Biological Chemistry* 40732–40744.

MAESAKO, M. ET AL. (2013):
'Continuation of exercise is necessary to inhibit high fat diet-induced beta-amyloid deposition and memory deficit in amyloid precursor protein transgenic mice',
in: *PLoS One* 8.9, e72796. ISSN: 1932-6203 (Electronic) 1932-6203 (Linking). DOI: 10.1371/journal.pone.0072796. URL: https://www.ncbi.nlm.nih.gov/pubmed/24023774.

MANGIARINI, LAURA ET AL. (1996):
'Exon 1 of the HD Gene with an Expanded CAG Repeat Is Sufficient to Cause a Progressive Neurological Phenotype in Transgenic Mice',
in: *Cell* 87.

MANNING-BOG, A. B. ET AL. (2002):
'The herbicide paraquat causes up-regulation and aggregation of alpha-synuclein in mice: paraquat and alpha-synuclein',
in: *J Biol Chem* 277.3, pp. 1641–4. ISSN: 0021-9258 (Print) 0021-9258 (Linking). DOI: 10.1074/jbc.C100560200. URL: https://www.ncbi.nlm.nih.gov/pubmed/11707429.

MAZUCO, TÚLIO R. R. ET AL. (2019):
'LPS-induced sickness behavior is not affected by selenium but is switched off by psychogenic stress in rats',
in: *Veterinary Research Communications* 43, pp. 239–247.

MCCOY, MELISSA K. and MARK R. COOKSON (2011):
'DJ-1 regulation of mitochondrial function and autophagy through oxidative stress',
in: *Autophagy* 7.5, pp. 531–532. ISSN: 1554-8627. DOI: 10.4161/auto.7.5.14684. URL: https://dx.doi.org/10.4161/auto.7.5.14684.

MCNAUGHT, K. S. ET AL. (2002):
'Aggresome-related biogenesis of Lewy bodies',
in: *Eur J Neurosci* 16.11, pp. 2136–48. ISSN: 0953-816X (Print) 0953-816X (Linking). DOI: 10.1046/j.1460-9568.2002.02301.x. URL: https://www.ncbi.nlm.nih.gov/pubmed/12473081.

MENALLED, L. B. and M. F. CHESSELET (2002):
'Mouse models of Huntington's disease',
in: *Trends Pharmacol Sci* 23.1, pp. 32–9. ISSN: 0165-6147 (Print) 0165-6147 (Linking). DOI: 10.1016/s0165-6147(00)01884-8. URL: https://www.ncbi.nlm.nih.gov/pubmed/11804649.

MENDE-MUELLER, L. M. ET AL. (2001):
'Tissue-specific proteolysis of Huntingtin (htt) in human brain: evidence of enhanced levels of N- and C-terminal htt fragments in Huntington's disease striatum',
in: *J Neurosci* 21.6, pp. 1830–7. ISSN: 1529-2401 (Electronic) 0270-6474 (Print) 0270-6474 (Linking). DOI: 10.1523/JNEUROSCI.21-06-01830.2001. URL: https://www.ncbi.nlm.nih.gov/pubmed/11245667.

MEREDITH, G. E. and D. J. RADEMACHER (2011):
'MPTP mouse models of Parkinson's disease: an update',
in: *J Parkinsons Dis* 1.1, pp. 19–33. ISSN: 1877-718X (Electronic) 1877-7171 (Print) 1877-7171 (Linking). DOI: 10.3233/JPD-2011-11023. URL: https://www.ncbi.nlm.nih.gov/pubmed/23275799.

MIRANDA-MORALES, E. ET AL. (2017):
'Implications of DNA Methylation in Parkinson's Disease',
in: *Front Mol Neurosci* 10, p. 225. ISSN: 1662-5099 (Print) 1662-5099 (Electronic) 1662-5099 (Linking). DOI: 10.3389/fnmol.2017.00225. URL: https://www.ncbi.nlm.nih.gov/pubmed/28769760.

MISHIZEN-EBERZ, AMANDA J. ET AL. (2005):
'Cleavage of α-Synuclein by Calpain: Potential Role in Degradation of Fibrillized and Nitrated Species of α-Synuclein',
in: *ACS Chemical Neuroscience* 7818–7829.

MO, C., A. J. HANNAN and T. RENOIR (2015):
'Environmental factors as modulators of neurodegeneration: insights from gene-environment interactions in Huntington's disease',
in: *Neurosci Biobehav Rev* 52, pp. 178–92. ISSN: 1873-7528 (Electronic) 0149-7634 (Linking). DOI: 10.1016/j.neubiorev.2015.03.003. URL: https://www.ncbi.nlm.nih.gov/pubmed/25770041.

MOON, HYO EUN and SUN HA PAEK (2015):
'Mitochondrial Dysfunction in Parkinson's Disease',
in: *Experimental Neurobiology* 24.2, pp. 103–116. ISSN: 1226-2560. DOI: 10.5607/en.2015.24.2.103. URL: https://dx.doi.org/10.5607/en.2015.24.2.103.

MORRIS, JILL K. ET AL. (2010):
'Neurodegeneration in an animal model of Parkinson's disease is exacerbated by a high-fat diet',
in: *American Journal of Physiology.*

MORRIS, M. C., E. A. GILLIAM and L. LI (2014):
'Innate immune programing by endotoxin and its pathological consequences',
in: *Front Immunol* 5, p. 680. ISSN: 1664-3224 (Print) 1664-3224 (Linking). DOI: 10.3389/fimmu.2014.00680. URL: https://www.ncbi.nlm.nih.gov/pubmed/25610440.

MULDER, W. J. M. ET AL. (2019):
'Therapeutic targeting of trained immunity',
in: *Nat Rev Drug Discov* 18.7, pp. 553–566. ISSN: 1474-1784 (Electronic) 1474-1776 (Print) 1474-1776 (Linking). DOI: 10.1038/s41573-019-0025-4. URL: https://www.ncbi.nlm.nih.gov/pubmed/30967658.

MULLIN, S. and A. SCHAPIRA (2013):
'alpha-Synuclein and mitochondrial dysfunction in Parkinson's disease',
in: *Mol Neurobiol* 47.2, pp. 587–97. ISSN: 1559-1182 (Electronic) 0893-7648 (Print) 0893-7648 (Linking). DOI: 10.1007/s12035-013-8394-x. URL: https://www.ncbi.nlm.nih.gov/pubmed/23361255.

NAKAMURA, K. (2013):
'alpha-Synuclein and mitochondria: partners in crime?',
in: *Neurotherapeutics* 10.3, pp. 391–9. ISSN: 1878-7479 (Electronic) 1933-7213 (Print) 1878-7479 (Linking). DOI: 10.1007/s13311-013-0182-9. URL: https://www.ncbi.nlm.nih.gov/pubmed/23512373.

NEHER, J. J. and C. CUNNINGHAM (2019):
'Priming Microglia for Innate Immune Memory in the Brain',
in: *Trends Immunol* 40.4, pp. 358–374. ISSN: 1471-4981 (Electronic) 1471-4906 (Linking). DOI: 10.1016/j.it.2019.02.001. URL: https://www.ncbi.nlm.nih.gov/pubmed/30833177.

NETEA, M. G., J. DOMINGUEZ-ANDRES ET AL. (2020):
'Defining trained immunity and its role in health and disease',
in: *Nat Rev Immunol* 20.6, pp. 375–388. ISSN: 1474-1741 (Electronic) 1474-1733 (Linking). DOI: 10.1038/s41577-020-0285-6. URL: https://www.ncbi.nlm.nih.gov/pubmed/32132681.

NETEA, M. G., L. A. JOOSTEN ET AL. (2016):
'Trained immunity: A program of innate immune memory in health and disease',
in: *Science* 352.6284, aaf1098. ISSN: 1095-9203 (Electronic) 0036-8075 (Linking). DOI: 10.1126/science.aaf1098. URL: https://www.ncbi.nlm.nih.gov/pubmed/27102489.

NG, C. W. ET AL. (2013):
'Extensive changes in DNA methylation are associated with expression of mutant huntingtin',
in: *Proceedings of the National Academy of Sciences* 110.6, pp. 2354–2359. ISSN: 0027-8424. DOI: 10.1073/pnas.1221292110. URL: https://dx.doi.org/10.1073/pnas.1221292110.

NIES, Y. H. ET AL. (2021):
'MicroRNA Dysregulation in Parkinson's Disease: A Narrative Review',
in: *Front Neurosci* 15, p. 660379. ISSN: 1662-4548 (Print) 1662-453X (Linking). DOI: 10.3389/fnins.2021.660379. URL: https://www.ncbi.nlm.nih.gov/pubmed/33994934.

NOPOULOS, PEGGY C. (2016):
'Huntington disease: a single-gene degenerative disorder of the striatum',
in: *Dialogues Clin Neurosci* 18.1, pp. 91–98. ISSN: 1958-5969 (Electronic), 1294-8322 (Print). DOI: 10.31887/DCNS.2016.18.1/pnopoulos. URL: https://www.ncbi.nlm.nih.gov/pubmed/27069383.

NORONHA, S. S. R. ET AL. (2019):
'Association of high-fat diet with neuroinflammation, anxiety-like defensive behavioral responses, and altered thermoregulatory responses in male rats',
in: *Brain Behav Immun* 80, pp. 500–511. ISSN: 1090-2139 (Electronic) 0889-1591 (Linking). DOI: 10.1016/j.bbi.2019.04.030. URL: https://www.ncbi.nlm.nih.gov/pubmed/31022457.

NOVATI, A., H. P. NGUYEN and J. SCHULZE-HENTRICH (2022):
'Environmental stimulation in Huntington disease patients and animal models',
in: *Neurobiol Dis* 171, p. 105725. ISSN: 1095-953X (Electronic) 0969-9961 (Linking). DOI: 10.1016/j.nbd.2022.105725. URL: https://www.ncbi.nlm.nih.gov/pubmed/35427742.

NUBER, S. ET AL. (2013):
'A progressive dopaminergic phenotype associated with neurotoxic conversion of alpha-synuclein in BAC-transgenic rats',
in: *Brain* 136.Pt 2, pp. 412–32. ISSN: 1460-2156 (Electronic) 0006-8950 (Linking). DOI: 10.1093/brain/aws358. URL: https://www.ncbi.nlm.nih.gov/pubmed/23413261.

OKOCHI, M. ET AL. (2000):
'Constitutive phosphorylation of the Parkinson's disease associated alpha-synuclein',
in: *J Biol Chem* 275.1, pp. 390–7. ISSN: 0021-9258 (Print) 0021-9258 (Linking). DOI: 10.1074/jbc.275.1.390. URL: https://www.ncbi.nlm.nih.gov/pubmed/10617630.

OLANOW, C. W. ET AL. (2004):
'Lewy-body formation is an aggresome-related process: a hypothesis',
in: *Lancet Neurol* 3.8, pp. 496–503. ISSN: 1474-4422 (Print) 1474-4422 (Linking). DOI: 10.1016/S1474-4422(04)00827-0. URL: https://www.ncbi.nlm.nih.gov/pubmed/15261611.

OUESLATI, ABID (2016):
'Implication of Alpha-Synuclein Phosphorylation at S129 in Synucleinopathies: What Have We Learned in the Last Decade?',
in: *Journal of Parkinson's Disease* 6.1, pp. 39–51. ISSN: 1877-7171. DOI: 10.3233/jpd-160779. URL: https://dx.doi.org/10.3233/jpd-160779.

OULLIER, THIBAULD ET AL. (2020):
Optimizing filter trap assay for the detection of aggregated alpha-synuclein in brain samples,
Online Database.

PAJARES, M. ET AL. (2020):
'Inflammation in Parkinson's Disease: Mechanisms and Therapeutic Implications',
in: *Cells* 9.7. ISSN: 2073-4409 (Electronic) 2073-4409 (Linking). DOI: 10.3390/cells9071687. URL: https://www.ncbi.nlm.nih.gov/pubmed/32674367.

PALPAGAMA, THULANI H. ET AL. (2019):
'The Role of Microglia and Astrocytes in Huntington's Disease',
in: *Frontiers in Molecular Neuroscience* 12, p. 258. ISSN: 1662-5099. DOI: 10.3389/fnmol.2019.00258. URL: https://www.ncbi.nlm.nih.gov/pubmed/31708741.

PANG, S. Y. ET AL. (2019):
'The interplay of aging, genetics and environmental factors in the pathogenesis of Parkinson's disease',
in: *Transl Neurodegener* 8, p. 23. ISSN: 2047-9158 (Print) 2047-9158 (Electronic) 2047-9158 (Linking). DOI: 10.1186/s40035-019-0165-9. URL: https://www.ncbi.nlm.nih.gov/pubmed/31428316.

PANICKER, N. ET AL. (2019):
'Fyn kinase regulates misfolded alpha-synuclein uptake and NLRP3 inflammasome activation in microglia',
in: *J Exp Med* 216.6, pp. 1411–1430. ISSN: 1540-9538 (Electronic) 0022-1007 (Print) 0022-1007 (Linking). DOI: 10.1084/jem.20182191. URL: https://www.ncbi.nlm.nih.gov/pubmed/31036561.

PARK, J. S. ET AL. (2022):
'LDHB Deficiency Promotes Mitochondrial Dysfunction Mediated Oxidative Stress and Neurodegeneration in Adult Mouse Brain',
in: *Antioxidants (Basel)* 11.2. ISSN: 2076-3921 (Print) 2076-3921 (Electronic) 2076-3921 (Linking). DOI: 10.3390/antiox11020261. URL: https://www.ncbi.nlm.nih.gov/pubmed/35204143.

PFEFFERKORN, C. M., Z. JIANG and J. C. LEE (2012):
'Biophysics of alpha-synuclein membrane interactions',

in: *Biochim Biophys Acta* 1818.2, pp. 162–71. ISSN: 0006-3002 (Print) 0006-3002 (Electronic) 0006-3002 (Linking). DOI: 10.1016/j.bbamem.2011.07.032. URL: https://www.ncbi.nlm.nih.gov/pubmed/21819966.

PIRCS, K. ET AL. (2018):
'Huntingtin Aggregation Impairs Autophagy, Leading to Argonaute-2 Accumulation and Global MicroRNA Dysregulation',
in: *Cell Rep* 24.6, pp. 1397–1406. ISSN: 2211-1247 (Electronic). DOI: 10.1016/j.celrep.2018.07.017. URL: https://www.ncbi.nlm.nih.gov/pubmed/30089251.

POEHLER, A. M. ET AL. (2014):
'Autophagy modulates SNCA/alpha-synuclein release, thereby generating a hostile microenvironment',
in: *Autophagy* 10.12, pp. 2171–92. ISSN: 1554-8635 (Electronic) 1554-8627 (Print) 1554-8627 (Linking). DOI: 10.4161/auto.36436. URL: https://www.ncbi.nlm.nih.gov/pubmed/25484190.

POEWE, W. ET AL. (2017):
'Parkinson Disease',
in: *Nature Reviews Disease Primers* 3, p. 17013.

PORTER, K. J. ET AL. (2010):
'Regulation of lipopolysaccharide-induced inflammatory response and endotoxemia by beta-arrestins',
in: *J Cell Physiol* 225.2, pp. 406–16. ISSN: 1097-4652 (Electronic) 0021-9541 (Print) 0021-9541 (Linking). DOI: 10.1002/jcp.22289. URL: https://www.ncbi.nlm.nih.gov/pubmed/20589830.

POULADI, M. A. ET AL. (2010):
'Full-length huntingtin levels modulate body weight by influencing insulin-like growth factor 1 expression',
in: *Hum Mol Genet* 19.8, pp. 1528–38. ISSN: 1460-2083 (Electronic) 0964-6906 (Print) 0964-6906 (Linking). DOI: 10.1093/hmg/ddq026. URL: https://www.ncbi.nlm.nih.gov/pubmed/20097678.

QUINTIN, J. ET AL. (2014):
'Innate immune memory: towards a better understanding of host defense mechanisms',
in: *Curr Opin Immunol* 29, pp. 1–7. ISSN: 1879-0372 (Electronic) 0952-7915 (Linking). DOI: 10.1016/j.coi.2014.02.006. URL: https://www.ncbi.nlm.nih.gov/pubmed/24637148.

RAMASWAMY, S., J. L. MCBRIDE and J. H. KORDOWER (2007):
'Animal models of Huntington's disease',
in: *ILAR J* 48.4, pp. 356–73. ISSN: 1084-2020 (Print) 1084-2020 (Linking). DOI: 10.1093/ilar.48.4.356. URL: https://www.ncbi.nlm.nih.gov/pubmed/17712222.

RASHEED, MADIHA ET AL. (2021):
'Epigenetic Regulation of Neuroinflammation in Parkinson's Disease',
in: *International Journal of Molecular Sciences* 22.9, p. 4956. ISSN: 1422-0067. DOI: 10.3390/ijms22094956. URL: https://dx.doi.org/10.3390/ijms22094956.

REINER, ANTON, IOANNIS DRAGATSIS and PAULA DIETRICH (2011):
'Genetics and neuropathology of Huntington's disease',
in: *Int Rev Neurobiol* 98, pp. 325–72. ISSN: 2162-5514 (Electronic), 0074-7742 (Print), 0074-7742 (Linking). DOI: 10.1016/B978-0-12-381328-2.00014-6. URL: https://www.ncbi.nlm.nih.gov/pubmed/21907094.

RISIGLIONE, P. ET AL. (2021):
'Alpha-Synuclein and Mitochondrial Dysfunction in Parkinson's Disease: The Emerging Role of VDAC',
in: *Biomolecules* 11.5. ISSN: 2218-273X (Electronic) 2218-273X (Linking). DOI: 10.3390/biom11050718. URL: https://www.ncbi.nlm.nih.gov/pubmed/34064816.

RODRIGUEZ, R. M., B. SUAREZ-ALVAREZ and C. LOPEZ-LARREA (2019):
'Therapeutic Epigenetic Reprogramming of Trained Immunity in Myeloid Cells',
in: *Trends Immunol* 40.1, pp. 66–80. ISSN: 1471-4981 (Electronic) 1471-4906 (Linking). DOI: 10.1016/j.it.2018.11.006. URL: https://www.ncbi.nlm.nih.gov/pubmed/30595189.

ROIZIN, L. ET AL. (1974):
'Electron microscope and enzyme studies in cerebral biopsies of Huntington's chorea',
in: *Trans Am Neurol Assoc* 99, pp. 240–3. ISSN: 0065-9479 (Print) 0065-9479 (Linking). URL: https://www.ncbi.nlm.nih.gov/pubmed/4282536.

ROOS, R. A. (2010):
'Huntington's disease: a clinical review',
in: *Orphanet J Rare Dis* 5, p. 40. ISSN: 1750-1172 (Electronic) 1750-1172 (Linking). DOI: 10.1186/1750-1172-5-40. URL: https://www.ncbi.nlm.nih.gov/pubmed/21171977.

ROSENCRANS, WILLIAM M. ET AL. (2021):
'α-Synuclein emerges as a potent regulator of VDAC-facilitated calcium transport',
in: *ScienceDirect* 95.

ROTERMUND, C. ET AL. (2014):
'Diet-induced obesity accelerates the onset of terminal phenotypes in alpha-synuclein transgenic mice',
in: *J Neurochem* 131.6, pp. 848–58. ISSN: 1471-4159 (Electronic) 0022-3042 (Linking). DOI: 10.1111/jnc.12813. URL: https://www.ncbi.nlm.nih.gov/pubmed/24995537.

RUBINSZTEIN, DAVID C. and JENNY CARMICHAEL (2003):
'Huntington's disease: molecular basis of neurodegeneration',
in: *Expert Reviews in Molecular Medicine* 5.20, pp. 1–21. ISSN: 1462-3994. DOI: 10.1017/s1462399403006549. URL: https://dx.doi.org/10.1017/s1462399403006549.

RUNWAL, G. ET AL. (2019):
'LC3-positive structures are prominent in autophagy-deficient cells',
in: *Sci Rep* 9.1, p. 10147. ISSN: 2045-2322 (Electronic) 2045-2322 (Linking). DOI: 10.1038/s41598-019-46657-z. URL: https://www.ncbi.nlm.nih.gov/pubmed/31300716.

RUSKIN, DAVID N. ET AL. (2011):
'A ketogenic diet delays weight loss and does not impair working memory or motor function in the R6/2 1J mouse model of Huntington's disease',
in: *Elsevier* 103.

SABA AID, ROBERT LANGENBACH FRANCESCA BOSETTI (2008):
'Neuroinflammatory response to lipopolysaccharide is exacerbated in mice genetically deficient in cyclooxygenase-2',
in: *Journal of Neuroinflammation.*

SANTOS, D. ET AL. (2015):
'The Impact of Mitochondrial Fusion and Fission Modulation in Sporadic Parkinson's Disease',
in: *Mol Neurobiol* 52.1, pp. 573–86. ISSN: 1559-1182 (Electronic) 0893-7648 (Linking). DOI: 10.1007/s12035-014-8893-4. URL: https://www.ncbi.nlm.nih.gov/pubmed/25218511.

SANTOS, F. and W. DEAN (2004):
'Epigenetic reprogramming during early development in mammals',
in: *Reproduction* 127.6, pp. 643–51. ISSN: 1470-1626 (Print) 1470-1626 (Linking). DOI: 10.1530/rep.1.00221. URL: https://www.ncbi.nlm.nih.gov/pubmed/15175501.

SAUDOU, F. and S. HUMBERT (2016):
'The Biology of Huntingtin',
in: *Neuron* 89.5, pp. 910–26. ISSN: 1097-4199 (Electronic) 0896-6273 (Linking). DOI: 10.1016/j.neuron.2016.02.003. URL: https://www.ncbi.nlm.nih.gov/pubmed/26938440.

SAUNDERS, J. A. ET AL. (2012):
'CD4+ regulatory and effector/memory T cell subsets profile motor dysfunction in Parkinson's disease',
in: *J Neuroimmune Pharmacol* 7.4, pp. 927–38. ISSN: 1557-1904 (Electronic) 1557-1890 (Print) 1557-1890 (Linking). DOI: 10.1007/s11481-012-9402-z. URL: https://www.ncbi.nlm.nih.gov/pubmed/23054369.

SC, WARBY ET AL. (2009):
'CAG expansion in the Huntington disease gene is associated with a specific and targetable predisposing haplogroup',
in: *The American Journal of Human Genetics* 89.

SCHEIBLICH, HANNAH ET AL. (2021):
'Microglial NLRP3 Inflammasome Activation upon TLR2 and TLR5 Ligation by Distinct α-Synuclein Assemblies',
in: *The Journal of Immunology* 207.8, pp. 2143–2154. DOI: 10.4049/jimmunol.2100336.

SCHILLING, G. ET AL. (1995):
'Expression of the Huntington's disease (IT15) protein product in HD patients',
in: *Hum Mol Genet* 4.8, pp. 1365–71. ISSN: 0964-6906 (Print) 0964-6906 (Linking). DOI: 10.1093/hmg/4.8.1365. URL: https://www.ncbi.nlm.nih.gov/pubmed/7581375.

SCHULTE, J. and J. T. LITTLETON (2011):
'The biological function of the Huntingtin protein and its relevance to Huntington's Disease pathology',
in: *Curr Trends Neurol* 5, pp. 65–78. ISSN: 0972-8252 (Print) 0972-8252 (Linking). URL: https://www.ncbi.nlm.nih.gov/pubmed/22180703.

SEPULVEDA, D. ET AL. (2022):
'Contribution of Autophagy-Lysosomal Pathway in the Exosomal Secretion of Alpha-Synuclein and Its Impact in the Progression of Parkinson's Disease',
in: *Front Mol Neurosci* 15, p. 805087. ISSN: 1662-5099 (Print) 1662-5099 (Electronic) 1662-5099 (Linking). DOI: 10.3389/fnmol.2022.805087. URL: https://www.ncbi.nlm.nih.gov/pubmed/35250476.

SEREDENINA, T. and R. LUTHI-CARTER (2012):
'What have we learned from gene expression profiles in Huntington's disease?',
in: *Neurobiol Dis* 45.1, pp. 83–98. ISSN: 1095-953X (Electronic) 0969-9961 (Linking). DOI: 10.1016/j.nbd.2011.07.001. URL: https://www.ncbi.nlm.nih.gov/pubmed/21820514.

SERGE PRZEDBORSKI, MIQUEL VILA and VERNICE JACKSON-LEWIS (2003):
'Series Introduction: Neurodegeneration: What is it and where are we?',
in: *The Journal of Clinical Investigation* 111(1): 3–10.

SEVGI, F. ET AL. (2021):
'Imaging of alpha-Synuclein Aggregates in a Rat Model of Parkinson's Disease Using Raman Microspectroscopy',
in: *Front Cell Dev Biol* 9, p. 664365. ISSN: 2296-634X (Print) 2296-634X (Electronic) 2296-634X (Linking). DOI: 10.3389/fcell.2021.664365. URL: https://www.ncbi.nlm.nih.gov/pubmed/34568310.

SHEN, Z., X. BAO and R. WANG (2018):
'Clinical PET Imaging of Microglial Activation: Implications for Microglial Therapeutics in Alzheimer's Disease',
in: *Front Aging Neurosci* 10, p. 314. ISSN: 1663-4365 (Print) 1663-4365 (Electronic) 1663-4365 (Linking). DOI: 10.3389/fnagi.2018.00314. URL: https://www.ncbi.nlm.nih.gov/pubmed/30349474.

SHERER, T. B. ET AL. (2003):
'Subcutaneous rotenone exposure causes highly selective dopaminergic degeneration and alpha-synuclein aggregation',
in: *Exp Neurol* 179.1, pp. 9–16. ISSN: 0014-4886 (Print) 0014-4886 (Linking). DOI: 10.1006/exnr.2002.8072. URL: https://www.ncbi.nlm.nih.gov/pubmed/12504863.

SHERER, TODD B. ET AL. (2003):
'Mechanism of Toxicity in Rotenone Models of Parkinson's Disease',
in: *The Journal of Neuroscience* 23.34, pp. 10756–10764. ISSN: 0270-6474. DOI: 10.1523/jneurosci.23-34-10756.2003. URL: https://dx.doi.org/10.1523/jneurosci.23-34-10756.2003.

SHERWOOD, E. R. ET AL. (2022):
'Innate Immune Memory and the Host Response to Infection',

in: *J Immunol* 208.4, pp. 785–792. ISSN: 1550-6606 (Electronic) 0022-1767 (Linking). DOI: 10.4049/jimmunol.2101058. URL: https://www.ncbi.nlm.nih.gov/pubmed/35115374.

SHIMOJI, M. ET AL. (2005):
'Absence of inclusion body formation in the MPTP mouse model of Parkinson's disease',
in: *Brain Res Mol Brain Res* 134.1, pp. 103–8. ISSN: 0169-328X (Print) 0169-328X (Linking). DOI: 10.1016/j.molbrainres.2005.01.012. URL: https://www.ncbi.nlm.nih.gov/pubmed/15790534.

SHOSHAN-BARMATZ, V. ET AL. (2010):
'VDAC, a multi-functional mitochondrial protein regulating cell life and death',
in: *Mol Aspects Med* 31.3, pp. 227–85. ISSN: 1872-9452 (Electronic) 0098-2997 (Linking). DOI: 10.1016/j.mam.2010.03.002. URL: https://www.ncbi.nlm.nih.gov/pubmed/20346371.

SINGER, E. ET AL. (2021):
'The Novel Alpha-2 Adrenoceptor Inhibitor Beditin Reduces Cytotoxicity and Huntingtin Aggregates in Cell Models of Huntington's Disease',
in: *Pharmaceuticals (Basel)* 14.3. ISSN: 1424-8247 (Print) 1424-8247 (Electronic) 1424-8247 (Linking). DOI: 10.3390/ph14030257. URL: https://www.ncbi.nlm.nih.gov/pubmed/33809220.

SMITH, K. M. ET AL. (2006):
'Dose ranging and efficacy study of high-dose coenzyme Q10 formulations in Huntington's disease mice',
in: *Biochim Biophys Acta* 1762.6, pp. 616–26. ISSN: 0006-3002 (Print) 0006-3002 (Linking). DOI: 10.1016/j.bbadis.2006.03.004. URL: https://www.ncbi.nlm.nih.gov/pubmed/16647250.

SNEAD, D. and D. ELIEZER (2014):
'Alpha-synuclein function and dysfunction on cellular membranes',
in: *Exp Neurobiol* 23.4, pp. 292–313. ISSN: 1226-2560 (Print) 2093-8144 (Electronic) 1226-2560 (Linking). DOI: 10.5607/en.2014.23.4.292. URL: https://www.ncbi.nlm.nih.gov/pubmed/25548530.

SNOW, B. J. ET AL. (2000):
'Pattern of dopaminergic loss in the striatum of humans with MPTP induced parkinsonism',
in: *J Neurol Neurosurg Psychiatry* 68.3, pp. 313–6. ISSN: 0022-3050 (Print) 1468-330X (Electronic) 0022-3050 (Linking). DOI: 10.1136/jnnp.68.3.313. URL: https://www.ncbi.nlm.nih.gov/pubmed/10675212.

SOMMER, A. ET AL. (2018):
'Th17 Lymphocytes Induce Neuronal Cell Death in a Human iPSC-Based Model of Parkinson's Disease',
in: *Cell Stem Cell* 23.1, 123–131 e6. ISSN: 1875-9777 (Electronic) 1875-9777 (Linking). DOI: 10.1016/j.stem.2018.06.015. URL: https://www.ncbi.nlm.nih.gov/pubmed/29979986.

SONG, H. ET AL. (2023):
'Epigenetic modification in Parkinson's disease',
in: *Front Cell Dev Biol* 11, p. 1123621. ISSN: 2296-634X (Print) 2296-634X (Electronic) 2296-634X (Linking). DOI: 10.3389/fcell.2023.1123621. URL: https://www.ncbi.nlm.nih.gov/pubmed/37351278.

SPILLANTINI, MARIA GRAZIA ET AL. (1997):
'α-Synuclein in Lewy bodies',
in: *Nature* 388.6645, pp. 839–840. ISSN: 0028-0836. DOI: 10.1038/42166. URL: https://dx.doi.org/10.1038/42166.

SQUITIERI, FERDINANDO ET AL. (2005):
'Juvenile Huntington's disease: Does a dosage-effect pathogenic mechanism differ from the classical adult disease?',
in: *ScienceDirect* 127.

SRINIVASAN, E. ET AL. (2021):
'Alpha-Synuclein Aggregation in Parkinson's Disease',
in: *Front Med (Lausanne)* 8, p. 736978. ISSN: 2296-858X (Print) 2296-858X (Electronic) 2296-858X (Linking). DOI: 10.3389/fmed.2021.736978. URL: https://www.ncbi.nlm.nih.gov/pubmed/34733860.

STEFANIS, L. (2012):
'alpha-Synuclein in Parkinson's disease',
in: *Cold Spring Harb Perspect Med* 2.2, a009399. ISSN: 2157-1422 (Electronic) 2157-1422 (Linking). DOI: 10.1101/cshperspect.a009399. URL: https://www.ncbi.nlm.nih.gov/pubmed/22355802.

STEFFAN, J. S. (2010):
'Does Huntingtin play a role in selective macroautophagy?',
in: *Cell Cycle* 9.17, pp. 3401–13. ISSN: 1551-4005 (Electronic) 1538-4101 (Print) 1551-4005 (Linking). DOI: 10.4161/cc.9.17.12718. URL: https://www.ncbi.nlm.nih.gov/pubmed/20703094.

STEFFAN, J. S. ET AL. (2001):
'Histone deacetylase inhibitors arrest polyglutamine-dependent neurodegeneration in Drosophila',
in: *Nature* 413.6857, pp. 739–43. ISSN: 0028-0836 (Print) 0028-0836 (Linking). DOI: 10.1038/35099568. URL: https://www.ncbi.nlm.nih.gov/pubmed/11607033.

STORSTEIN, OLE-BJØRN TYSNES ANETTE (2017):
'Epidemiology of Parkinson's disease',
in: *Journal of Neural Transmission* 901–905.

STRATOULIAS, VASSILIS ET AL. (2019):
'Microglial subtypes: diversity within the microglial community',
in: *EMBO* 38(17).

SUL, OK-JOO ET AL. (2017):
'Lipopolysaccharide (LPS)-Induced Autophagy Is Responsible for Enhanced Osteoclastogenesis',
in: *Molecules and Cells* 40, pp. 880–887.

SULZER, D. ET AL. (2017):
'T cells from patients with Parkinson's disease recognize alpha-synuclein peptides',
in: *Nature* 546.7660, pp. 656–661. ISSN: 1476-4687 (Electronic) 0028-0836 (Print) 0028-0836 (Linking). DOI: 10.1038/nature22815. URL: https://www.ncbi.nlm.nih.gov/pubmed/28636593.

SWEENEY, P. ET AL. (2017):
'Protein misfolding in neurodegenerative diseases: implications and strategies',
in: *Transl Neurodegener* 6, p. 6. ISSN: 2047-9158 (Print) 2047-9158 (Electronic) 2047-9158 (Linking). DOI: 10.1186/s40035-017-0077-5. URL: https://www.ncbi.nlm.nih.gov/pubmed/28293421.

T. MAIURI T. WOLOSHANSKY, J. XIA and R. TRUANT (2013):
'The huntingtin N17 domain is a multifunctional CRM1 and Ran-dependent nuclear and cilial export signal',
in: *Human Molecular Genetics* 22.

YU-TAEGER, L. ET AL. (2012):
'A novel BACHD transgenic rat exhibits characteristic neuropathological features of Huntington disease',
in: *J Neurosci* 32.44, pp. 15426–38. ISSN: 1529-2401 (Electronic) 0270-6474 (Linking). DOI: 10.1523/JNEUROSCI.1148-12.2012. URL: https://www.ncbi.nlm.nih.gov/pubmed/23115180.

TAI, Y. F. ET AL. (2007):
'Imaging microglial activation in Huntington's disease',
in: *Brain Res Bull* 72.2-3, pp. 148–51. ISSN: 0361-9230 (Print) 0361-9230 (Linking). DOI: 10.1016/j.brainresbull.2006.10.029. URL: https://www.ncbi.nlm.nih.gov/pubmed/17352938.

TAKAHASHI, TETSUYA ET AL. (2002):
'Tyrosine 125 of alpha-synuclein plays a critical role for dimerization following nitrative stress',
in: *Brain Res* 938.1-2, pp. 73–80. ISSN: 0006-8993 (Print), 0006-8993 (Linking). DOI: 10.1016/s0006-8993(02)02498-8. URL: https://www.ncbi.nlm.nih.gov/pubmed/12031537.

TANG, WAN-YEE and SHUK-MEI HO (2007):
'Epigenetic reprogramming and imprinting in origins of disease',

in: *Reviews in Endocrine and Metabolic Disorders* 8.2, pp. 173–182. ISSN: 1389-9155. DOI: 10.1007/s11154-007-9042-4. URL: https://dx.doi.org/10.1007/s11154-007-9042-4.

TANSEY, M. G. ET AL. (2022):
'Inflammation and immune dysfunction in Parkinson disease',
in: *Nat Rev Immunol* 22.11, pp. 657–673. ISSN: 1474-1741 (Electronic) 1474-1733 (Print) 1474-1733 (Linking). DOI: 10.1038/s41577-022-00684-6. URL: https://www.ncbi.nlm.nih.gov/pubmed/35246670.

TAY, T. L. ET AL. (2018):
'Unique microglia recovery population revealed by single-cell RNAseq following neurodegeneration',
in: *Acta Neuropathol Commun* 6.1, p. 87. ISSN: 2051-5960 (Electronic) 2051-5960 (Linking). DOI: 10.1186/s40478-018-0584-3. URL: https://www.ncbi.nlm.nih.gov/pubmed/30185219.

THOMPSON, L. M. ET AL. (2009):
'IKK phosphorylates Huntingtin and targets it for degradation by the proteasome and lysosome',
in: *J Cell Biol* 187.7, pp. 1083–99. ISSN: 1540-8140 (Electronic) 0021-9525 (Print) 0021-9525 (Linking). DOI: 10.1083/jcb.200909067. URL: https://www.ncbi.nlm.nih.gov/pubmed/20026656.

THORNE, N. J. and D. A. TUMBARELLO (2022):
'The relationship of alpha-synuclein to mitochondrial dynamics and quality control',
in: *Front Mol Neurosci* 15, p. 947191. ISSN: 1662-5099 (Print) 1662-5099 (Electronic) 1662-5099 (Linking). DOI: 10.3389/fnmol.2022.947191. URL: https://www.ncbi.nlm.nih.gov/pubmed/36090250.

TIEU, K. (2011):
'A guide to neurotoxic animal models of Parkinson's disease',
in: *Cold Spring Harb Perspect Med* 1.1, a009316. ISSN: 2157-1422 (Electronic) 2157-1422 (Linking). DOI: 10.1101/cshperspect.a009316. URL: https://www.ncbi.nlm.nih.gov/pubmed/22229125.

TRONCOSO-ESCUDERO, P. ET AL. (2020):
'On the Right Track to Treat Movement Disorders: Promising Therapeutic Approaches for Parkinson's and Huntington's Disease',
in: *Front Aging Neurosci* 12, p. 571185. ISSN: 1663-4365 (Print) 1663-4365 (Electronic) 1663-4365 (Linking). DOI: 10.3389/fnagi.2020.571185. URL: https://www.ncbi.nlm.nih.gov/pubmed/33101007.

VALENZUELA-ARZETA, I. E. ET AL. (2023):
'LPS Triggers Acute Neuroinflammation and Parkinsonism Involving NLRP3 Inflammasome Pathway and Mitochondrial CI Dysfunction in the Rat',
in: *Int J Mol Sci* 24.5. ISSN: 1422-0067 (Electronic) 1422-0067 (Linking). DOI: 10.3390/ijms24054628. URL: https://www.ncbi.nlm.nih.gov/pubmed/36902058.

VALOR, L. M. (2015):
'Transcription, epigenetics and ameliorative strategies in Huntington's Disease: a genome-wide perspective',
in: *Mol Neurobiol* 51.1, pp. 406–23. ISSN: 1559-1182 (Electronic) 0893-7648 (Linking). DOI: 10.1007/s12035-014-8715-8. URL: https://www.ncbi.nlm.nih.gov/pubmed/24788684.

VAN RAAMSDONK, J. M. ET AL. (2005):
'Cognitive dysfunction precedes neuropathology and motor abnormalities in the YAC128 mouse model of Huntington's disease',
in: *J Neurosci* 25.16, pp. 4169–80. ISSN: 1529-2401 (Electronic) 0270-6474 (Print) 0270-6474 (Linking). DOI: 10.1523/JNEUROSCI.0590-05.2005. URL: https://www.ncbi.nlm.nih.gov/pubmed/15843620.

VARDA SHOSHAN-BARMATZ, EDUARDO N. MALDONADO and YAKOV KRELIN (2010):
'VDAC1 at the crossroads of cell metabolism, apoptosis and cell stress',
in: *The Journal of Cellular Pathology* 1.

VARUGHESE, J. T., S. K. BUCHANAN and A. S. PITT (2021):
'The Role of Voltage-Dependent Anion Channel in Mitochondrial Dysfunction and Human Disease',
in: *Cells* 10.7. ISSN: 2073-4409 (Electronic) 2073-4409 (Linking). DOI: 10.3390/cells10071737. URL: https://www.ncbi.nlm.nih.gov/pubmed/34359907.

VEKRELLIS, K. ET AL. (2011):
'Pathological roles of alpha-synuclein in neurological disorders',
in: *Lancet Neurol* 10.11, pp. 1015–25. ISSN: 1474-4465 (Electronic) 1474-4422 (Linking). DOI: 10.1016/S1474-4422(11)70213-7. URL: https://www.ncbi.nlm.nih.gov/pubmed/22014436.

VERMA, D. ET AL. (2017):
'Anti-mycobacterial activity correlates with altered DNA methylation pattern in immune cells from BCG-vaccinated subjects',
in: *Sci Rep* 7.1, p. 12305. ISSN: 2045-2322 (Electronic) 2045-2322 (Linking). DOI: 10.1038/s41598-017-12110-2. URL: https://www.ncbi.nlm.nih.gov/pubmed/28951586.

VILLAR-PIQUE, A., T. LOPES DA FONSECA AND T. F. OUTEIRO (2016):
'Structure, function and toxicity of alpha-synuclein: the Bermuda triangle in synucleinopathies',
in: *J Neurochem* 139 Suppl 1, pp. 240–255. ISSN: 1471-4159 (Electronic) 0022-3042 (Linking). DOI: 10.1111/jnc.13249. URL: https://www.ncbi.nlm.nih.gov/pubmed/26190401.

VLAG, M. VAN DER, R. HAVEKES AND P. R. A. HECKMAN (2020):
'The contribution of Parkin, PINK1 and DJ-1 genes to selective neuronal degeneration in Parkinson's disease',
in: *Eur J Neurosci* 52.4, pp. 3256–3268. ISSN: 1460-9568 (Electronic) 0953-816X (Print) 0953-816X (Linking). DOI: 10.1111/ejn.14689. URL: https://www.ncbi.nlm.nih.gov/pubmed/31991026.

WAKABAYASHI, KOICHI ET AL. (2007):
'The Lewy body in Parkinson's disease: molecules implicated in the formation and degradation of alpha-synuclein aggregates',
in: *Neuropathology* 27.5, pp. 494–506. ISSN: 0919-6544 (Print), 0919-6544 (Linking). DOI: 10.1111/j.1440-1789.2007.00803.x. URL: https://www.ncbi.nlm.nih.gov/pubmed/18018486.

WALKER, F. O. (2007):
'Huntington's disease',
in: *Lancet* 369.9557, pp. 218–28. ISSN: 1474-547X (Electronic) 0140-6736 (Linking). DOI: 10.1016/S0140-6736(07)60111-1. URL: https://www.ncbi.nlm.nih.gov/pubmed/17240289.

WANG, YU ET AL. (2012):
'Phosphorylated α-Synuclein in Parkinson's Disease',
in: *Science Translational Medicine* 4.121, 121ra20.

WANKER, E. E. (2000):
'Protein aggregation and pathogenesis of Huntington's disease: mechanisms and correlations',
in: *Biol Chem* 381.9-10, pp. 937–42. ISSN: 1431-6730 (Print) 1431-6730 (Linking). DOI: 10.1515/BC.2000.114. URL: https://www.ncbi.nlm.nih.gov/pubmed/11076024.

WAREHAM, L. K. ET AL. (2022):
'Solving neurodegeneration: common mechanisms and strategies for new treatments',
in: *Mol Neurodegener* 17.1, p. 23. ISSN: 1750-1326 (Electronic) 1750-1326 (Linking). DOI: 10.1186/s13024-022-00524-0. URL: https://www.ncbi.nlm.nih.gov/pubmed/35313950.

WELLINGTON, C. L. ET AL. (2002):
'Caspase cleavage of mutant huntingtin precedes neurodegeneration in Huntington's disease',
in: *J Neurosci* 22.18, pp. 7862–72. ISSN: 1529-2401 (Electronic) 0270-6474 (Print) 0270-6474 (Linking). DOI: 10.1523/JNEUROSCI.22-18-07862.2002. URL: https://www.ncbi.nlm.nih.gov/pubmed/12223539.

WEN, J. ET AL. (2023):
'Dietary High-Fat Promotes Cognitive Impairment by Suppressing Mitophagy',
in: *Oxid Med Cell Longev* 2023, p. 4822767. ISSN: 1942-0994 (Electronic) 1942-0900 (Print) 1942-0994 (Linking). DOI: 10.1155/2023/4822767. URL: https://www.ncbi.nlm.nih.gov/pubmed/36718278.

WENDELN, A. C. ET AL. (2018):
'Innate immune memory in the brain shapes neurological disease hallmarks',

in: *Nature* 556.7701, pp. 332–338. ISSN: 1476-4687 (Electronic) 0028-0836 (Linking). DOI: 10.1038/s41586-018-0023-4. URL: https://www.ncbi.nlm.nih.gov/pubmed/29643512.

WESTERMANN, B. (2010):
'Mitochondrial fusion and fission in cell life and death',
in: *Nat Rev Mol Cell Biol* 11.12, pp. 872–84. ISSN: 1471-0080 (Electronic) 1471-0072 (Linking). DOI: 10.1038/nrm3013. URL: https://www.ncbi.nlm.nih.gov/pubmed/21102612.

WHITTAKER, DANIEL S ET AL. (2022):
'Dietary ketosis improves circadian dysfunction as well as motor symptoms in the BACHD mouse model of Huntington's disease',
in: *Frontiers in Nutrition* 9, p. 1034743. DOI: 10.3389/fnut.2022.1034743.

WÜLLNER, ULLRICH ET AL. (2016):
'DNA methylation in Parkinson's disease',
in: *Journal of Neurochemistry* 139, pp. 108–120. ISSN: 0022-3042. DOI: 10.1111/jnc.13646. URL: https://dx.doi.org/10.1111/jnc.13646.

WYSS-CORAY, T. and L. MUCKE (2002):
'Inflammation in neurodegenerative disease–a double-edged sword',
in: *Neuron* 35.3, pp. 419–32. ISSN: 0896-6273 (Print) 0896-6273 (Linking). DOI: 10.1016/s0896-6273(02)00794-8. URL: https://www.ncbi.nlm.nih.gov/pubmed/12165466.

XIONG, H. ET AL. (2009):
'Parkin, PINK1, and DJ-1 form a ubiquitin E3 ligase complex promoting unfolded protein degradation',
in: *J Clin Invest* 119.3, pp. 650–60. ISSN: 1558-8238 (Electronic) 0021-9738 (Print) 0021-9738 (Linking). DOI: 10.1172/JCI37617. URL: https://www.ncbi.nlm.nih.gov/pubmed/19229105.

YANG, H. M. ET AL. (2017):
'Microglial Activation in the Pathogenesis of Huntington's Disease',
in: *Front Aging Neurosci* 9, p. 193. ISSN: 1663-4365 (Print) 1663-4365 (Linking). DOI: 10.3389/fnagi.2017.00193. URL: https://www.ncbi.nlm.nih.gov/pubmed/28674491.

YAO, CONG-HUI ET AL. (2019):
'Mitochondrial Fusion Supports Increased Oxidative Phosphorylation During Cell Proliferation',
in: *eLife* 8, e41351. DOI: 10.7554/eLife.41351. URL: https://doi.org/10.7554/eLife.41351.

YARIBASH, SHAKILA, KEYHAN MOHAMMADI and MAHMOOD ALIZADEH SANI (2025):
'Alpha-Synuclein Pathophysiology in Neurodegenerative Disorders: A Review Focusing on Molecular Mechanisms and Treatment Advances in Parkinson's Disease',
in: *Cell Mol Neurobiol* 45, p. 30. DOI: 10.1007/s10571-025-01544-2.

YEH, H. and T. IKEZU (2019):
'Transcriptional and Epigenetic Regulation of Microglia in Health and Disease',
in: *Trends Mol Med* 25.2, pp. 96–111. ISSN: 1471-499X (Electronic) 1471-4914 (Linking). DOI: 10.1016/j.molmed.2018.11.004. URL: https://www.ncbi.nlm.nih.gov/pubmed/30578089.

YOO, G., Y. K. SHIN and N. K. LEE (2023):
'The Role of alpha-Synuclein in SNARE-mediated Synaptic Vesicle Fusion',
in: *J Mol Biol* 435.1, p. 167775. ISSN: 1089-8638 (Electronic) 0022-2836 (Linking). DOI: 10.1016/j.jmb.2022.167775. URL: https://www.ncbi.nlm.nih.gov/pubmed/35931109.

ZARRANZ, J. J. ET AL. (2004):
'The new mutation, E46K, of alpha-synuclein causes Parkinson and Lewy body dementia',
in: *Ann Neurol* 55.2, pp. 164–73. ISSN: 0364-5134 (Print) 0364-5134 (Linking). DOI: 10.1002/ana.10795. URL: https://www.ncbi.nlm.nih.gov/pubmed/14755719.

ZHANG, W. ET AL. (2023):
'Role of neuroinflammation in neurodegeneration development',
in: *Signal Transduct Target Ther* 8.1, p. 267. ISSN: 2059-3635 (Electronic) 2095-9907 (Print) 2059-3635

(Linking). DOI: 10.1038/s41392-023-01486-5. URL: https://www.ncbi.nlm.nih.gov/pubmed/37433768.

ZHANG, XIAOMING ET AL. (2021):
'Epigenetic regulation of innate immune memory in microglia',
Unpublished Work. DOI: 10.1101/2021.05.30.446351. URL: https://dx.doi.org/10.1101/2021.05.30.446351.

ZHAO, J. ET AL. (2019):
'Neuroinflammation induced by lipopolysaccharide causes cognitive impairment in mice',
in: *Sci Rep* 9.1, p. 5790. ISSN: 2045-2322 (Electronic) 2045-2322 (Linking). DOI: 10.1038/s41598-019-42286-8. URL: https://www.ncbi.nlm.nih.gov/pubmed/30962497.

ZHENG, H. F. ET AL. (2013):
'Autophagic impairment contributes to systemic inflammation-induced dopaminergic neuron loss in the midbrain',
in: *PLoS One* 8.8, e70472. ISSN: 1932-6203 (Electronic) 1932-6203 (Linking). DOI: 10.1371/journal.pone.0070472. URL: https://www.ncbi.nlm.nih.gov/pubmed/23936437.

ZHOU, T. ET AL. (2017):
'Microglia Polarization with M1/M2 Phenotype Changes in rd1 Mouse Model of Retinal Degeneration',
in: *Front Neuroanat* 11, p. 77. ISSN: 1662-5129 (Print) 1662-5129 (Linking). DOI: 10.3389/fnana.2017.00077. URL: https://www.ncbi.nlm.nih.gov/pubmed/28928639.

ZHU, B. ET AL. (2022):
'The immunology of Parkinson's disease',
in: *Semin Immunopathol* 44.5, pp. 659–672. ISSN: 1863-2300 (Electronic) 1863-2297 (Print) 1863-2297 (Linking). DOI: 10.1007/s00281-022-00947-3. URL: https://www.ncbi.nlm.nih.gov/pubmed/35674826.

ZHU, R. ET AL. (2022):
'The role of microglial autophagy in Parkinson's disease',
in: *Front Aging Neurosci* 14, p. 1039780. ISSN: 1663-4365 (Print) 1663-4365 (Electronic) 1663-4365 (Linking). DOI: 10.3389/fnagi.2022.1039780. URL: https://www.ncbi.nlm.nih.gov/pubmed/36389074%20https://www.ncbi.nlm.nih.gov/pmc/articles/PMC9664157/pdf/fnagi-14-1039780.pdf.